Title

A Molecular and genetic analysis of the fer protein tyrosine kinase gene of Drosophila melanogaster

Permalink

https://escholarship.org/uc/item/33r453dt

Author

Paulson, Robert F.

Publication Date

1993

Peer reviewed|Thesis/dissertation

A Molecular and Genetic Analysis of the <u>fer</u> protein tyrosine kinase gene

of <u>Drosophila melanogaster</u>

by

Robert F. Paulson

DISSERTATION

Submitted in partial satisfaction of the requirements for the degree of

DOCTOR OF PHILOSOPHY

in

Biochemistry

in the

GRADUATE DIVISION

of the

UNIVERSITY OF CALIFORNIA

San Francisco

This thesis is dedicated to my family, who keep me going during the rough times and helped me celebrate the good times.

Acknowledgements:

I would like to thank Mike Bishop for all the advice and guidence that he has given me over the past seven years. Mike has not only been a mentor during this time but also a good friend. The success that I might achieve in the future will be due to the superb training I received in Mike's lab.

I would also like to thank the members of my thesis committee, Harold Varmus and Tom Kornberg. Harold has always been very supportive and helpful. He always gave me the impression that he thought I knew what I was talking about and for that I will always be grateful. Tom has provided a critical analysis of my work that helped me through out my work. My only regret is that I did not take advantage of both Harold and Tom's advice more frequently.

In the time I have spent in graduate school at UCSF, I have had the opportunity to interact with a large number of people. I would not have survived my first year at UCSF if it had not been for the support of my fellow classmates. In particular I would like to thank John Chant, Dave Waring, Bruce Patterson, Joe Ogas, Dan Frank, Joanna Gilbert, Trey Simmons, Jill Heemskirk, Janet Chenevert, Roland Bainton, and countless others with whom I discussed science and other more important topics, commiserated with and drank a few beers .

I would like to the all the people with whom I have had a chance to inetract with in Mike's lab. I feel that I have learned something from most all of them. I would especially like to thank Jeanne Magram, for being my best friend when she was in the lab. I would also like to thank Kathy Weston for helping me update my personal appearance. Some of the other people who made my stay in the Bishop lab a nice one, Martin Eilers, Bob Finney,

Josh Kaplan, Mike Simon, Monica Vetter, Audrey Foster, Alan Rodgers, Martin McMahon, Richard Lang, Sabina Schirm, Steve Robbins (who must take over the reins as manager of the Bishop lab softball team). A special thank you goes to Jean Jackson and Nancy Quintrell for their help and good cheer over the years. I would also like to thank the members of the *Drosophila* group for their insight and support.

My initial interest in a career in science was sparked by the influences of two teachers. My high school chemistry teacher Harlan Larsen taught me that science was fun and I appreciate the time and effort he put into teaching me chemistry. Larry Dumas at Northwestern University was nice enough to let me work in his lab during my senior year. I got my first taste of research there, and I am grateful for that opportunity.

Last but certainly not least, I would like to thank my family. My Mom and Dad, Gene and Adrienne Paulson, have given me the support and love necessary to finish this thesis. My siblings, Anne and Mike, Tom, and Mary who were always there to make me laugh when I needed to the most. Finally, I want to thank my wife Amy, whose love, support, and editorial skills made this thesis possible. Amy has put up with all my faults and helped me find new strengths. I have to thank my son Andy for his unconditional love that helped me get through the worst of days.

A Genetic and Molecular Analysis of the *fer* protein tyrosine kinase gene of *Drosophila melanogaster*.

Robert F. Paulson

Non-receptor tyrosine kinases (NRTKs) were first identified as the transforming genes carried by acutely transforming retroviruses. Although the viral isolates of these genes are able to transform cells in culture, the normal function of NRTKs during development is not well understood. In order to analyze the function of an NRTK during development, I have utilized the well established genetics of *Drosophila melanogaster* to investigate the function of the *fer* tyrosine kinase gene during *Drosophila* development.

fer encodes a non-receptor tyrosine kinase most closely related to the c-*fps*/*fes* family of NRTKs. The molecular characterization of the *fer* gene has revealed that the transcription unit is quite large, >50 kilobases (kb). Two mRNAs of 3.3 kb and 2.3 kb are transcribed from the gene. The 3.3 kb mRNA encodes a 92.5 kilodalton protein . The second mRNA encodes a 45 kilodalton protein. Analysis of the expression of the two mRNAs has revealed that both messages are expressed at the same times during development. In situ hybridization analysis of the spatial distribution of the two transcripts showed that both messages were coexpressed in the same tissues during embryogenesis.

Three mutant alleles of the *fer* gene were identified. Two of these alleles have rearrangements in the *fer* gene and both of these alleles fail to produce full length p92.5^{fer}. 50-75% of the mutant progeny die either as third instar larvae or pupae depending on the allele combination. The surviving mutant adults exhibited rough eyes that lack the proper number and localization of the interommatidial bristles. *fer* mutants also showed a defect

in macrochaete development, with one or two macrochaete missing on some of the mutant flies. The development of the indirect flight muscles was also affected. Sections of mutant flies showed that the muscles were disorganized and some muscles failed to develop. In addition, mutations in two genes, *Son of sevenless* and *disabled* were shown to enhance the rough eye phenotype of *fer* mutants.

J. Michael Bishop

Professor of Microbiology and Immunology

Director of the G.W. Hooper Foundation

Thesis adivisor.

Table of Contents

List of Tables

List of Figures

Chapter 1

Chapter 2

Chapter 3

Appendix 1

Introduction

Activated oncogenes, tumor suppressor genes, and cancer.

The development of a multicellular organism is a complex and highly regulated process. One key aspect of this process is the coordinate regulation of cell proliferation and cell differentiation. Throughout an organism's lifetime, the different cell types that make up the organism must be produced at the right time, and in the right number, and these cells must function in the correct location for as long as they are needed by the organism. Any defects in the mechanisms that regulate these processes can have profound consequences on the development and the life of the organism.

Cancer is a diverse collection of diseases that are caused by a breakdown in the processes that regulate normal cellular proliferation and differentiation. The large number of different diseases that are classified as cancer underscores the complexity of these processes. By characterizing the genetic lesions present in the cancer cell, we can start to identify important components of the regulatory mechanisms which control cell proliferation and differentiation.

The regulation of cell proliferation can be divided into two opposing regulatory networks. One network is involved in the stimulation of cells to proliferate, while the other network is concerned with inhibiting cell proliferation. The signals produced by these two networks must be precisely coordinated in order for normal development to occur. A disruption in either of the regulatory networks can cause the unregulated proliferation that is the hallmark of the cancer cell (Bishop 1987; Bishop 1991). Genes that act positively to stimulate proliferation are called oncogenes. Mutations in oncogenes that cause the unregulated stimulation of cell proliferation act as dominant mutations, and are referred to as activated oncogenes. Genes that

act negatively to inhibit cell proliferation are called tumor suppressors. Mutations that cause the complete loss of activity of a tumor suppressor gene behave genetically as recessive mutations, and can also lead to unregulated cell proliferation.

The study of acutely transforming retroviruses provided many of the initial clues to the identities of some of the gene products involved in the stimulation of cell proliferation. Early work showed that these retroviruses carried dominant acting transforming genes. The transforming genes, however were not viral in origin and it was later shown that the retroviruses had transduced normal cellular genes. During the transduction process and subsequent viral replication, these genes were mutated in such a way that expression of these genes after viral infection of a cell now induced transformation (Varmus 1989). The integration of a retrovirus upstream or downstream of an oncogene can also cause oncogene activation (Nusse 1986). The strong transcription enhancer of the retrovirus causes inappropriate expression of the oncogene which in turn leads to transformation of the cell. In mice, insertions of MMTV near the *wnt-1* gene have been shown to cause expression of *wnt-1* in mammary epithelial cells that do not normally express the gene. The expression of *wnt-1* leads to the development of mammary tumors in these mice. This observation illustrates an important point. Oncogene activation does not always involve a mutation in the oncogene protein, but rather it can be caused by the inappropriate expression of an otherwise wildtype oncogene.

Unlike cancer in animals, human cancer, with few exceptions, does not involve the action of tumor viruses. Consequently, in order to identify oncogenes involved in the development of human cancers, researchers turned

to tumor cells to look for activated oncogenes (Bishop 1987). Tumor cell DNA was isolated and then transfected into NIH 3T3 cells. Those cells that took up an activated oncogene from the tumor cell DNA were transformed and the human DNA responsible for the transformation was cloned. Using this assay, a mutated *ras* gene was isolated from DNA derived from a bladder carcinoma (Varmus 1989). This result was the first evidence that human tumors contained activated oncogenes. The DNA transfection assay has since been used to identify many other activated oncogenes. It is not surprising that many of the oncogenes identified in the DNA transfection assay had been previously identified as activated oncogenes involved in transformation by retroviruses.

The study of chromosomal translocations associated with certain cancers is another tool that has been used to identify activated oncogenes in human tumors In some cases, chromosomal translocations have led to the formation of gene fusions between oncogenes and other genes resulting in the activation of the oncogene (Korsmeyer 1992). The Philadelphia chromosome observed in Chronic myelogenous Leukemia contains a translocation that fuses the *abl* tyrosine kinase gene with the *BCR* gene. Translocations can also move oncogenes so that they are now under new transcriptional control. Translocations involving the *myc* gene and the immunoglobulin heavy chain locus cause an unregulated expression of *myc* in lymphomas.

Tumor cells often exhibit amplified regions of DNA. When these amplified regions were characterized it was discovered that oncogenes are often amplified in tumors (Bishop 1987; Bishop 1991). The amplification of an oncogene causes high level expression of that gene and can contribute cell transformation. Studies of several types of cancer has shown that the

presence of an amplified oncogene is indicative of the progression of a tumor to a later stage. Amplification of *N-myc* in neuroblastomas is only seen in late stage tumors (Schwab and Amler 1990).

The hypothesis that the normal function of oncogenes is to stimulate cell proliferation has been strongly supported by the functional characterization of these genes. Oncogenes encode a wide variety of protein products from secreted growth factors to nuclear transcription factors. *v-sis*, an activated oncogene isolated from the Simian sarcoma virus, encodes a mutated form of the ß chain of Platelet Derived Growth Factor (Varmus 1989). *neu*, an oncogene that was identified by the DNA transfection assay, encodes a receptor tyrosine kinase, related to the Epidermal Growth Factor Receptor (Bargmann, Hung et al. 1986). Stimulation of *neu* by its ligand results in a mitogenic signal (Peles, Bacus et al. 1992). The *ras* oncogene has been isolated both as a retroviral oncogene and as an activated oncogene in DNA transfection assays. *ras* encodes a low molecular weight GTP binding protein that plays a key role in signaling by receptor tyrosine kinases (Barbacid 1987). *c-myc*, an oncogene which has been identified by a number of different ways, encodes a nuclear transcription factor that plays a key, but poorly understood role in the control of the cell cycle (Bishop 1991).

Dominant mutations that cause the activation of oncogenes cannot account for all the events necessary for the formation of a tumor in an animal (Sager 1989; Marshall 1991). Early experiments done with transformed and non-transformed variants of a cell line showed that the transformed phenotype was suppressed when cells from the two cell lines were fused. Further experiments showed that the suppression activity was associated with certain chromosomes. These results suggested that the mutations

present in these cancer cells were genetically recessive. The study of several inherited cancers showed that although each disease appeared to be inherited as an autosomal dominant mutation, the kinetics of each disease could be explained at the molecular level as a need for two recessive mutations with one of the necessary mutations already present in the germline. Molecular characterization of the gene mutated in familial Retinoblastoma showed that this disease was caused by two recessive mutations in the RB gene with one mutation already present in the germline of people predisposed to the disease. In addition, careful karotypic analysis of various tumor cells has shown that these cells contained numerous deletions and rearrangements. Molecular analysis of these tumor cells has demonstrated a loss of heterozygosity at many loci. All of these results have pointed to the existence of a group of recessive mutations that contribute to the formation of a tumor. The genes that define this group of mutations are called tumor suppressor genes. These genes are involved in the negative regulation of cell proliferation.

Because tumor suppressor genes are recessive mutations, the molecular characterization of these genes has been very difficult. Analysis of the few tumor suppressor genes that have been cloned has revealed that in tumor cells, the tumor suppressor genes contain mutations that result in a in a loss of activity. All types of mutations, point mutations, deletions, rearrangements, and insertions of retroviruses that inactivate the tumor suppressor gene have been observed in tumor cells. In addition, dominant negative mutations in one allele of a tumor suppressor have been shown to be able to inactivate the function of the other allele (Herskowitz 1987).

The normal functions of tumor suppressor gene products may be as varied as those identified for oncogenes. The tumor suppressor gene isolated from chromosome 18 in colorectal carcinomas called *DCC* encodes a transmembrane protein with similarity to cell adhesion molecules (Fearon, cho et al. 1990). Although the mechanism of *DCC* function is not understood, *DCC* is thought to function in cell-cell signaling that may block cell proliferation. The gene mutated in Neurofibromatosis type 1, *NF1*, encodes a GTPase activating protein for the *ras* gene product (Xu, O'Connell et al. 1990). *NF1* acts to turn off the cell proliferation signal mediated by *ras*. Three other tumor suppressor genes have been shown to encode nuclear proteins that presumably function by regulating transcription of genes important for cell proliferation. The Wilm's Tumor gene, *WT1*, encodes a zinc finger protein similar to the early response gene *egr* (Call, Glaser et al. 1990). *WT1* has been shown to bind to *egr* binding sites and may act to block the function of this class of early response genes. The Retinoblastoma gene product is a nuclear phosphoprotein that binds DNA in a site specific manner (Lee, To et al. 1988). *RB* binding sites have been shown to be upstream of the *c-fos* oncogene, and *RB* is thought to repress the transcription of *c-fos* (Robbins, Horowitz et al. 1990). *p53* is another nuclear tumor suppressor. *p53* also binds DNA in sequence specific manner. Several experiments have suggested that *p53* may be involved in regulating the progression into the S phase of the cell cycle (Hartwell 1992; Livingstone, white et al. 1992).

In recent years it has become increasing clear that both the activation of oncogenes and the loss of tumor suppressor gene activity is necessary for the development of cancer. Studies of several different types of cancer, most notably colon cancer, have shown that a number genetic lesions are necessary

for the final cancer phenotype to manifest itself (Fearon and Vogelstein 1990; Bishop 1991). It is now generally accepted that with each new mutation the progression of a tumor moves along. Interestingly, the order of the mutations is not as important as the total number of mutations for the progression of a tumor. In colon cancer, where the different stages of tumor progression have been characterized, different tumors often exhibit different sequences of mutagenic events, but all final stage tumors contain approximately the same number of mutations (Fearon and Vogelstein 1990).

The events that lead to the progression of a tumor are very complex. The mutations that lead to progression of a tumor are different for the different types of cancer. In addition a mutation in a given oncogene or a tumor suppressor gene can have different effects on the progression of different tumors (Bishop 1991). Mutations in RB appear to be initiating events for the development of retinoblastoma and osteosarcoma as demonstrated by the fact that germline mutations in RB predispose an individual to these types of tumors. However, mutations in RB are also observed at high frequency in small cell carcinoma of the lung and in breast and bladder carcinomas, cancers which are not prevalent in individuals with germline RB mutations. In these tumors, it appears that mutations in RB are a contributing factor to the progression of the tumor.

Another factor that contributes to the progression of a tumor is genetic instability (Hartwell 1992). It is well known that tumor cells contain large numbers of genetic alterations including deletions, rearrangements , translocations, both losses of parts of chromosomes and losses of entire chromosomes, and DNA amplification. An important step in tumor progression may be the loss of genetic stability. During the progression of the

tumor some of the tumor cells have acquire the ability to amplify their DNA. In addition, the frequency of both chromosome loss and the loss of heterozygosity at different loci is greatly increased in tumor cells. The genetic instability leads to an increase in the number of genetic lesions a tumor cell suffers, which in turn contributes to the progression of the disease. In some instances genetic instability is caused by genes that are not considered oncogenes or tumor suppressor genes. Mutations in DNA repair enzymes are known to cause Xeroderma pigmentosa, an inherited form of skin cancer. In other cases, the wild type alleles of oncogenes and tumor suppressors may act to maintain genetic stability, while mutations in these genes lead to genetic instability in tumor cells. Loss of *p53* function in a cell confers upon the cell the ability to amplify its DNA (Livingstone, white et al. 1992). Likewise, in a mouse model for skin cancer mutations in *ras* appear to be the initiating event for later genetic lesions necessary for the progression of the tumor. One of the lesions that occurs in these tumors is the amplification of *ras* itself and it is thought that the activated *ras* gene may play a role in this event (Bishop 1987).

Using *Drosophila* to study the function of oncogenes and tumor suppressor genes.

The heterogeneous phenotypes presented by cancer cells which reflect the complex aneuploid genotypes of cancer cells makes the study of the function of oncogenes and tumor suppressor genes very difficult. Ideally, we would like to study the function of each oncogene or tumor suppressor gene in isolation. If we can understand the normal function of these genes then we will be able to better understand the effects of mutations that alter these genes in cancer cells. The characterization of the function of both the

mutated and wild type alleles of many oncogenes and tumor suppressor genes in cultured cells has provided a great deal of insight into the role of these genes during carcinogenesis. Cell lines, however, do not completely recapitulate the events that occur in the whole organism. The use of transgenic mice and homologous recombination knock out mutations in mice have added to our knowledge of the function of oncogenes and tumor suppressors during both the normal development of the organism and during carcinogenesis. Unfortunately, mice are not amenable to the further genetic analysis, that allow for the identification of newgene products that might functionally interact with the gene products of oncogenes and tumor suppressor genes. In order to perform a more complete genetic analysis of oncogene and tumor suppressor gene function, we must turn to a simpler organism where the genetic analysis is more accessable. *Drosophila melanogaster* is an organism with which we are able to perform such a genetic analysis.

The study of cancer using *Drosophila* as a model system started with the observation that genes similar to oncogenes were present in the *Drosophila* genome (Shilo and Weinberg 1981, Hoffman-Falk, Einat et al. 1983; Hoffmann 1989). Many of these oncogene homologs were cloned by low stringency screening of *Drosophila* genomic libraries. However, before a genetic analysis of oncogene function could be done, mutations in these genes had to be isolated. Although the existence of human tumor suppressor genes had only been hypothesized at this time, several recessive *Drosophila* mutations had already been identified that caused an unregulated growth phenotype, and the molecular characterization of these genes had started (Gateff 1982; Bryant 1987; Gateff and Mechler 1989).

In 1987, when I started this thesis project, sixteen oncogene homologs and at least fourteen recessive "tumor mutants" had been identified in *Drosophila* . For six of the oncogene homologs, mutations had been isolated, however, only one of these mutations, the *abl* mutation, had been induced in a gene that had first been cloned by low stringency. Three of the recessive tumor mutations had also been cloned. Since that time the number of *Drosophila* mutations in oncogenes that have been identified has more than doubled. This increase is due not only to the identification of mutations in oncogene homologs that were cloned by low stringency but also to the demonstration that several previously isolated mutations that affect development were in fact mutations in oncogene homologs. Several more recessive tumor mutant genes recently have been cloned from *Drosophila*. However, none of them appear to correspond to any of the tumor suppressor genes isolated from human tumors, and to my knowledge no homologs of the human tumor repressor genes have been identified in *Drosophila* (table A).

With the identification of mutations in *Drosophila* oncogene homologs and the cloning of recessive tumor suppressor genes, a genetic analysis of their function has been possible. The characterization of the phenotypes exhibited by the mutants has helped identify some of the *in vivo* functions of the wild type products of these genes, and the use of suppressor-enhancer analysis has led to the identification of other proteins that interact with these genes products. In this section of the introduction I will discuss some of the recent results that not only have increased our understanding of oncogene and tumor suppressor gene function but also have identified experimental systems that show great promise for clarifying the mechanism of oncogene and tumor suppressor gene function.

Table A
Oncogene homologs and tumor suppressor mutants of *Drosophila melanogaster*.

Gene	Vertebrate homolog	Cloning method	Mutations
Nuclear Oncogenes:			
myb[1]	c-myb	low stringency	yes
ets 2[2]	c-ets	low stringency	no
dorsal[3]	rel, NFkB	mutant cloned	yes
fos[4]	c-fos	protein purified	no
jun[5]	c-jun	protein purified	no
Receptor tyrosine kinases			
DER[6]	EGFR, neu	low stringency	yes
DIR[7]	Insulin R	low strigency	no
sevenless[8]	c-ros?	mutant cloned	yes
torso[9]	PDGFR?	mutant cloned	yes
Dtrk	c-trk	low stringency	no
breathless[10]	FGF R	low stringency	yes
Non-receptor tyrosine kinases			
abl[11]	c-abl	low stringency	yes
src64B[12]	c-src	low stringency	no
src29A[13]	c-src	low stringency	no
fer[14]	c-fer	low stringency	yes
Serine-threonine kinases			
l(1)pole hole[15]	c-raf	low stringency	yes
GTP binding proteins			
ras 1[16]	H-ras	low stringency	yes
ras 2[16]	K-ras	low stringency	no
rap 1 (ras 3)[16]	rap1/k-rev 1	low stringency	yes
Growth factors			
decapentaplegic[17]	TGF-ß	mutant cloned	yes
wingless[18]	wnt-1	mutant cloned and low stringency	yes
spitz[19]	EGF/TGF alpha	mutant cloned	yes

References

(Hoffman-Falk, Einat et al. 1983 [11]; Neuman-Silberberg, Schejter et al. 1984 [16]; Katzen, Kornberg et al. 1985 [1]; Livneh, Glazer et al. 1985 [6]; Simon, Drees et al. 1985 [12]; Petruzelli, Herrera et al. 1986 [7]; Banerjee, Renfranz et al. 1987 [8]; Gregory, Kammermeyer et al. 1987 [13]; Hafen, Basler et al. 1987 [8]; Padgett, Johnson et al. 1987 [17]; Rijsewijk, Schuermann et al. 1987 [18]; Nishida, Hata et al. 1988 [15]; Perkins, Dailey et al. 1988 [4,5]; Pribyl, Watson et al. 1988 [2]; Sprenger, Stevens et al. 1989 [9]; Katzen, Monterras et al. 1991 [14]; Klambt, Glazer et al. 1992 [10]; Rutledge, Zhang et al. 1992 [19])

Recessive tumor mutations of *Drosophila melanogaster*.

mutation	gene cloned	vertebrate homolog
Neurogenic genes		
Notch[2]	yes	cell surface molecule with EGF repeats
Delta[5]	yes	Similar to Notch
mastermind[9]	yes	none
Bigbrain[9]	yes	similar to amino acid transporter
enhancer of split[9]	yes	gene complex, HLH proteins and a G protein
Imaginal Disc overgrowth mutants		
lethal(2)giant larvae[3]	yes	cadherin like cell adhesion molecule
lethal(1)discs large[7,11]	yes	guanylate kinase
lethal(2)fat[10]	yes	cadherin like cell adhesion molecule
lethal(2)giant discs[4]	no	
lethal(3)c43[4]	no	
tumorous discs[1,6]	no	
discs overgrown[8]	no	
Benign germ cell tumor mutants		
fused[1,6]	yes	Serine threonine kinase
ovarian tumor[1,6]	yes	?

References;

(Gateff 1982 [1]; Kidd, Lockett et al. 1983 [2]; Mechler, Mcginnis et al. 1985 [3]; Bryant 1987 [4]; Kopczynski, Alton et al. 1988 [5]; Gateff and Mechler 1989 [6]; Woods and Bryant 1989 [7]; Jursnich, Fraser et al. 1990 [8]; Campos-Ortega and Jan 1991 [9]; Mahoney, Weber et al. 1991 [10]; Woods and Bryant 1991 [11])

Oncogene homologs and pattern formation during embryogenesis: *dorsal, decapentaplegic,* and *wingless.*

The dorsoventral polarity of the *Drosophila* embryo is determined by the interaction of more than two dozen genes (Govind and Steward 1991). Several groups of genes act at different times during development to initially establish the polarity of the egg and to later establish the polarity of the embryo. One group of genes is expressed maternally and is required for both the proper development of the egg shell and the proper development of embryonic polarity. This group includes the *torpedo* alleles of the RTK gene *DER* (Clifford and Schupach 1989). *ras* has been shown to function downstream of *DER* in this pathway (Doyle and Bishop 1993). The analysis of the function of receptor tyrosine kinases (RTKs) will be discussed in more detail later in this introduction.

A second group of genes that are also maternally expressed are required for the proper polarity of the embryo. This group specifies a signaling pathway that sets up a ventral signal responsible for determining the dorsoventral polarity of the embryo. This pathway utilizes a signal that is localized to the ventral portion of the of the perivitelline space, a space located between the vitelline membrane and the embryo (Govind and Steward 1991). The signal, which appears to be encoded by the *spatzle* gene, binds to the *Toll* gene product. *Toll* encodes a transmembrane receptor with homology to the platelet GP1b thrombin receptor. The final result of this signaling process is a translocation of the *dorsal* protein to the nucleus, in a ventral to dorsal nuclear gradient in the syncitial blastoderm (Steward, Zusman et al. 1988). *dorsal* has been cloned and it encodes a protein similar to that encoded by the oncogene *c-rel* (Steward 1987). Recently, *dorsal* and

rel have been shown to be highly homologous to the mammalian transcription factor NF-kB (Lenardo and Baltimore 1989; Gilmore 1990). In mammalian cells, the activity of the NFkB protein is regulated by controlling the subcellular localization of the protein. Inactive NFkB protein is sequestered in the cytoplasm by an inhibitor called IkB (Baeuerle and Baltimore 1988). In response to an extracellular signal, NFkB translocates to the nucleus and acts as a transcriptional regulator. In a situation similar to the mammalian system, *cactus,* a gene that negatively regulates the activity of the *dorsal* protein in the nuclei on the dorsal side of the embryo, has been shown to be homologous to IkB (Geisler, Bergmann et al. 1992; Kidd 1992). Since *dorsal* and *cactus* bear such a strong resemblance to NFkB and IkB, the genetic analysis of the dorsoventral signal transduction pathway will provide great insight into the mechanism by which *rel* and NFkB are activated in mammalian cells.

The establishment of a ventral to dorsal nuclear gradient of the *dorsal* protein in the syncitial blastoderm leads to the restricted expression of zygotic genes that specify the dorsoventral polarity of the embryo. Among these genes that are regulated by the concentration of *dorsal* protein is *decapentaplegic (dpp)*. *dpp* expression in wildtype embryos is limited to the dorsal side of the embryo (St. Johnson and Gelbart 1987). However in *dorsal* mutants, *dpp* is expressed over the entire dorsal-ventral axis, and the embryos are dorsalized. On the other hand, *dpp* mutants exhibit a ventralized phenotype suggesting that *dpp* may be important for proper development of the dorsal structures in the embryo. Further genetic analysis has revealed that *dpp* does indeed play a role in the regulation of genes important for the development of dorsal structures. Cloning of *dpp* has

revealed that the gene is a member of the TGF ß family of growth factors (Padgett, Johnson et al. 1987). In the future, the genetic analysis of *dpp* function will help in the understanding of the mechanism by which TGF ß functions in vertebrates.

Another growth factor homologue, *wingless (wg)*, has been shown to be involved in pattern formation during *Drosophila* embryogenesis. *wg* is required for the proper development of the cells of the posterior compartment of each segment of the embryo (Ingham 1988). A loss of *wg* function results in all the cells of the segment adopting the fate of the cell of the anterior compartment. Genetic experiments have shown that the cells that express *wg* are not the cells that actually require *wg* for proper development (Heuvel, Nusse et al. 1989). These results are consistent with the idea that *wg* encodes a secreted factor that affects cells nearby. Cloning of the *wg* gene revealed that the gene is similar to the vertebrate *wnt-1* oncogene that is activated by the insertion of MMTV in mouse breast tumors (Rijsewijk, Schuermann et al. 1987). Further genetic analysis has revealed that *wg* functions to maintain the expression of *engrailed*, another segment polarity gene, in the cells of the posterior compartment. Although many genes that are important for the determination of segment polarity have been identified, a candidate gene encoding the receptor for *wg* has not yet been identified. Further genetic analysis of the function of *wg* is sure to provide new information about the mechanism by which this family of growth factors function.

Drosophila myb an oncogene homologue that appears to affect cell division.

A homologue of the vertebrate nuclear oncogene *myb* was isolated from a *Drosophila* genomic library by low stringency hybridization. *myb* mRNA is expressed throughout the *Drosophila* life cycle. All mitotically active tissues express *myb* as well as a few post-mitotic tissues (Katzen, Kornberg et al. 1985). A mutation in the *myb* gene has been isolated and initial characterization of the phenotype suggests that *myb* may play a role in the regulation of cell division. Although the mutation is lethal at 25° C, some adults survive at 18°C. These flies show defects in wing development and the abdominal cuticle is not completely formed. Further analysis of the wing defects revealed that the cells of the wing fail to undergo their final mitosis (Katzen, Kornberg et al. 1993). The exact nature of the defect in cell division is not understood.

Tumor suppressor genes in *Drosophila*.

More than twenty *Drosophila* mutations have been reported to result in the unregulated growth of cells. These mutations are recessive mutations and the wildtype versions of these genes are thought to encode proteins that negatively regulate growth. Much recent work has focused on the isolation of these tumor suppressor genes and the characterization of their gene products. One group of seven mutations cause an overgrowth of cells in the imaginal discs (Bryant 1987). Recently, several of these mutations have been characterized in some detail.

The seven mutations that affect the proliferation of cells in imaginal discs can be subdivided into two classes. The first class of mutations cause a hyperplastic growth of the imaginal discs. However, the cells of the disc maintain their columnar epithelial structure and their ability to differentiate. Two mutations in this class, *l(3)discs overgrown (l(3)dco)* and *l(3)c43hs1*,

appear to have defects in gap junction communication (Jursnich, Fraser et al. 1990). Transformed vertebrate cells in culture also exhibit defects in gap junction communication (Atkinson and Sheridan 1985). It has been hypothesized that communication among cells via gap junctions is an important aspect of contact inhibition of cell proliferation. Recently another mutation in this class has been cloned. The *fat* gene encodes a transmembrane protein of over 5000 amino acids that contains 34 domains similar to those observed in the cell adhesion molecule cadherin, four EGF like repeats and a unique cytoplasmic domain (Mahoney, Weber et al. 1991). Based upon its similarity to the cadherin class of cell adhesion molecules, *fat* is thought to regulate cell proliferation and morphogenesis by selective cell-cell interactions.

The second class of mutations that results in the overgrowth of imaginal disc cells, causes the cells lose their columnar epithelial structure and their ability to differentiate (Bryant 1987). There are two mutations in this class and both of genes that cause this type of mutant phenotype, *l(2)giant larvae (l(2) gl)* and *l(3) discs large (l(3) dlg)*, have been cloned (Mechler, Mcginnis et al. 1985; Woods and Bryant 1989; Woods and Bryant 1991). *l(2)gl* encodes a protein that is detected on the cell surface. Like *fat*, the *l(2)gl* gene product shows some limited homology to extracellular domains of the cadherin family of cell adhesion molecules (Klambt, Muller et al. 1989). Based upon the structure of the gene and the phenotype of the mutations it is hypothesized that *l(2) gl* regulates cell growth by controlling cell-cell interactions through the regulation of cell adhesion.

The protein encoded by *l(3)dlg* contains several domains that are similar to domains observed in other proteins. The *l(3)dlg* gene product

contains a filamentous region that is similar to the hemaglutinin of whooping cough virus, an opa repeat region, an SH3 domain, and a domain that is similar to the catalytic domain of yeast guanylate kinase (Woods and Bryant 1991). The function of guanylate kinase is to phosphorylate GMP to form GDP, and recent reports have shown that the *l(3)dlg* gene product can function as a guanylate kinase. The *l(3)dlg* protein is localized to the septate junctions of the imaginal disc cells. These structures correspond to the tight junctions seen in vertebrate epithelial cells. These data suggest that *l(3)dlg* may function to regulate the amount of GTP available for a GTP mediated signaling pathway that affects imaginal disc cell proliferation by controlling cell-cell interactions at the level of septate junction formation.

An additional mutation that has been shown to affect the growth and differentiation of imaginal disc cells is called *abnormal wing discs (awd)* (Dearolf, Hersperger et al. 1988; Biggs, Hersperger et al. 1990). However, unlike the mutations that cause overgrowth of imaginal disc cells, mutations in *awd* cause extensive cell death abnormal morphology of the imaginal disc cells. *awd* has been cloned and like *dlg, awd* also encodes a protein involved in the synthesis of GTP, a nucleoside diphosphate kinase which phosphorylates GDP to make GTP. *awd* has also been shown to be 78% identical to the vertebrate gene *nm23* which is down regulated in metastatic tumor cells (Biggs, Hersperger et al. 1990). One mutant allele of *awd* called *awd*[killer of prune] shows a synthetic lethal interaction with the *prune* mutation (Ruggieri and McCormick 1991). Recently, the *prune* gene has been cloned and it has been shown to encode a protein that shows similarity to the *ras* GTPase activating protein, GAP (Teng, Engele et al. 1991). These results suggest that the interaction between *awd* and *prune* may be due to both of

them playing a role in regulating the function of a *ras* like GTP binding protein.

Although there is no data to suggest that *awd* and *l(3)dlg* interact, the identification of two genes involved in the formation of GTP that both appear to regulate the growth and development of imaginal disc cells suggests that the regulation of GTP levels in a cell can play a key role in regulating cell proliferation. The identification of a vertebrate homologue of *l(3)dlg* and an investigation of its role in regulating cell proliferation is needed.

The study of tyrosine kinase mutants: *sevenless*, *torso*, *DER*, and *abl*.

The genetic analysis of receptor tyrosine kinase mutations in the *sevenless (sev)* (Banerjee, Renfranz et al. 1987; Hafen, Basler et al. 1987), *torso (tor)* (Sprenger, Stevens et al. 1989), and *DER* (Shilo and Raz 1991) genes has been one of the most productive areas of oncogene research. Each of these RTKs functions in a different developmental pathway. *sev* is required for the development of the R7 photoreceptor cell of the eye, *tor* functions during the determination of terminal structures of the embryo, while *DER* plays a wider role, functioning during oogenesis (*torpedo* alleles), embryonic development (*faint little ball* alleles), and in eye development (*Ellipse* alleles).

Although these three RTKs function in different places and at different times during *Drosophila* development, genetic analysis of the mechanism by which they function has revealed that signaling by each of these RTKs is mediated by a similar set of downstream proteins. Two genetic screens, one that screened for enhancers of a temperature sensitive *sev* allele, and a second that screened for suppressors of a *tor* gain of function allele have identified a number of signaling molecules that act downstream of several

different RTKs (Simon, Bowtell et al. 1991; Doyle and Bishop 1993). Among the mutations that were isolated and have been molecularly characterized were mutations that affected the *ras* mediated signaling pathway. Mutations in the *ras 1* gene interact with mutations *sev, tor,* and *DER*. These results demonstrate the wide range of developmental processes that require *ras 1* activity. Consequently, it is not surprising that homozygous *ras 1* mutations are lethal (Simon, Bowtell et al. 1991).

The function of *ras* genes in *Drosophila* has also been investigated by studying the consequences of expression of activated versions of *ras* genes (Bishop and Corces 1988; Fortini, Simon et al. 1992). Mutations analogous to the codon 12 mutation observed in mutated *ras* genes isolated from human tumors have been engineered into both the *Drosophila ras1* and *Drosophila ras 2* genes. In the case of *ras 1* the activated version was expressed from the sevenless promoter-enhancer, while the activated *ras 2* was expressed from either the heat shock promoter or its own promoter. For both *ras 1* and *ras 2*, expression of the activated mutants caused defects in development. All the cells that expressed activated *ras 1* adopted the R7 photoreceptor cell fate which caused a rough eye phenotype in these flies. These results showed that the function of the *sev* RTK in the development of photoreceptor cell R7 is to activate the *ras 1* mediated signaling pathway. Expression of the activated *ras 2* gene caused several different defects depending on the promoter used. Nonspecific expression from the heat shock promoter caused a rough eye phenotype, while expression from its own promoter causes a defect in wing development. Enhancer-suppressor analysis of these activated *ras* phenotypes will allow for the identification of some of the genes that function downstream of *ras* genes.

Three other mutations that affect *ras 1* function were also shown to interact with mutations in *sev*. *Son of sevenless (Sos)* encodes a guanine nucleotide exchange factor for *ras*, *gap 1* encodes a GTPase activating protein for *ras*, and *Roughened* encodes a *rap 1/krev 1* homologue that acts as an antagonist to *ras* function (Harihan, Carthew et al. 1991; Rogge, Karlovich et al. 1991; Simon, Bowtell et al. 1991; Bonfini, Karlovich et al. 1992; Gaul, Mardon et al. 1992). In addition to functioning downstream of *sev*, genetic analysis has shown that *Sos* also functions downstream of both the *tor* and *DER* RTKs.

In addition to these mutations that directly affect the function of *ras 1*, three other mutations have been shown to be downstream of more than one of these RTKs. *dork* encodes an SH2-SH3 containing protein that similar to the proteins encoded by the *sem-5* gene of *C. elegans* and the *GRB 2* gene of mammals (Rubin 1991; Simon, Bowtell et al. 1991; Clark, Stern et al. 1992; Lowenstein, Daly et al. 1992; Rubin and al. 1992). These proteins interact with RTKs and with *sos* via their SH2 and SH3 domains, and provide a physical link between the RTK and the *ras* mediated signaling pathway. *corkscrew (csw)* is a mutant in a phosphotyrosine phosphatase similar to the vertebrate *PTP 1C* protein (Perkins, Larsen et al. 1992). The function of this protein in RTK signaling in *Drosophila* and the function of its counterpart in vertebrate cells is not known. The third mutation that has been shown to interact with mutations in RTKs is *l(1) pole hole* (Ambrosio, Mahowald et al. 1989). The gene mutated in *l(1)pole hole* encodes the *Drosophila* homologue of the vertebrate *raf* oncogene. *raf* encodes a serine-threonine kinase that has been shown to be activated by RTKs in mammalian cells. In *Drosophila*, *raf* has been shown to act downstream of both *sev* and *tor* (Doyle and Bishop

1993). A genetic analysis of *raf* function in flies has recently identified a suppressor of *raf* mutations . The *Drosophila suppressor of raf (sor)* encodes a protein that is similar to the protein encoded by the vertebrate activator of MAP kinase gene (Tsuda, Inoue et al. 1993). These data obtained from the studies of *dork, csw,* and *Drosophila raf* suggest that not only is the *ras* mediated signaling pathway of vertebrates conserved in *Drosophila,* but also that genes like *raf* that are thought to act downstream of *ras* are conserved as well.

The study of non-receptor tyrosine kinases (NRTKs) has not progressed as quickly as the study of RTKs. Several NRTK genes have been identified in *Drosophila,* however only one mutation in a *Drosophila* NRTK gene has been isolated, a mutation in the *Drosophila abl* homolog. Analysis of NRTK mutations in mice and of the *abl* mutation in *Drosophila* has been complicated by the weak pleiotropic phenotypes exhibited by these mutations. These complex phenotypes probably result from a combination of two specific properties of NRTKs. Unlike RTKs which initiate a signal in response to the binding of ligand, NRTKs probably do not initiate signals. Instead they are probably involved in the modulation of signals. As a result mutations in NRTKs do not result in a loss of the signal but rather in a change in the quality of the signal. The phenotype of such a defect in signal transduction would be more subtle than the complete loss of a signal as is observed in RTK mutations. The other property of NRTKs that contribute to their weak mutant phenotypes is that their function may be compensated for by other gene products. It seems clear from the analysis of mice homozygous for mutations in NRTK genes that these mice do not express mutant phenotypes in all the cells that express the NRTK gene. Even those cells that express

high levels of the NRTK may not exhibit a mutant phenotype in homozygous mice. Both of these properties of NRTKs has made the study of the *Drosophila abl* mutations very complex.

Flies carrying mutations in the *Drosophila abl* gene exhibit a semilethal pleiotropic phenotype that does not seem to affect the tissue which expresses the highest level of *abl* mRNA, the central nervous system (CNS) (Henkemeyer, Gerteler et al. 1987). Further genetic analysis of the *abl* mutations has allowed for the identification of several mutations which can modify the phenotype of the *abl* mutant flies (Henkemeyer, Gerteler et al. 1987; Gertler, Bennett et al. 1989; Gertler, Doctor et al. 1990; Gertler, Hill et al. 1993). The analysis of mutations that enhance the *abl* phenotype has revealed that *abl* plays a more significant role in the development of the CNS than was evident from the phenotype of the original *abl* mutants. None of the mutations that enhance the *abl* mutant phenotype and that have been cloned correspond to any of the genes that are thought to interact with *abl* in mammalian cells. It is not clear whether these genes represent signaling molecules that are downstream of *abl* or whether they represent components of a signaling pathway that in some way compensates for the loss of *abl* function in the CNS (Hoffmann 1991). If the former possibility is true then signaling through NRTKs may involve downstream molecules that are different from those identified to act downstream of RTKs. However, if these mutations affect other signaling pathways that can compensate for defects in *abl* dependent signaling, then these pathways will have to be characterized and accounted for in future genetic screens in order to isolate mutations in genes that actually do function downstreamof *abl*.

The analysis of mutations in *Drosophila abl* has also illustrated another aspect of NRTK function. It may be that NRTKs only function to fine tune a signaling process. The observation that the mutant phenotype exhibited by the *abl* mutant flies can be rescued by a kinase defective allele of *abl*, suggests that the kinase activity of *abl* is not necessary for viability (Henkemeyer, West et al. 1990). However, *abl* mutant flies that also carry a mutation in an enhancer of *abl* gene are not rescued by the kinase defective *abl* gene. Characterization of the *abl¹* allele has provided another piece of evidence about the mechanism of *abl* function. The *abl¹* allele has a much stronger phenotype than a protein null mutation and the protein is not localized to the proper place in the cell (Henkemeyer, West et al. 1990). Taken together these data suggest that *abl* may function as part of a signaling complex. In an otherwise wildtype background, this signaling complex can function perfectly well without wild type levels of *abl* kinase activity as long as enough of the mutant *abl* protein is present to make the complex complete. However, if a second pathway that functions in parallel with the *abl* dependent pathway is mutated, then the abl signaling complex requires *abl* kinase activity.

The further study of NRTK function in *Drosophila* will require the use of more sophisticated genetic analysis. In order to identify gene products that function downstream of NRTKs, other pathways that might compensate for the function of an NRTK must be taken into account. Any future genetic screens for mutations that enhance or suppress NRTK mutations must therefore be done in a sensitized mutant background where the kinase activity of the NRTK is required, and the contribution of other signaling pathways is minimized.

In this thesis I will present my characterization of the transcription unit and the expression pattern of the *Drosophila fer* NRTK gene. In addition, I will present a genetic analysis of the function of *fer* during *Drosophila* development, and some preliminary experiments to identify gene products that may interact with the *fer* gene product.

Chapter 1

Characterization of the transcription unit and the expression pattern of the *fer* gene of *Drosophila melanogaster*.

Abstract

Previously we reported the isolation of a *fps/fes* related tyrosine
kinase gene from *Drosophila melanogaster* called *dfps85D*. Initial
characterization of the gene revealed that it is expressed as a 3.3 kilobase
(kb) mRNA which encodes a 92.5 kilodalton (kd) protein, p92.5$^{\text{dfps85D}}$. The
dfps85D gene product is approximately 60% similar to the gene products of
both the chicken *c-fps* gene and the vertebrate *c-fps* related gene, *c-fer*.
dfps85D is expressed through out the life cycle of the fly, but the expression is
regulated in a tissue specific manner (Katzen, Monterras et al. 1991). In
contrast to vertebrate *c-fps*, *dfps85D* mRNA is detected in a wide variety of
tissues. This pattern of expression is more similar to the expression pattern
observed for the mammalian *c-fer* gene. I have identified a second mRNA
expressed from the *dfps85D* locus. This mRNA is approximately 2.3 kb and
encodes a truncated protein that contains the carboxy terminal kinase
domain and the non catalytic SH2 domain of p92.5$^{\text{dfps85D}}$. However in the
2.3 kb mRNA, the sequence encoding the amino terminal 423 amino acids is
replaced with sequence encoding 10 new amino acids. The structure of the
this second *dfps85D* gene product is very similar to the testes specific *ferT*
gene product encoded by the vertebrate *c-fer* gene. On the basis of the wide
tissue distribution of the *dfps85D* mRNA and the presence of a second mRNA
that encodes a truncated protein, we feel that *dfps85D* is more similar to *c-fer*
than to *c-fps*. Therefore we propose that *dfps85D* be renamed *Drosophila fer*.
We have also characterized the transcription unit of the *fer* locus. The locus
is contained in >50 kb of genomic DNA. The intron-exon structure of the *fer*
gene is not at all similar to the gene structure of the vertebrate *c-fps* gene.

The expression of the two mRNAs during the life cycle of the fly was investigated by S1 nuclease protection analysis. Both mRNAs appear to be expressed at the same time during development, although the 3.3kb message is expressed at a higher level than the 2.3 kb message. In situ hybridization experiments using message specific probes on whole mount *Drosophila* embryos revealed that the two mRNAs are expressed in the same tissues during embryogenesis. The highest levels of expression were seen during the development of the gut and somatic musculature. Late in embryogenesis, both of the *fer* messages are also expressed in the ventral midline of the central nervous system. This analysis of *fer* expression during embryogenesis will help guide the dissection of the embryonic phenotype of *fer* mutants.

Introduction

The proto-oncogene *c-fps/fes* encodes a non-receptor tyrosine kinase that has been conserved in vertebrates. This gene was originally identified as a retroviral oncogene isolated from both avian and feline sarcoma viruses, *v-fps* and *v-fes* respectively. The 92 kd gene product of the *c-fps* gene is composed of three domains, a unique amino terminal domain, a non-catalytic regulatory domain called SH2, and a kinase domain (figure 1.1). Based on the structure of the gene product, *c-fps/fes* represents a distinct family of non-receptor tyrosine kinases (Pawson and Gish 1992). The unique amino terminal domain is approximately 47 kd, and makes up almost half of the protein. Unlike the *src* family of tyrosine kinases, the amino terminus of the *c-fps* gene product is not myristylated. p92$^{c\text{-}fps}$ has not been shown to associate with membranes. Rather, immunoflourescence experiments and biochemical fractionation have demonstrated that the protein is localized to

Figure 1.1
The *c-fps/fes* family of non-receptor tyrosine kinases

unique domain   SH2   Kinase
domain

p92^{cfps}

49%   46%   60%

p94^{c-fer}

50%   45%   60%

p92.5^{fer}
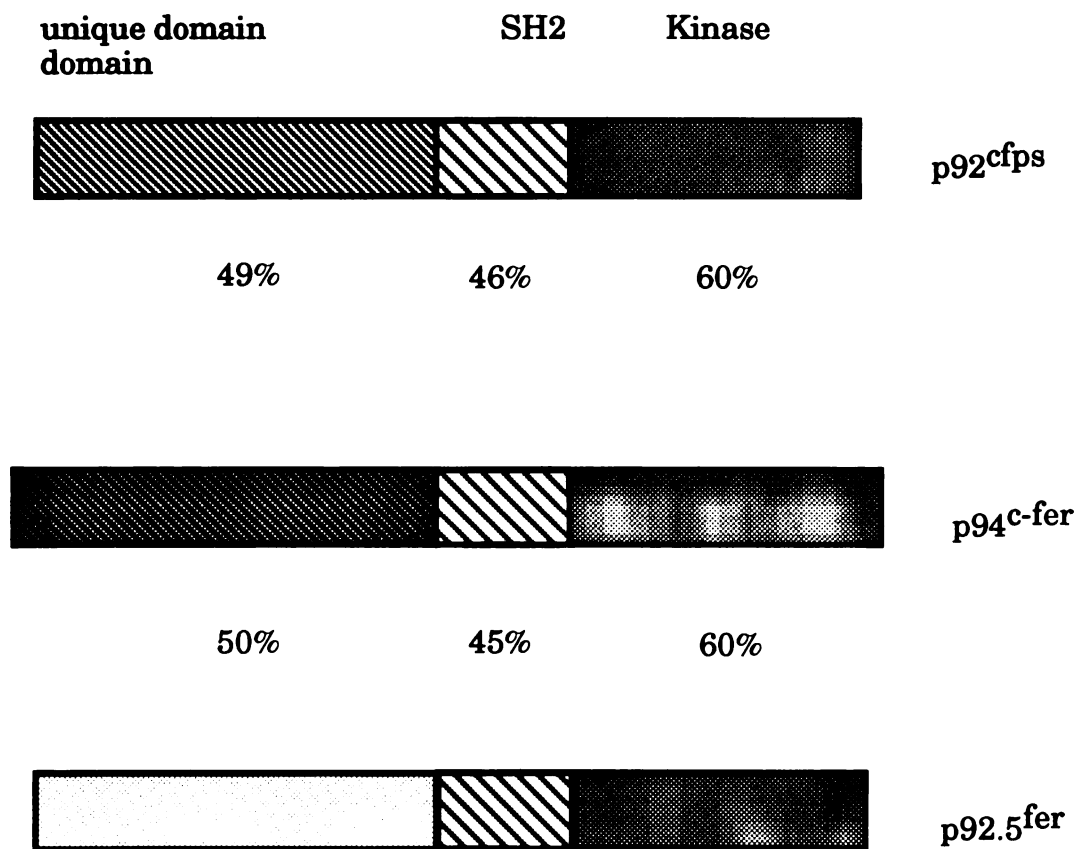
Legend figure 1.1:

The domain structure of the three members of the *fps/fes* family of non-receptor tyrosine kinases. The numbers under the different domains of p98^{cfps} and p94^{cfer} represent the amount of amino acid similarity including conservative changes between each of these proteins and p92.5^{fer}.

the cytoplasm (Young and Martin 1984). The SH2 domain, which was first described in v-fps and v-src, has now been identified in all non-receptor tyrosine kinases and in several other proteins involved in signal transduction. This domain binds phosphotyrosine residues, and it is thought that in non-receptor tyrosine kinases SH2 may be instrumental in binding substrates (Pawson and Gish 1992). The kinase domain of the *c-fps* contains all the signature amino acid sequences associated with tyrosine kinases. p92[c-fps] also has a major autophosphorylation site in the kinase domain, located at tyrosine 716 in chicken c-fps (Hanks, Quinn et al. 1988). This site is required for transformation by the v-fps gene product. The kinase domain of p92[c-fps] does not contain a regulatory tyrosine phosphorylation site analogous to tyrosine 527 in p60[src], and the mechanism by which the kinase activity is activated is unknown. The *c-fps* gene product is expressed primarily in hematopoietic cells of the granulocyte and macrophage lineage (Samarut, Mathey-prevot et al. 1985). The function of the gene product in these cells, however, is not known.

A second member of the *fps/fes* related tyrosine kinase gene family has recently been isolated from rats and humans. This gene called *c-fer* is highly similar to *c-fps* and is conserved in mammals (Hao, Heisterkamp et al. 1989; Pawson, Ltewin et al. 1989). The *c-fer* gene encodes a protein of 94 kd that cross reacts with *c-fps* antisera. Unlike the *c-fps* gene, the rat *c-fer* gene is expressed in a wide range of tissues including the kidney, brain, lung, ovaries and testes. In the testes, in addition to the 2.9 kb mRNA that encodes p94[fer], two smaller mRNAs of 1.3 and 2.4 kb are detected. The mouse homologue of the rat testes specific *c-fer* mRNA has been cloned. This

transcript, referred to as *ferT,* encodes a 51 kd protein that differs from the 94 kd *c-fer* protein at its amino terminus (Fischman, Edman et al. 1990). In *ferT* the amino terminal 412 amino acids of p94^{fer} are replaced with 44 new amino acids.

Previously we reported the isolation of a *fps/fes* like gene from *Drosophila melanogaster* called *dfps85D* (Katzen, Monterras et al. 1991). Initial characterization of the gene showed that *dfps85D* is expressed as a 3.3 kb mRNA encoding a 92.5 kd protein. The *dfps85D* gene product is equally similar to both the vertebrate *c-fps* and *c-fer* gene products. The 3.3 kb *dfps85D* mRNA first appears at the onset of gastrulation and continues to be expressed through out the life cycle of the fly. In situ hybridization experiments showed that the gene is expressed in a wide range of tissues during development. During embryogenesis the gene is expressed in the developing gut, and the somatic mesoderm that will give rise to the musculature of the larva. Near the end of embryogenesis expression is detected in the ventral midline of the central nervous system. At the larval stage of development, *dfps85D* is expressed in the eye disc behind the morphogenetic furrow in the developing ommatidia, and in all the other imaginal discs. In pupae, *dfps85D* mRNA is detected in all the developing adult muscle groups and in the optic lamina of the brain. Adult expression is limited to the retina, the gut, with lower levels in the testes and ovaries.

In this chapter, I describe the identification of a second *dfps85D* mRNA. This 2.3 kb mRNA encodes a truncated protein similar to the *ferT* testes specific gene product. In view of the similarity of the two *dfps85D* gene products to the vertebrate *c-fer* gene products, we propose that *dfps85D* be renamed *Drosophila fer*. I will also discuss the topography of the *fer* genomic

region and the structure of the transcription unit. The expression of the two mRNAs during the life cycle of the fly was investigated by S1 nuclease protection experiments. In addition, the tissue specific distribution of the two transcripts during embryogenesis was analyzed by in situ hybridization experiments utilizing message specific probes.

Results
Isolation of a second *fer* mRNA.

During the screen for cDNA clones of the 3.3 kb *fer* mRNA, two clones shorter than the 3.3 kb cDNA clone were also isolated. Both of these shorter clones diverged from the longest cDNA clone at the same point in the sequence. The divergence point was fifteen basepairs 5' to the sequences encoding the SH2 domain. One of the clones, clone 4.1, was subsequently shown to contain the genomic sequence immediately upstream of the divergence point. Since this genomic sequence does not have an open reading frame that includes the SH2 and kinase domains, I believe that cDNA clone 4.1 was derived from an unspliced mRNA. The second clone, 9C13, has unique sequence upstream of the divergence point and this sequence remains in frame with the downstream coding sequence of the SH2 and kinase domains. The unique sequence in clone 9C13 contains an AUG start codon that has the appropriate sequence to be used for translation initiation in *Drosophila* (Cavener 1987). In addition the start codon is downstream of stop codons in all three reading frames. These features of clone 9C13 suggest that this clone represents a second *fer* transcript.

Initial attempts to confirm the expression of the putative 9C13 transcript by Northern blot analysis were inconclusive because the 9C13

Figure 1.2
Sequence of the 2.3 kb mRNA from *dfer* .

```
AGCAATAGCAATCACAGTGCCTCACAGTCCACGATAATAACGAGCACGATCACCACCACCATAACG
ACTACAACTACCACGACGCCGTCCAAGGAAAACTCAAGACTGAAATTCAAAGTGCCCAAGATCCAG
AAGAAATCAAAGGCCATCCGCAATACATTCCGCTCCAAGTTGCTCAATTTCCAGTTGAAGCGGCTC
CAAGCCGTGCAAACAGTGCACCAAGAGACGTCGCATCCATCCCAGCAAAAGTGTCTTTGATTTTGC
CAAAGAGTTCGAGGTGGAACAACCGGCTGGTTCGGCGGCGGATGAGCAATTCTGCAACTGTCCGC
AGCTGGTCAAAAGCCTGTTAAGCCATCCGTCCAAATATCCGGCCACAAAGATCACCCGTTCGAGTC
CAGTTCTGGAGAGCTGGACGAGAACTCGGACTGGGACACTTGACAACGACGAGGAGGAGGAGGAT
```

```
                                          M   L   L   R   A   Q   P   G   A
AGCGCCAGTGACGACGTGCTCAGCATGAAGGATC ATG CTA TTG CGT GCC CAG CCT GGC GCC
     S   I   S   L   S   T   N   R   P   L   Y   E   E   E   W   F   H   G   V
AGT ATA TCG CTC TCC ACA AAT CGT CCG CTT TAC GAG GAG GAA TGG TTC CAT GGC GTT
     L   P   R   E   E   V   V   R   L   L   N   N   D   G   D   F   L   V   R
CTG CCG CGC GAG GAA GTG GTT CGA TTG CTG AAT AAC GAT GGT GAC TTC CTG GTC CGC
     E   T   I   R   N   E   E   S   Q   I   V   L   S   V   C   W   N   G   H
GAA ACG ATT CGA AAC GAG GAG AGC CAG ATT GTG CTC AGT GTC TGT TGG AAT GGC CAT
     K   H   F   I   V   Q   T   T   G   E   G   N   F   R   F   E   G   P   P
AAG CAC TTC ATT GTC CAG ACC ACC GGA GAG GGT AAT TTC CGG TTC GAG GGA CCA CCA
     F   A   S   I   Q   E   L   I   M   H   Q   Y   H   S   E   L   P   V   T
TTT GCC AGC ATC CAG GAG CTG ATC ATG CAT CAG TAT CAC TCG GAA TTG CCA GTG ACC
     V   K   S   G   A   I   L   R   R   T   V   C   R   E   R   W   E   L   S
GTG AAA TCG GGA GCC ATA CTC CGA CGA ACC GTT TGC CGG GAG CGC TGG GAG CTG AGC
     N   D   D   V   V   L   L   E   R   I   G   R   G   N   F   G   D   V   Y
AAC GAT GAT GTG GTA CTT CTG GAG AGG ATT GGT CGG GGA AAC TTT GGG GAT GTC TAC
     K   A   K   L   K   S   T   K   L   D   V   A   V   K   T   C   R   M   T
AAG GCC AAA CTG AAG TCC ACC AAA CTG GAT GTG GCT GTC AAA ACC TGT CGA ATG ACC
     L   P   D   E   Q   K   R   K   F   L   Q   E   G   R   I   L   K   Q   Y
CTG CCC GAC GAA CAG AAA CGT AAA TTC CTG CAG GAA GGG CGC ATC CTC AAG CAA TAC
     D   H   P   N   I   V   K   L   I   G   I   C   V   Q   K   Q   P   I   M
GAT CAT CCA AAT ATC GTA AAA TTG ATT GGC ATT TGT GTG CAG AAG CAG CCC ATC ATG
     I   V   M   E   L   V   L   G   G   S   L   L   T   Y   L   R   K   N   S
ATT GTC ATG GAA TTG GTG CTC GGT GGT TCG CTT TTA ACT TAT TTG CGC AAG AAC TCC
     N   G   L   T   T   R   E   Q   M   G   M   C   R   D   A   A   A   G   M
AAT GGC CTC ACC ACT CGC GAA CAA ATG GGC ATG TGC AGA GAT GCG GCG GCA GGC ATG
     R   Y   L   E   S   K   N   C   I   H   R   D   L   A   A   R   N   C   L
CGA TAT CTG GAG TCC AAA AAC TGC ATT CAT CGC GAT CTG GCG GCG CGT AAT TGT CTC
     V   D   L   E   H   S   V   K   I   S   D   F   G   M   S   R   E   E   E
GTT GAC TTG GAG CAC AGT GTG AAG ATC TCC GAT TTC GGA ATG TCT CGC GAG GAA GAG
     E   Y   I   V   S   D   G   M   K   Q   I   P   V   K   W   T   A   P   E
GAA TAT ATA GTT TCC GAT GGC ATG AAA CAA ATA CCT GTG AAG TGG ACA GCT CCC GAG
     A   L   N   F   G   K   Y   T   S   L   C   D   V   W   S   Y   G   I   L
GCC TTG AAT TTC GGC AAG TAC ACT TCG TTG TGC GAT GTG TGG TCC TAT GGC ATA CTG
     M   W   E   I   F   S   K   G   D   T   P   Y   S   G   M   T   N   S   R
ATG TGG GAG ATC TTC TCC AAG GGC GAC ACA CCC TAC TCC GGC ATG ACC AAC TCC AGA
     A   R   E   R   I   D   T   G   Y   R   M   P   T   P   K   S   T   P   E
GCC AGA GAG CGC ATC GAT ACG GGA TAT CGT ATG CCA ACG CCG AAG AGC ACG CCC GAG
     E   M   Y   R   L   M   L   Q   C   W   A   A   D   A   E   S   R   P   H
GAG ATG TAC CGA CTG ATG CTC CAG TGC TGG GCA GCC GAC GCC GAA TCC CGA CCG CAT
     F   D   E   I   Y   N   V   V   D   A   L   I   L   R   L   D   N   S   H
TTC GAT GAG ATC TAC AAT GTG GTG GAT GCA CTG ATT CTG CGC CTG GAC AAC AGC CAC
***
```

```
TAAGAGCGGCTCCATGCGGAACACTTAGCGTATACTCAACGTAGATTTAGTCAGCGCTTTTAAAGT
ACGTTACGTCCGAGGACTTGACAACGAGTTGCCTGTATTTATGAGATAGCACATACCTACTATACA
TTTTACCATATAAACCATATTTATATAGAGACATATATATTTTCTATCCATGTAAATGTAAATTTCGA
TGTGTACTGTAGTGTGTGTTTGCCTGACTGAGCGTATGTTTAAAATCCTTAATGTGCCAAAAACCGC
AAGAGATCTTAAAACAAAAAAAAAAGTGAAACGAAAAAAGATAAGAGAAAATAAAATAAAACTGAT
ATTGTGTGTCTGCTTGAACAAGGCGCTTGCTAACCTAAGCTCATGAATTTATATATTTTTGATTGTT
TTGTGTTTTGATTTTTAGGCAGTGATTCATAATTTGTAAATTATGCAATCCCTACGTTTGTCAATTTG
TTTCTAGACTTTGTATTCTATGTATATTTATTTACACCTAATTTACATTTCTACTTCGACTACGATTA
TGTTTACTCTAACACAACTAAGCTCTAAGTTAAAGCTTTAAGTTTTGCTGCGCTGCTGAAGTGAATA
AATAATATGTGTACTATATATATATATATAAAAAAAAAA
```

Legend figure 1.2:

The nucleotide sequence of the 2.3 kb mRNA with the amino acids translated above the coding sequence. The start site of the 5' untranslated region corresponds to the longest RACE clone (see figure 1.8). The 10 new amino acids at the amino terminus are shown in bold type.

mRNA is expressed at a low level. Using a more sensitive assay, S1 nuclease
protection, the expression of the second *fer* transcript was confirmed (see
figure 1.9B). The sequence of the 9C13 cDNA clone is shown in figure 1.2.
Primer extension analysis (data shown below) suggested that the 9C13 cDNA
clone was not a full length clone, and lacked approximately 100 bp from the 5'
end. Taking this observation into account the size of the second *fer* mRNA is
estimated to be 2.3 kb. The mRNA contains approximately 750 bp of unique
5' untranslated region and encodes a protein of 394 amino acids with a
predicted molecular weight of 45 kd. The gene product differs from p92.5[fer]
at the amino terminus where the amino terminal 423 amino acids are
replaced by 10 new amino acids.

Characterization of the *fer* genomic region.

The genomic region that encompasses *fer* was isolated by screening for
clones in a lambda phage library of *Drosophila* genomic DNA initially using
cDNA restriction fragments as probes and later using terminal restriction
fragments from the phage clones as probes. Genomic clones were restriction
mapped and a map of overlapping phage clones was generated. Using these
maps I determined that the *fer* locus is contained in >50 kb of DNA
(figure 1.3). Unfortunately we have been unable to isolate contiguous phage
clones that cover the entire *fer* locus. All the cDNA sequence, however, has
been accounted for in the phage clones isolated.

The positions of intron-exon boundaries were identified by sequencing
genomic clones using a series of sequencing primers whose sequence was
derived from cDNA sequence. The sequences of all the splice junctions
correspond to the consensus sequences for 5' and 3' splice junctions (Mount
1982). As diagrammed in figure 1.3, the 3.3 kb mRNA is made up of thirteen

Figure 1.3

Map of the *fer* genomic region and the *fer* transcripts and gene products
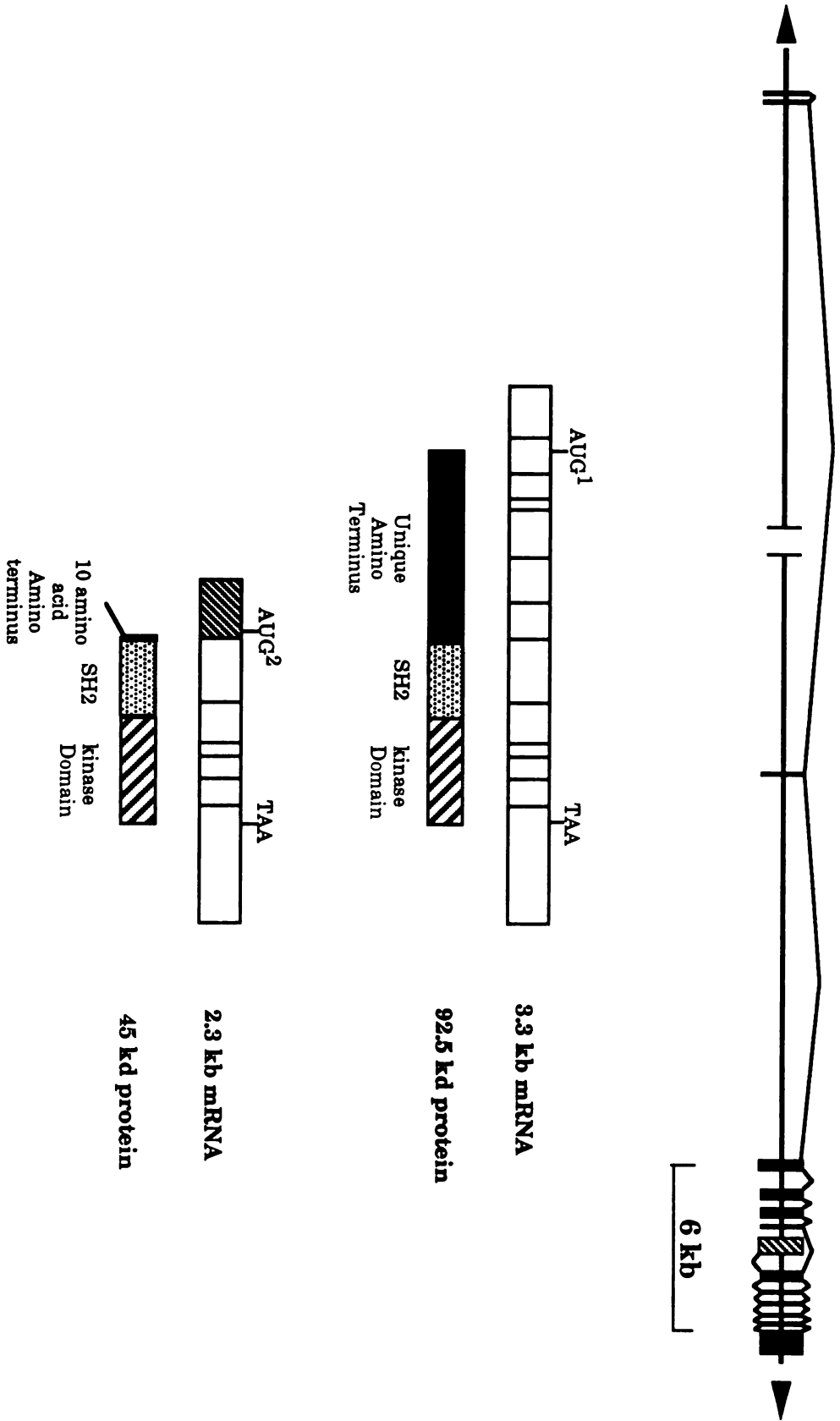
Legend figure 1.3:

Diagram of the *fer* locus with the exons and introns shown approximately to scale. The representations of the two mRNAs show the topography of he transcripts and the protein products are shown below. The ATG start codons and the TAA stop codons are indicated for both the mRNAs.

exons which are contained in a genomic region of >50 kb, while the 2.3 kb mRNA is made up of at least seven exons which are contained in a four kb region.

The sizes of the introns were determined in three ways. Some of the smaller introns were sequenced when the intron-exon boundaries were identified. The sizes of other introns were estimated using PCR. The PCR reactions utilized plasmids containing subclones of genomic DNA and primers derived from the sequence of two adjacent exons. The size of the intron was then determined to be the size of the PCR product minus the size of the exon sequences contained between the two primers. Finally, the sizes of the very large introns were estimated from the restriction maps of the genomic clones. The topography of the *fer* gene bears no resemblance to the genomic structure of the vertebrate *c-fps* gene (Huang, Hammond et al. 1985; Roebroek, Schalken et al. 1987). There is also no similarity in the organization of the exons that make up the different domains of the *c-fps* and *fer* gene products.

Mapping the transcription unit of *fer*.

The *fer* gene could generate the two mRNAs by either alternative splicing of the nascent *fer* transcript or initiation of transcription from two different promoters in the *fer* gene. In order to differentiate between these two possibilities, I mapped the transcription unit of the *fer* locus.

Primer extension analysis of the 3.3 kb mRNA showed that the longest cDNA we isolated was approximately 100-150 bp short of the true 5' end (data not shown). In order to map the 5' end of the mRNA, a uniformly labeled 190 bp S1 probe was generated that contained 168 bp of genomic sequence immediately upstream of the 5' end of the cDNA (see figure 1.4C).

Figure 1.4
Mapping the 5' end of the 3.3 kb *fer* mRNA
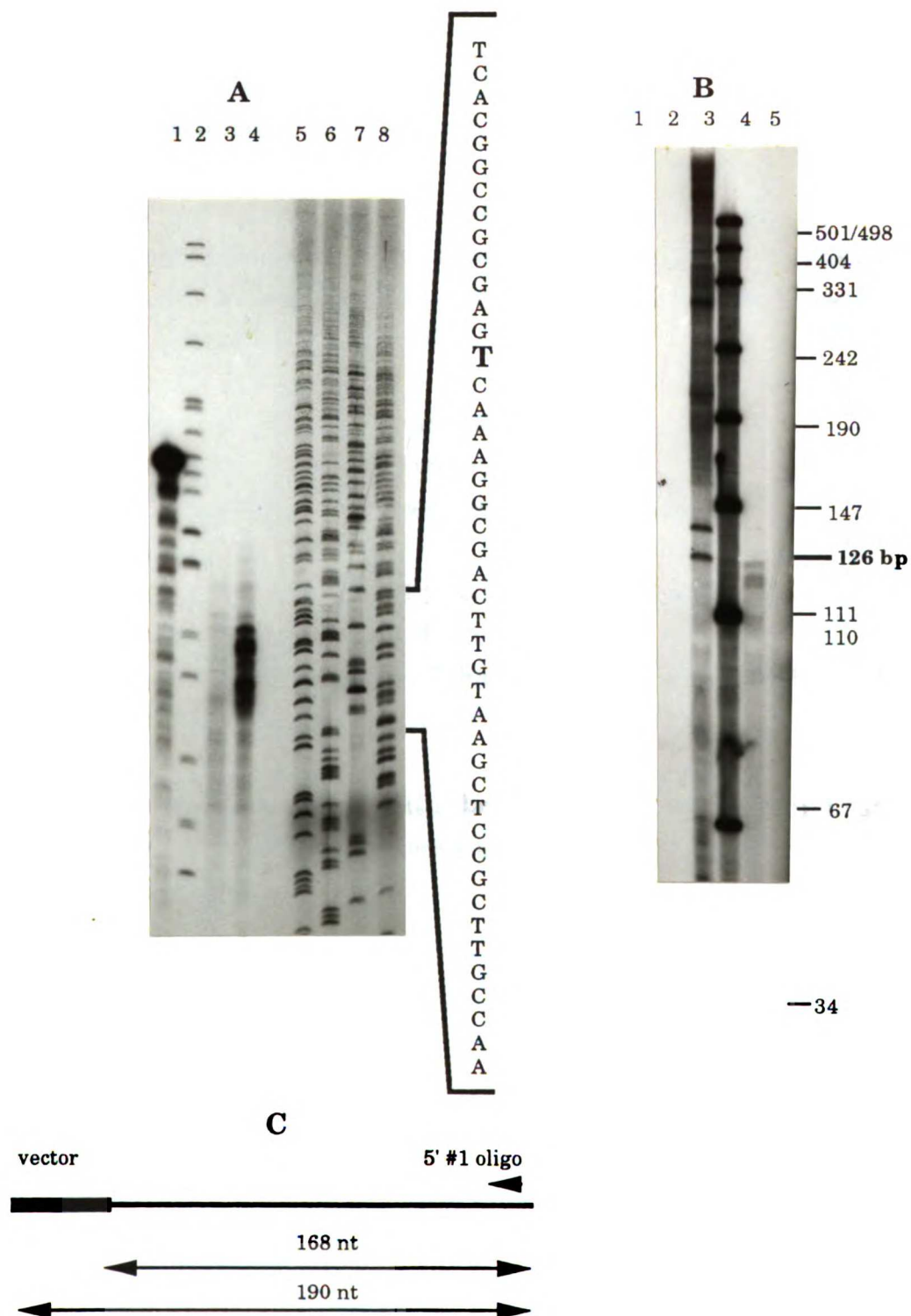
Legend figure 1.4:

A. S1 nuclease protection analysis of the 5' end of the 3.3 kb mRNA.

      Lane 1 Probe untreated

      Lane 2 Markers

      Lane 3 tRNA + probe + S1

      Lane 4 2-24 hour embryo poly A+ RNA + probe + S1

      Lanes 5-8 are a sequencing ladder using the 5' #1 oligo as the sequencing primer.

This primer is the same primer that was used to make the S1 probe, the sequence of the 5' end of the protected fragment is displayed to the right of the gel. The nucleotide that corresponds to the 5' end of the S1 nuclease protected fragment is marked with bold type.

B. S1 nuclease protection and primer extension analysis.

      Lane 1 tRNA primer extension reaction

      Lane 2 2-24 hour poly A+ RNA primer extension reaction.

      Lane 3 Markers

      Lane 4 S1 nuclease protection of 2-24 hour poly A+ RNA

      Lane 5 S1 nuclease protection tRNA control

      The arrow indicates the position of the S1 nuclease protected band the lower primer extension band of ~126 bp.

C. The S1 nuclease protection probe with the total size of the probe indicated 190 nt, and the size of the *fer* locus genomic sequence upstream of the 5' end of the cDNA indicated, 168 nt.
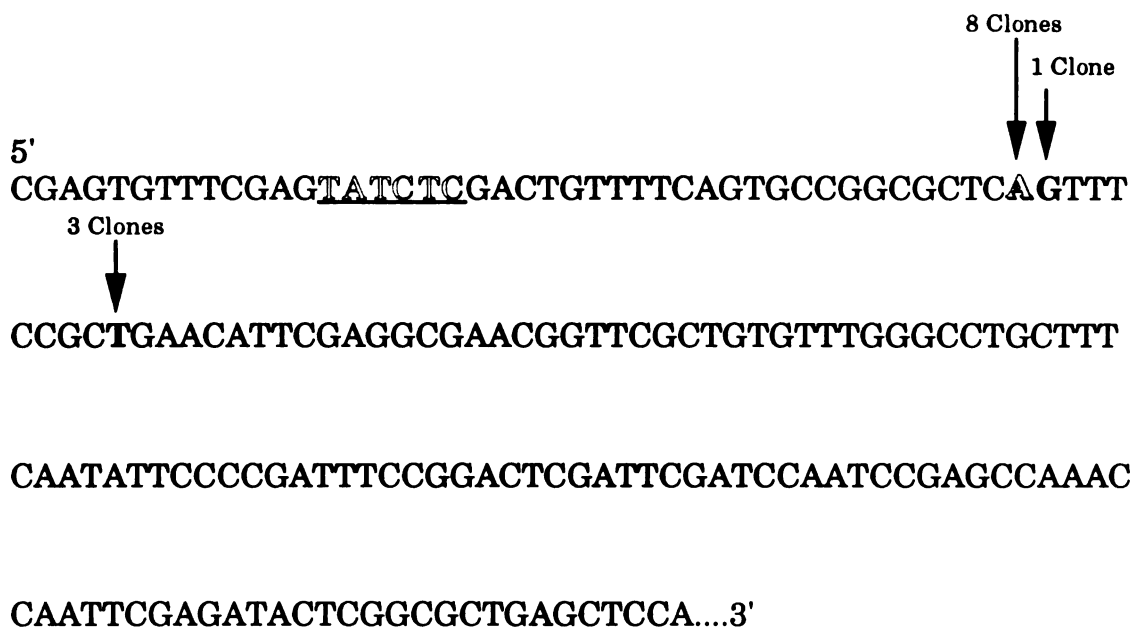
The S1 probe was hybridized with poly-A+ RNA isolated from embryos 2-24 hours after oviposition. The hybridization reaction was digested with S1 nuclease. A fragment of 126 bp was protected from S1 nuclease digestion. The sequence of the 5' end of the 126 bp S1 nuclease protected fragment was determined by sequencing a genomic subclone with the same primer used to make the S1 nuclease protection probe. The sequencing reactions were run on a sequencing gel in lanes adjacent to the S1 nuclease protection reactions (figure 1.4A). The sequence of the 5' end of the 126 bp protected fragment corresponds to basepair -241 relative to the AUG start codon of the 3.3 kb mRNA. Primer extension experiments using the same primer as that used to make the S1 probe were done to confirm that the 126 bp S1 protected fragment does correspond to the start site of transcription. Two extension products were detected, one of 126 bp that corresponds to the S1 protected band and a larger extension product of approximately 140 bp (figure 1.4B). The larger extension products, >150 bp, seen in figure 1.4B are due to nonspecific priming by the oligonucleotide. The presence of the 140 bp extension product suggests that there might be either an additional small exon 5' to the S1 probe or a second transcription start site.

In order to confirm basepair -241 as the transcriptional start site and rule out the possibility of an additional 5' exon, the 5' end of the mRNA was cloned using the RACE protocol (figure 1.5) (Frohman, Dush et al. 1988). Of the twelve RACE clones isolated, the 5' end of the eight longest clones corresponded to basepair -241, the transcription start site indicated by the 126 bp S1 nuclease protected fragment. However, the most persuasive evidence to confirm -241 as the start site of transcription came from the direct sequencing of the 5' end of the 3.3 kb mRNA. Although the quality of

the data was not sufficient for me to read the sequence of the mRNA directly due to technical difficulties, the length of the sequence corresponded to the length of a primer extension product of approximately 120-130 bp (figure 1.6). These data clearly ruled out the possibility of either an additional 5' exon or a second transcriptional start site. The genomic region upstream of the start site contains a TATCTC sequence which is similar to the consensus sequence for a TATA box element.

The mapping of the transcription unit for the 2.3 kb mRNA has been problematic. Primer extension experiments indicate that the start site of transcription is approximately 100-130 bp upstream of the end of the cDNA or approximately -491 to -521 relative to the initiator AUG codon (figure 1.7). The larger extension products in figure 6 are due to nonspecific priming by the Race 1 oligonucleotide. RACE cloning of the 5' end of the 2.3 kb mRNA was used to generate a number of clones. Although most of the clones were too short to be consistent with the primer extension results, one clone, #16, corresponded to transcriptional start site 106 bp upstream of the 5' end of the 9C13 cDNA (figure 1.8). This site was consistent with the primer extension data and corresponds to nucleotide -497. All attempts to use reverse transcriptase-PCR to connect exons 1 or 2 with the alternate exon of the 2.3 kb mRNA to show that this mRNA is derived by alternative were unsuccessful. Although our observations are consistent with the idea that the 2.3 kb mRNA is transcribed from a second promoter located between exons 7 and 8, RNAse protection mapping experiments to confirm this site as the start site of transcription have been inconclusive.

Figure 1.5
The positions of the 5' ends of the RACE clones of the
3.3 kb
fer **mRNA in the** *fer* **genomic sequence.**

8 Clones

1 Clone

5'
CGAGTGTTTCGAGTATCTCGACTGTTTTCAGTGCCGGCGCTCAGTTT

3 Clones

CCGCTGAACATTCGAGGCGAACGGTTCGCTGTGTTTGGGCCTGCTTT

CAATATTCCCCGATTTCCGGACTCGATTCGATCCAATCCGAGCCAAAC

CAATTCGAGATACTCGGCGCTGAGCTCCA....3'

Legend figure 1.5:

RACE cloning the 5' end of the 3.3 kb mRNA.

The arrows and the bold type indicate the 5' ends of the RACE clones in the genomic sequence of the *fer* locus, and the number clones that stopped at that site. The outlined A corresponds to the 5' end of the S1 nuclease protected fragment and the primer extension product. The TATCTC identifies a putative TATA box site in the genomic sequence upstream of the start site.

Figure 1.6
Direct sequencing of the 5' end of the3.3 kb *fer* mRNA
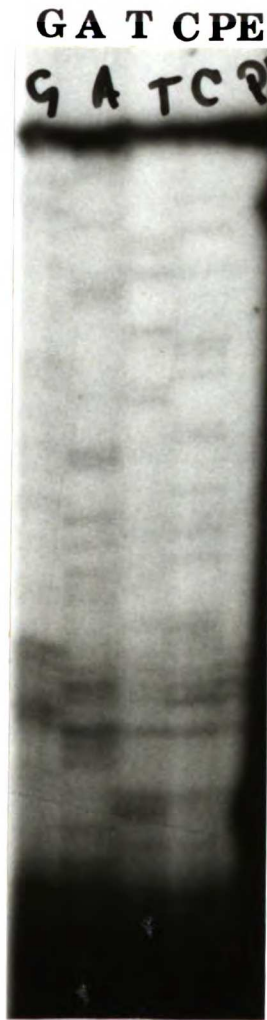
Legend figure 1.6:

Direct sequencing of the 5' end of the 3.3 kb mRNA.

Although the data are not of high quality, this gel clearly shows that the end of the RNA sequence corresponds to the end of the primer extension reaction. THis result confirms the results of the S1 nuclease protection and primer extension analysis.

Expression of the two *fer* mRNAs during development.

Since the 2.3 kb mRNA is difficult to detect on a Northern (RNA) blot, S1 nuclease protection analysis was performed on mRNA isolated at different times during the development of the fly. A 335 bp end labeled S1 nuclease protection probe was generated from the p9C13S1 plasmid as shown in figure 9A. The 2.3 kb mRNA protects a 312 bp fragment of the S1 probe, while the 3.3 kb mRNA protects a 110 bp fragment. This probe was hybridized to poly A+ selected RNA isolated from different stages of *Drosophila* developm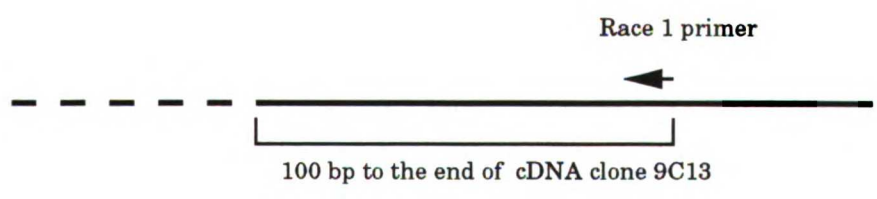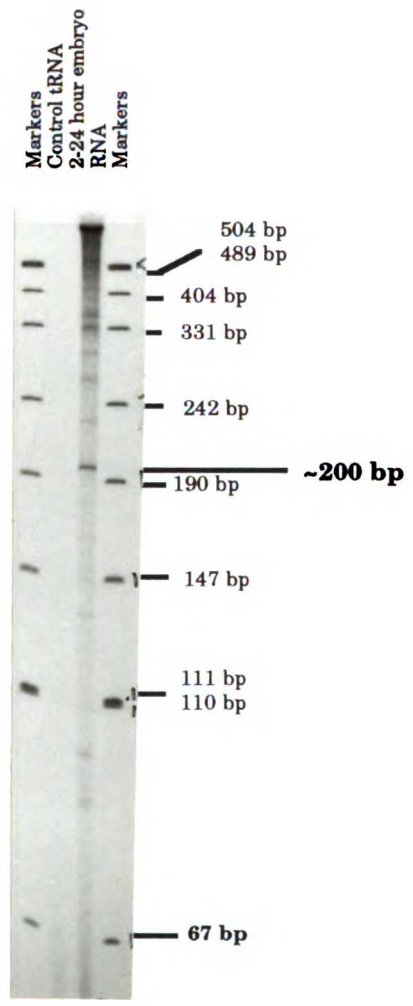ent, and the hybridization reaction was then digested with S1 nuclease. The pattern of protected fragments revealed that the expression pattern of the 2.3 kb mRNA mimics the expression pattern of the 3.3 kb RNA (figure 1.9B). However, the 2.3 kb RNA is expressed at a much lower level than the 3.3 kb mRNA.

Since the two mRNAs are expressed at the same time during development, in situ hybridization experiments on whole mount embryos were done to examine the tissue specific expression of the two mRNAs during embryogenesis. Message specific single stranded DNA probes labeled with digoxygenin substituted dUTP were made to the unique amino terminal coding region of the 3.3 kb mRNA and to the unique 5' untranslated region of the 2.3 kb mRNA (figure 1.10) (Tautz and Pfeifle 1989).

The in situ hybridization analysis of the expression pattern of the two *fer* mRNAs during embryogenesis revealed that both of the *fer* messages are expressed with a few exceptions in the same tissues; in the description below, unless otherwise noted, *fer* expression will refer to the expression of both the 2.3 kb and the 3.3 kb mRNAs. Embryos collected 0-2 hours after oviposition

Figure 1.7
Primer extension analysis of the 2.3 kb
fer mRNA.

Markers
Control tRNA
2-24 hour embryo RNA
Markers

504 bp
489 bp
404 bp
331 bp
242 bp
~200 bp
190 bp
147 bp
111 bp
110 bp
67 bp

Race 1 primer

100 bp to the end of cDNA clone 9C13

Legend figure 1.7:

Primer extension analysis of the 2.3 kb mRNA.

The lanes are labeled in the figure. The bands above the 200 bp band are due to non-specific primings (data not shown). The diagram below the gel shows the position of the Race 1 primer in the *fer* genomic sequence relative to the end of the 9C13 cDNA.

Figure 1.8
**Positions of the 5' ends of RACE clones in the *fer* genomic region
upstream of the 2.3 kb mRNA AUG start codon.**

5' CAGCAGTAATAATAATAATAATAATAAAAATACCAGTAGCAATAGC

AATCACAGTGCCTCACAGTCCACGATAATAACGAGCACGATCACCAC

CACCATAACGACTACAACTACCACGACGCCGTCCAAGGAAAACTCAA

GACTGAAATTCAAAGTGCCCAAGATCCAGAAGAAATCAAAGGCCATC

CGCAATACATTCCGCTCCAAGTTGCTCAATTTCCAGTTGAAGCGGCT

CCAAGCCGTGCAAACAGTGCACCAAGAGACGTCGCATCCATCCCAG

CAAAAGTGTCTTTGATTTTGCCAAAGAGTTCGAGGTGGAACAACCGG

CTGGTTCGGCGGCGGATGAGCAATTCTGCAACTGTCCGCAGCTGGTC
AAAAGCCTGTTAAGCCATCCGTCCAAATATCCGGCCACAAAGATCAC
CCGTTCGAGTCCAGTTCTGGAGAGCTGGACGAGAACTCGGACTGGGA
CACTTGACAACGACGAGGAGGAGGAGGATAGCGCCAGTGACGACGT
GCTCAGCATGAAGGATCATGCTA...3'

Legend figure 1.8:

Positions of the 5' ends of the RACE clones in the *fer* genomic sequence

upstream of the AUG start codon of the 2.3 kb mRNA.

The arrows and the bold face type indicate the positions of the 5' ends of the

RACE clones. The outlined A shows the position of the longest RACE clone,

that may represent the start site of transcription for the 2.3 kb mRNA. The

AUG start codon of the 2.3 kb mRNA is underlined.

Figure 1.9
S1 nuclease protection analysis of the expression of the 2.3 kb and 3.3 kb mRNAs
during *Drosophila* development.

A
The Probe

fer S1 oligo

345 nt.

110 nt. | Protected by the 3.3 kb mRNA

312 nt. | Protected by the 2.3 kb mRNA

B

1 2 3 4 5 6 7   8 9

345 nt ——

——312 nt

——110 nt
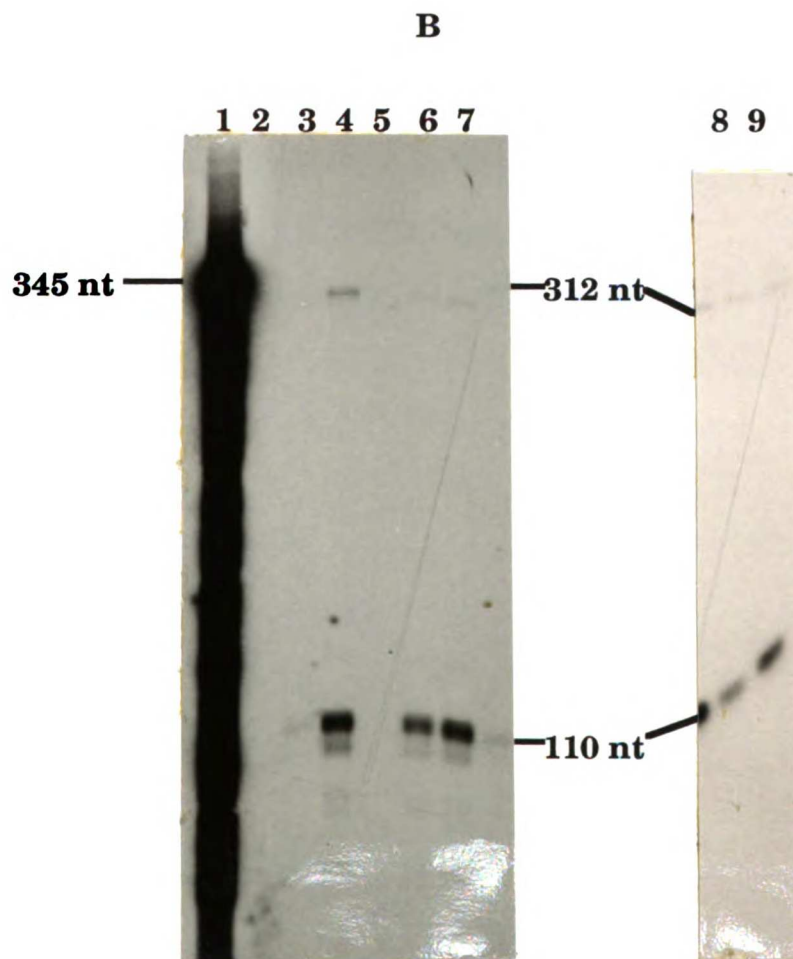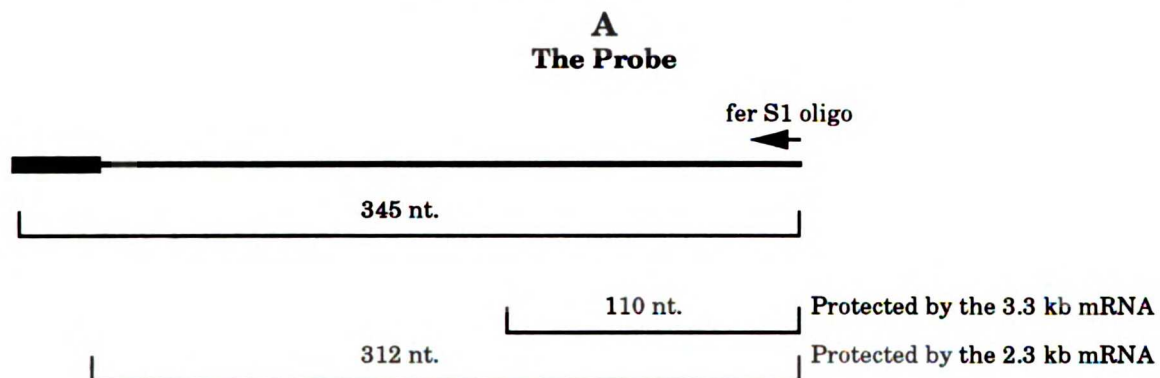
Legend figure 1.9:

S1 nuclease protectionanalysis of the expression of the two mRNAs during the lfe cycle of the fly.

A. Diagram of the S1 probe used in these experiments and the sizes of the fragments protected by the 3.3 kb mRNA and the 2.3 kb mRNA.

B. The S1 nuclease protection analysis.

    Lane 1 Markers

    Lane 2 Probe undigested with S1 nuclease

    Lane 3 tRNA control digested with S1 nuclease.

    Lane 4 0-2 hour embryo poly A+ RNA digested with S1.

    Lane 5 2-24 hour embryo poly A+ RNA digested with S1.

    Lane 6 Third instar larvae poly A+ RNA digested with S1.

    Lane 7 Pupal poly A+ RNA digested with S1.

    Lane 8 Adult male poly A+ RNA digested with S1.

    Lane 9 Adult female poly A+ RNA digested with S1.

The size of the probe alone and the protected fragments are indicated by the arrows.

(hr. a.o.), or those in stages 1-4 as defined by Campos-Ortega and
Hartenstein, showed no *fer* expression in the syncitial blastoderm or in the
cells of the cellular blastoderm (Campos-Ortega and Hartenstein 1985)
(figure 1.11). In 2-4 hr. a.o. embryos,(stages 5-9), the initial events of
gastrulation are starting to occur. Both of the mRNAs were detected at
several sites of morphogenetic movements (figure 1.11). The cephalic furrow
and the mesodermal tube which is formed after the invagination of the
ventral furrow expressed *fer*. In addition, I observed *fer* mRNA in the
aminoproctodeal invagination, with slightly higher expression in the cells of
the proctodeum. The cells of the proctodeum are the primordia of the
hindgut. Throughout the early stages of
embryogenesis, stages 1-9, the two messages are expressed at approximately
the same level.

During stages 10-11 of embryogenesis, or 4-6 hr. a.o., the first
differences in the level of expression between the two mRNAs became
apparent. The 2.3 kb mRNA was expressed at a lower level compared to the
3.3 kb mRNA. The sites of expression , however, continued to be the same for
both messages (figure 1.12). During these stages of development, the
germband elongates, and *fer* message was detected in the mesoderm of the
germband extended embryo. We continued to see expression in the
proctodeum, and *fer* mRNA was now evident in the posterior midgut
primordeum and the anterior midgut primordeum. The primordeum of the
forgut, the stomodeum, is starting to invaginate at the anterior end of the
embryo during this time period, and it was also expressing *fer*. Finally, I

Figure 1.10
mRNA specific probes used for in situ
hybridization to whole mount _Drosophila_
embryos.

3.3 kb mRNA specific probes

450 bp antisense probe

Pst 1   Pst 1

+686   +1749

398 bp sense probe

2.3 kb mRNA specific probes

186 bp antisense probe

Pvu II   ATG^2 NcoI   EcoRI

-166   +74

164 bp sense probe
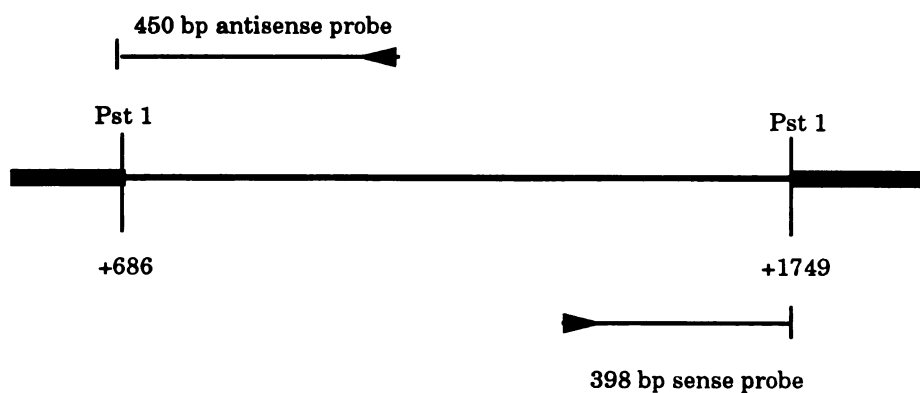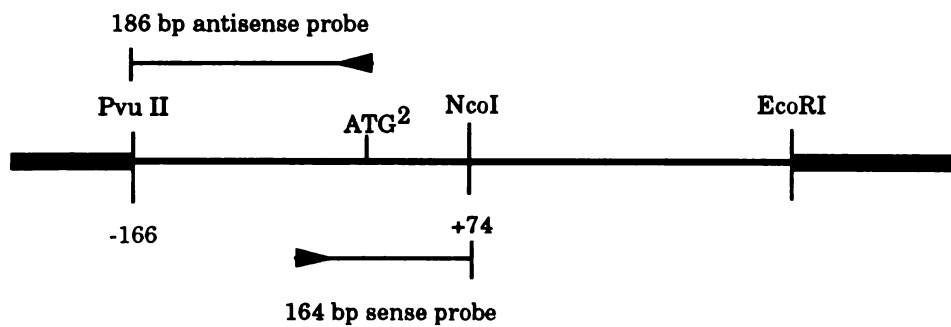
Legend figure 1.10:

The message specific probes used for the in situ hybridization experiments.

(See the methods and materials for details on their synthesis.)

Figure 1.11 In situ hybridization analysis of *Drosophila* whole mount embryos
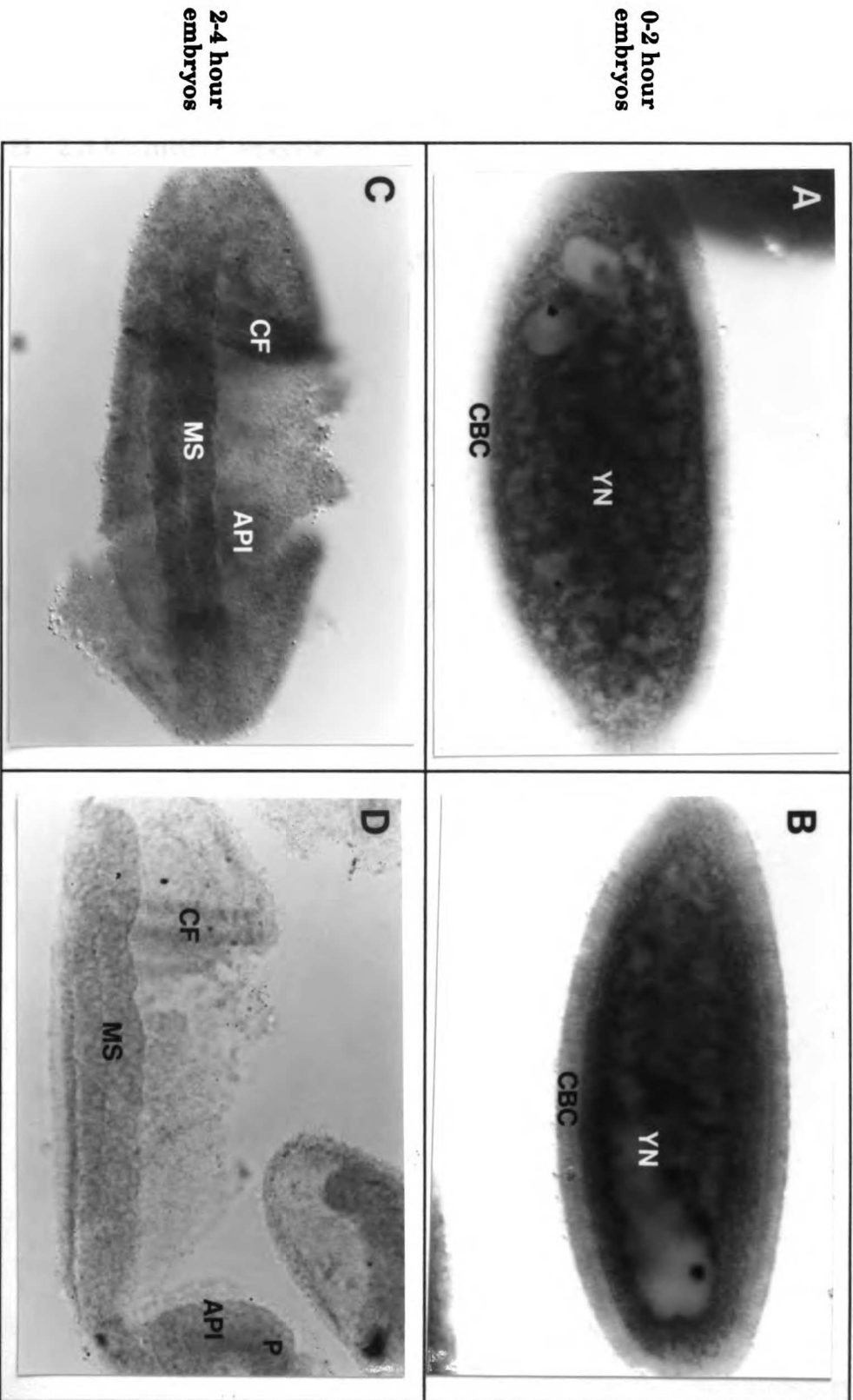
Legend Figure 1.11:

A and B are 0-2 hour embryo insitu hybridizations.

    A. 3.3 kb mRNA specific probe.

    B. 2.3 kb mRNA specific probe.

C and D are 2-4 hour embryo in situ hybridizations.

    C. 3.3 kb mRNA specific probe.

    D. 2.3 kb mRNA specific probe.

Abbreviations: CF, cephalic furrow; MS, mesoderm; API, aminoproctodeal invagination; P, proctodeum; CBC, cellular blastoderm cells; YN, yolk nuclei.

See text for analysis of the expression pattern.

observed *fer* expression in the clypeolabrum, an ectoderm derived structure which will contribute to the formation of the pharynx during stages 10-11.

fer message in the stomodeum, the anterior midgut, and the posterior midgut continued to be observed during embryonic stages 11-13 or 6-10 hr. a.o. (figure 1.12). Overall the expression of the 2.3 kb mRNA was still reduced when compared to the larger mRNA. The mesodermal layer expression of the *fer* mRNAs continued as the mesoderm is divided into the somatic and visceral mesoderm. The former will give rise to the somatic musculature of the larva and the latter will give rise to the smooth muscle of the gut. In the head region of the embryo, mRNA was detected in the clypeolabrum and the dorsal ridge, and there also appears to be expression in the developing mandible and maxilla which will be incorporated into the forgut at a later stage.

By stages 14-16 of embryogenesis (10-14 hr. a.o.) the anterior and posterior midgut primordia have fused to form the midgut. I observed *fer* expression in the newly formed midgut (figure 1.13A). *fer* message was observed in both the visceral muscles of the midgut and the gut epithelial cells. At the junction of the forgut and the midgut *fer* was expressed in a new structure that is forming called the proventriculus. This structure will act as part of the gastric valve. The somatic musculature which is now segmental in appearance, showed expression of the 3.3 kb message and weak expression of the 2.3 kb message. Finally in the head region, *fer* mRNA continued to be observed in the pharynx and the clypeolabrum.

During the final two stages of embryogenesis, stages 16-17, (14-18 hr. a.o.) *fer* mRNA persisted in the forgut, midgut, hindgut, and the proventriculus as shown in figure 1.13B. Overall, the expression in the

Figure 1.12 In situ hybridization analysis of *Drosophila* whole mount embryos
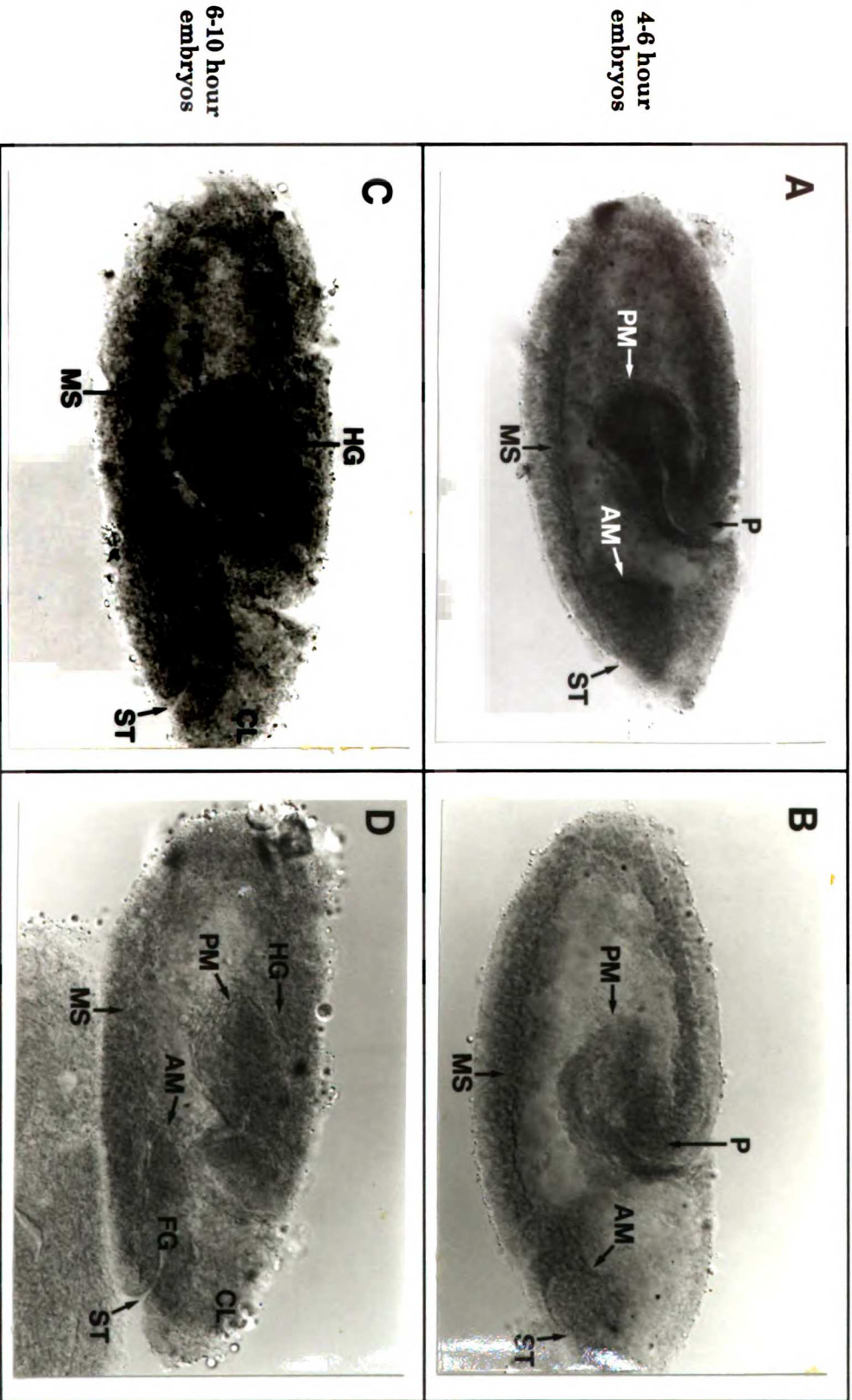
Legend figure 1.12:

A and B are 4-6 hour embryo in situ hybridizations.

    A. 3.3 kb mRNA specific probe.

    B. 2.3 kb mRNA specific probe.

C and D are 6-10 hour embryo in situ hybridizations.

    C. 3.3 kb mRNA specific probe.

    D. 2.3 kb mRNA specific probe.

Abbreviations: AM, anterior midgut primordium; PM posterior midgut primordium; P, proctodeum; ST stomodeum; MS, mesoderm; HG, hindgut; FG, forgut; CL, clypeolabrum.

somatic musculature was reduced with the expression of the 2.3 kb mRNA showing the greatest reduction. In the head region I detected *fer* message in the pharynx, frontal sac, and in a diffuse pattern in the ventral anterior region. One new site of expression was seen during these stages, along the ventral midline of the ventral nerve cord. This site is the only location in the nervous system where *fer* mRNA was detected. In late stage 17 embryos, 18-24 hr. a.o., the expression of *fer* dramatically decreased (figure 1.14). I could not detect the 2.3 kb mRNA and the 3.3kb mRNA was only observed in the ventral midline of the ventral nerve cord. All other expression ceased.

Discussion

The *fer* gene encodes a non-receptor tyrosine kinase related to the *c-fps/fes* family of tyrosine kinases. Initial characterization of the gene identified a 3.3 kb *fer* mRNA that encoded a 92.5 kd protein. I have characterized a second mRNA expressed by the *fer* gene. This message is approximately 2.3 kb and encodes a truncated protein with a predicted molecular weight of approximately 45 kd, p45^{fer}. The gene product has an unusual structure. Although it contains the SH2 and kinase domains of p92.5^{fer}, the amino terminal 423 amino acids are replaced with 10 amino acids. This change in the structure of the amino terminal domain may have a profound effect on the function of p45^{fer}. Although the study of vertebrate *c-fps/fes* and *c-fer* has not provided any insight into the function of the amino terminal domain, studies of the *v-fps* gene have proven to be more informative. There is some evidence that the amino terminal domain of the protein may act to regulate the activity of *v-fps* by controlling the subcellular localization of the protein. A naturally occurring variant of *v-fps* isolated

Figure 1.13A In situ hybridization analysis of *Drosophila* whole mount embryos
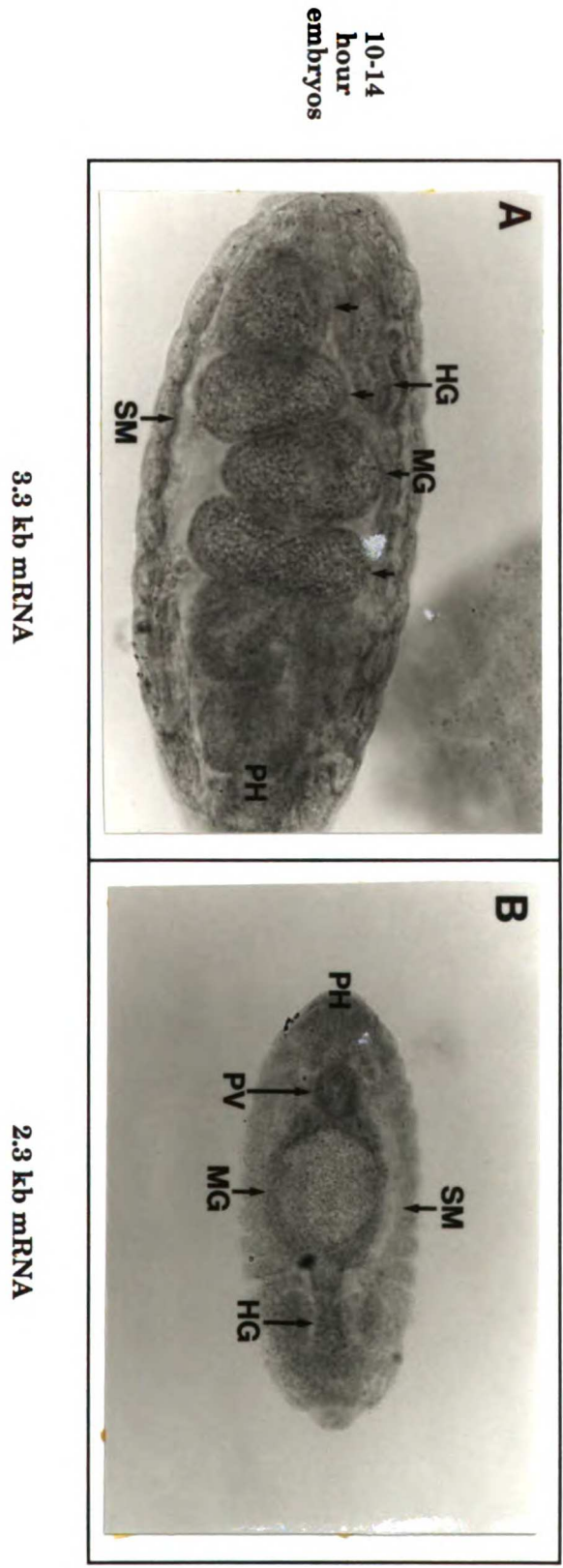
Legend figure 1.13A:

A and B are 10-14 hour embryo in situ hybridizations.

    A. 3.3 kb mRNA specific probe. Small arrows point to the constrictions of the midgut, large arrow to the hindgut.

    B. 2.3 kb mRNA specific probe.

Abbreviations: SM, somatic musculature; HG, hindgut; MG, midgut; PH, pharynx; PV, proventriculus.

Figure 1.13B In situ hybridization analysis of *Drosophila* whole mount embryos

14-18hour embryos
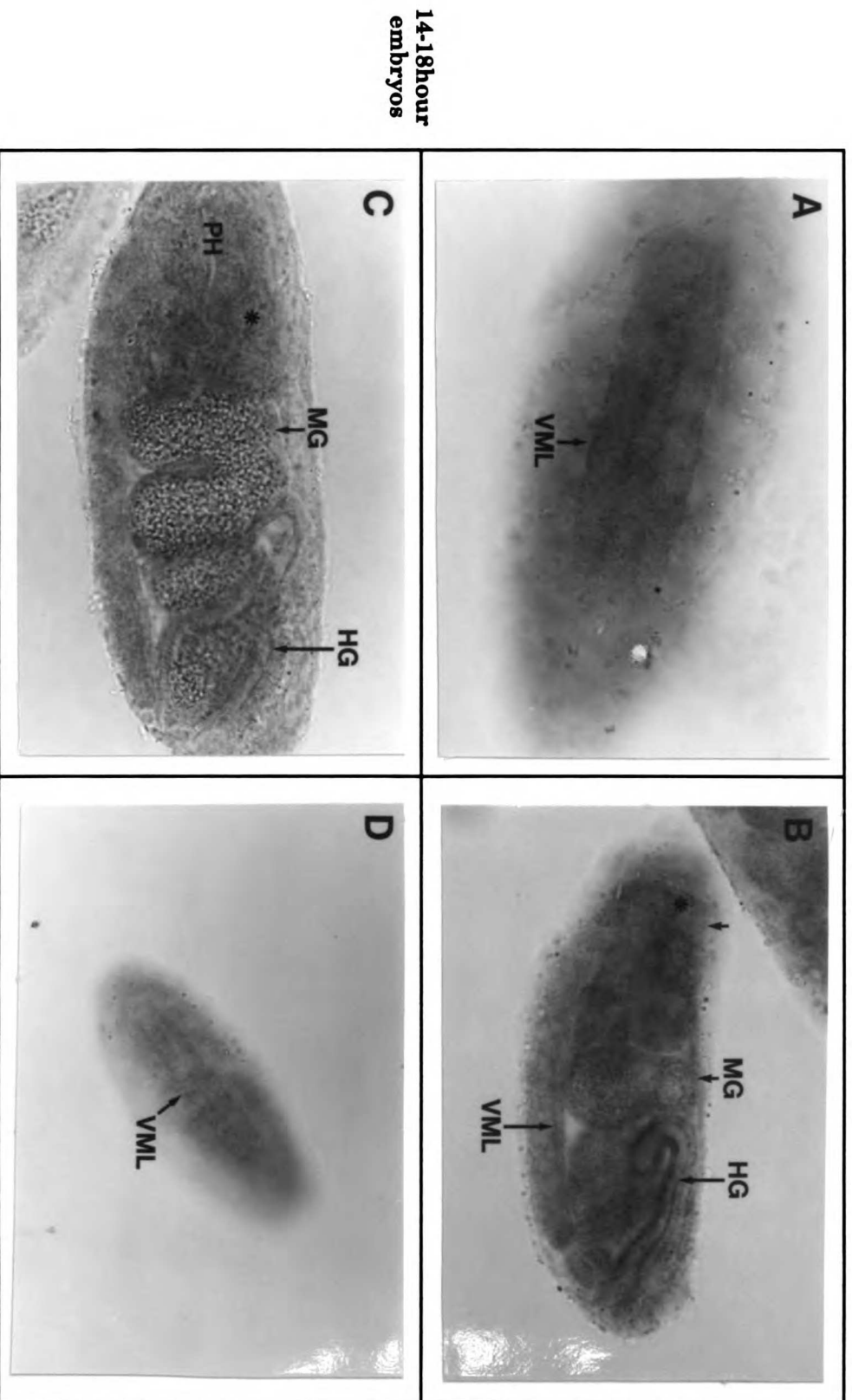
3.3 kb mRNA

2.3 kb mRNA

Legend Figure 1.13B:

A-D are 14-18 hour embryo in situ hybridizations.

    A and B. 3.3 kb mRNA specific probe.

        A. Ventral midline of the CNS expression.

        B. Expression elsewhere in the embryo.

    C and D. 2.3 kb mRNA specific probe.

        C. Expression in the embryo.

        D. Ventral midline of the CNS expression.

Abbreviations: VML, ventral midline of the CNS; PH, pharynx; MG, midgut; HG, hindgut; *, staining in the head region of unidentified tissue.

Figure 1.14 In situ hybridization analysis of *Drosophila* whole mount embryos

18-24 hour embryos
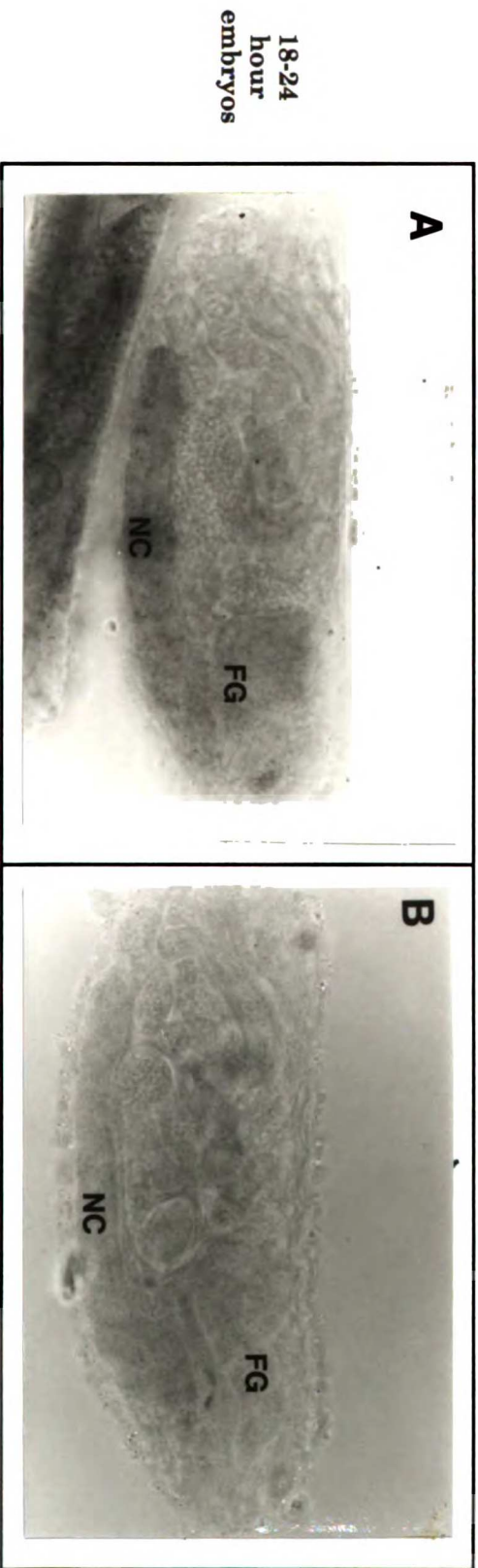
3.3 kb mRNA

2.3 kb mRNA

Legend figure 1.14:

A and B are 18-24 hour embryo in situ hybridizations.

    A. 3.3 kb mRNA specific probe.

    B. 2.3 kb mRNA specific probe.

Abbreviations: FG, forgut; NC, nerve cord.

from the PRCII avian sarcoma virus has allowed researchers to study a *v-fps* gene that is missing most of its amino terminal domain. PRCII *v-fps* contains a deletion of 340 amino acids from its amino terminal domain. In contrast to the potent transforming ability of the *v-fps* gene isolated from the Fujinami sarcoma virus, (FSV), PRCII *v-fps* only causes partial transformation of cells in culture and is weakly tumorogenic in chickens. Although the transformed phenotypes elicited by these two *v-fps* genes is different, biochemical analysis has shown that the two gene products exhibit approximately equal kinase activity. The subcellular localization of the two *v-fps* proteins , however, is very different (Woolford and Beemon 1984). Biochemical fractionation and immunoflorescence experiments revealed that FSV $p130^{v-fps}$ is associated with the plasma membrane in a salt sensitive manner. In contrast, PRCII $p105^{v-fps}$ is not associated with the plasma membrane, but appears to be associated with a dense membrane fraction in a salt resistant fashion (Feldman, Wang et al. 1983; Woolford and Beemon 1984). Since the main difference between the these two proteins is the aminoterminal deletion present in PRCII *v-fps*, these results suggest that this domain may be important for the proper localization of the *v-fps* gene product.

The amino terminal domain of $p92.5^{fer}$ may act as a protein-protein interaction domain to control the subcellular localization of the *fer* protein. Several members of the *src* family of tyrosine kinases have been shown to interact with transmembrane receptor proteins through their unique amino terminal domains. The interaction between *lck* and *CD4* in T cells is a prime example (Shaw, Amrein et al. 1989). If the 92.5 kd *fer* protein interacts with a receptor or a cytoplasmic protein via its amino terminal domain, then the loss of that domain in $p45^{fer}$ would preclude any similar interactions with

other proteins. The spectrum of proteins with which p45^{fer} would interact may therefore be different from that with which p92.5^{fer} would interact.

The *cfps/fes* gene is the prototype gene of a family of non-receptor tyrosine kinases that is conserved in vertebrates . This family also includes the *c-fer* gene, a related tyrosine kinase originally isolated from rat and human, but also found in mice. Expression of *c-fps/fes* is limited to hematopoietic cells of the granulocyte and macrophage lineages, while *c-fer* expression is seen in a wide range of tissues including brain, lung and kidney (Samarut, Mathey-prevot et al. 1985; Pawson, Ltewin et al. 1989). In contrast to *c-fps/fes* that expresses a single mRNA encoding a 92 kd protein, *c-fer* expresses two mRNAs that encode a 94 kd protein and testes specific 51 kd protein (Fischman, Edman et al. 1990). The 92.5 kd *fer* gene product is equally similar to both *c-fps/fes* and *c-fer* gene products. However, *fer* shares several other similarities with *c-fer*. Both of the genes are expressed in a wide range of tissues, and they both express a second mRNA that encodes a truncated form of the protein. On the basis of these similarities it would appear that *fer* may be the *Drosophila* homologue of the mammalian *c-fer* gene. Closer examination of the data reveals that there are some differences between the two genes. Although the *c-fer* genomic region has not been characterized in detail, preliminary characterization of the *ferT* transcript suggests that the organization of *fer* shares some similarity to the organization of the *c-fps* gene (Fischman, Edman et al. 1990). The topography of the *fer* locus, however, is quite different from that of the *c-fps/fes* genes of vertebrates (figure 1.15) (Huang, Hammond et al. 1985; Roebroek, Schalken et al. 1987). The differences between the genomic

structure of *c-fer* and *fer* do not discount the idea that *fer* is the *Drosophila c-fer* gene homologue. Many *Drosophila* genes considered to be homologues of vertebrate genes based on amino acid sequence similarity have different genomic organization.

fer and *c-fer* also differ in the structure of the truncated gene products encoded by the 2.3 kb *dfer* mRNA and the *ferT* mRNA. The amino terminal domain of p45^{fer} is 10 residues in length and begins four residues amino terminal to the start of the SH2 domain, while p51^{ferT} has a new amino terminus of 44 amino acids that begins 36 residues amino terminal to the start of the SH2 domain (Fischman, Edman et al. 1990). The sequences of the new amino acids present in each of the proteins do not share any similarity (figure 1.16). In addition, the expression of the *ferT* transcript is limited to pachytene stage spermatids of post pubescent mice, while the 2.3 kb *fer* transcript is expressed in the same tissues as the 3.3 kb *fer* transcript is expressed. Since we do not understand the function of these truncated proteins encoded by the 2.3 kb *fer* mRNA and the *ferT* mRNA, the significance of these differences between *dfer* and *fer* is not known. The differences may simply represent changes that have occurred since the evolutionary divergence of vertebrates and insects.

The expression pattern of the two *fer* mRNAs during *Drosophila* embryogenesis suggests a role for the *fer* gene in the development of gut and the somatic musculature. *fer* is expressed in cells undergoing major morphogenetic movements during embryogenesis. Early in development both messages are seen in the cephalic furrow, in the aminoproctodeal invagination, and in the invagination of the ventral furrow. Later during embryogenesis both *fer* messages are observed in the cells of the invaginating

Figure 1.15
Comparison of the *Drosophila fer* genomic region
and the vertebrate *c-fps* genomic region.

6 kb

1 kb
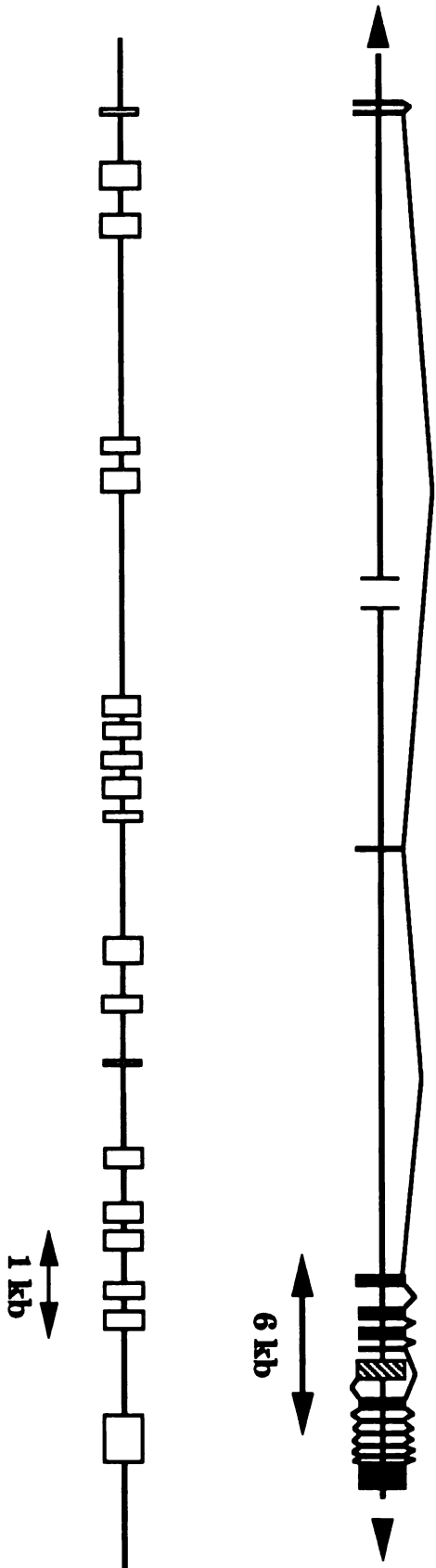
Legend figure 1.15:

Comparison of the intron -exon structure of the *Drosophila fer* gene and the mammalian *c-fps* gene. The scale of each diagram is indicated below the diagram.

Figure 1.16
Amino acid sequence comparison of *Drosophila* p45^{fer} and Murine ferT.

p45
ferT **MDKSMECPHCEGVLEPESDPQFSKKCSIPLSPGPS** (1-35)

p45   MLL (1-3)
ferT **SSEILRYK**RRKERLSKFESIRHSIAGIIKSPKSV* (36-70)

p45 **RAQPGAS** ISLSTNRPLYEEEWFHGVLPREEVVRLL (4-38)
ferT GSS TVCDVISVGE* * *A*HD* Y* * AI * * I * AQE** (71-105)

p45 NNDGDFLVRETI R NE+ESQIVLSVCWNGH+KHFIV (39-73)
ferT KQQ * * * * ** *SHGKPG* Y++* ** * YS D* QRR* * *I (106-140)

p45 QTTGEGNF+RFEGPPFASIQELIMHQYHSEL PVTV (74-108)
ferT * FV++ D* LY* * * *TG*SN*PQ**D *H FNTKQVI *K (141-175)

p45 KSGAI LRRTVC RE+ RWELSNDDVVLLERIGRGNFGD (109-143)
ferT * * *VV*LNPI PKDKK* V*NHE* * S*G* LL*K* * * * E (176-210)

p45 VYKAKLKSTKLDVAVKTCRMTLPDEQKRKFLQEGRI (144-178)
ferT * * * GT* *+ D*TP ** I* * *KE D* *Q* L* I* ** * *AK* (211-245)

p45 LKQYDHPNIVKLIGICVQKQPI MIVMELVLGGSLL (179-213)
ferT * * * * * * * * *** * ***VCT * R* *VY *I * ** *P * *DF* (246-280)

p45 TYLRKNSNGL TTREQMGMCRDAAAGMRYLESKNCI (214-248)
ferT *F ** * RKDEKKLKQLV RF SL* V* * * * L * * ** * * ** (281-315)

p45 HRDLAARNCLVDLEHSVKISDFGMSREEEE++ YIV (249-283)
ferT * * * * * * ** * * * *GENNTL* *** * * * * *Q* DGGV*+S (316-350)

p45 SDGMKQIPVKWTAPEALNFGKYTSLCDVWSYGILM (284-318)
ferT * S* L * *** I * * * *A * * * *Y* R* S*ES * * * *F ** *L (351-385)

p45 WE IFSKGDTPYSGMTNSRARER I DTGYRMPTPKST (319-353)
ferT * *T** L* VC** P* * * *QQ* * *QVE R* * * * SA*QNC (386-420)

p45 PEEMYRLMLQCWAADAESRPHFDE I YNVVDALILR (354-388)
ferT * **VFTI*MK** DYKP*N **K*NDLHKELTVIKKM (421-455)

p45 LDNSH (389-393)
ferT I T   (456-457)

Legend figure 1.16:

Alignment of the amino acid sequences of p45^{fer} and p51^{ferT}. The * denote identities and conserved changes. The new amino acids that make up the unique domains of each protein are underlined with p51^{ferT} in bold type.

stomodeum. There is no evidence to suggest that the *fer* gene products are directly involved in the initiation of these movements or in the movements themselves. Rather it is more likely that they are involved in the development of the structures derived from these morphogenetic movements. The observation that expression of both the *fer* mRNAs persists during the development of the structures derived from the morphogenetic movements supports this hypothesis. After the aminoproctodeal invagination, the invaginating cells give rise to the posterior midgut primordia and the primordia of the hindgut. The *fer* messages are observed in all these tissues. In addition *fer* is expressed in all the tissues that are derived from the ventral furrow, the anterior midgut primordia, the visceral mesoderm, and the somatic mesoderm. In fact the expression in the somatic mesoderm continues until late in embryogenesis after the somatic muscles have made their attachments on the body wall epidermis.

The expression of the two *fer* mRNAs in the developing gut is particularly interesting. *fer* transcripts are first detected as the primordia of the different portions of the gut are formed and continues until the end of organogenesis. During gut development, expression of *fer* is not limited to a particular cell type. Expression is seen in both the gut epithelium, and in the visceral mesoderm that will form the visceral musculature of the gut. Furthermore, *fer* mRNA is not limited to a particular germ layer. The gut epithelium is derived from both the ectoderm and the endoderm, and the visceral muscles are derived from the mesoderm (Campos-Ortega and Hartenstein 1985). Since *fer* mRNA is not limited to any cell type or to a particular germ layer, *fer* may be involved in a signaling process that is common to all these tissues. Analysis of the embryonic phenotype of *fer*

mutants that we have recently isolated may give some clue to its function during gut development.

Unlike the *fer* expression during the development of the gut and somatic musculature, the expression of the two *fer* messages along the midline of the ventral nerve cord is first observed after this structure is already formed. The midline is a specialized region that plays a key role in the axonal guidance and the formation of the axonal commissures in the central nervous system (Klambt, Jacobs et al. 1991). The expression of *fer* in the cells of the ventral midline does not start until late during embryogenesis, stages 16-17, at a time when the pattern of commissures in each segment is already formed. Most of the genes that affect the development of the ventral midline are expressed much earlier than stage 16. It is possible that the function of this late expression of *fer* may be to finish the differentiation process or perhaps *fer* may play role in the normal functioning of the larval nervous system.

One striking observation about the expression pattern of the two *fer* mRNAs is that both of the genes appear to be expressed in the same tissues at the same time. If my hypothesis is correct that the 2.3 kb *fer* mRNA is expressed from a second promoter, then the two promoters must be coordinately regulated. The in situ hybridization experiments also suggest that the two gene products function in the same cells. The two proteins may act coordinately in signal transduction or one of the proteins may control the function of the other. The elucidation of the functions of these two *fer* gene products will have to wait until mutations that remove one of the gene products or the other can be identified, and their phenotypes studied.

Chapter 2

Isolation and characterization of mutations in the *fer* gene

Abstract

The vertebrate *c-fps/fes* gene is the prototype of a family of non-receptor tyrosine kinases. Very little is known about the mechanism of action of these kinases or the physiological function of this family of tyrosine kinases during development. The *fer* gene of *Drosophila melanogaster* encodes a non-receptor tyrosine kinase most closely related to the *c-fps/fes* family of non-receptor tyrosine kinases. The identification of this new member of the *c-fps/fes* family in *Drosophila* permits us to use genetic analysis to investigate the function of *fer* during *Drosophila* development. We have identified an enhancer trap line, E134, that contains a P element insertion into *fer*. Using this P element insertion line, we have isolated a *fer* mutant complementation group that contains two X-ray induced mutations and one P element induced imprecise excision mutation. Two members of this complementation group have rearrangements in the *fer* gene. Both of these rearranged alleles, fer^{X42} and $fer^{P35.3}$, do not make full length $p92.5^{fer}$ protein. Depending on the combination of alleles, the mutations are semi-lethal, with 25-50% of the expected mutant progeny surviving to adults. The lethal period is between the late larval stage and the pupal stage. Analysis of the mutant adults that survive revealed that the tissues affected by the mutations correlate with the sites of *fer* expression. The mutant adults are missing one or two macrochaete, the large mechanosensory bristles on the head and thorax of the fly, and they have rough eyes, that lack the normal number and the normal spacing of interommatidial bristles. In addition the development of the thoracic muscles is disturbed. In eclosed mutant adults, the structure of the indirect flight muscles is abnormal, and pharate adults of strong alleles of *fer* show a disruption of the development of the thoracic muscles. Further

characterization of these mutants will help us to identify the cellular processes in which *fer* plays a role. These mutant alleles can also be used to identify second site mutations that enhance or suppress the *fer* mutant phenotype. The characterization of these second site mutations will provide insight into the mechanism of *fer* function, which in turn may increase our understanding of the function of the *c-fps/fes* family of tyrosine kinase in vertebrates.

Introduction

Non-receptor tyrosine kinases (NRTKs) were first identified as retroviral oncogenes isolated from acutely transforming retroviruses. This class of tyrosine kinase possesses several characteristic features that distinguish NRTKs from the receptor class of tyrosine kinases. The most obvious feature is that the NRTKs do not contain transmembrane domains, and are therefore cytoplasmic in localization. In fact, not only have NRTKs been shown to be localized in all areas of the cytoplasm, including the cytoplasmic side of membranes, but they have also been shown to be localized in the nucleus (Van Etten, Jackson et al. 1989). In addition to the kinase domain, all NRTKs contain a non-catalytic regulatory domain called SH2, that is present either by itself or in combination with a second domain called SH3 (Pawson and Gish 1992). The SH2 domain binds phosphotyrosine and is thought to be important in the binding of substrates and regulatory molecules to the kinase domain. SH3 domains have been implicated in the interaction of proteins with cytoskeletal elements.

Unlike receptor tyrosine kinases which are activated upon the binding of a ligand, the mechanism of activation is understood for only a few NRTKs

(Ullrich and Schlessinger 1990). Some NRTKs have been shown to interact with the cytoplasmic tails of receptors that lack enzymatic activities. The binding of the ligand by these receptors is thought to transmit a signal to the tyrosine kinase associated with it, activating the kinase activity. One member of the *src* family of NRTKs, *lck* interacts with the cytoplasmic tails of the CD4 and CD8 receptors in T cells (Shaw, Amrein et al. 1989). Crosslinking of CD4 at the cell surface causes an increase in lck kinase activity. Similarly, another member of the *src* family, *fyn*, has been shown to interact with the T cell receptor CD3 complex (Gassmann, Guttinger et al. 1992). Crosslinking of CD3 complex results in an activation of fyn kinase activity. However not all NRTKs have been shown to associate with receptors, and the mechanisms by which they are activated are still unknown.

Although the mechanism of activation of NRTKs is not well understood, several NRTKs have been shown to play key roles in signal transduction. The binding of antigen by the T cell receptor stimulates T cells to proliferate and to carry out differentiated functions. The rapid tyrosine phosphorylation of proteins that occurs after the binding of antigen by the T cell receptor complex is thought to initiate a signal transduction cascade that results in the activation of T cell responses. T cell lines that lack *lck* are unable to respond to antigen binding by their T cell receptor and are not induced to differentiate (Straus and Weiss 1992). Furthermore, over expression of an activated form of *lck* kinase causes the cells to become hypersensitive to stimulation through the T cell receptor (Abraham, Miceli et al. 1991). Similarly, the thymic isoform of the *fyn* tyrosine kinase gene is also involved in the induction of responses caused by antigen binding to the T cell

receptor. The expression of a kinase defective *fyn* gene product acts as a dominate negative mutation, blocking the response of the cells to T cell receptor ligands (Cooke, Abraham et al. 1991). Over expression of *fyn* in T cell lines also causes an enhanced response to T cell receptor ligands (Cooke, Abraham et al. 1991). Therefore it appears that two NRTKs are involved in the signaling pathway that results in the stimulation of T cell responses after antigen binding.

The response of cells to interferon a and ß has recently been shown to be mediated by a NRTK. A mutant cell line that is unable to respond to interferon alpha treatment has been shown to have a defect in the *tyk2* tyrosine kinase (Velazquez, Fellous et al. 1992). There is good evidence to suggest that the induction of gene expression by interferon may involve the direct phosphorylation of ISGF 3a transcription factor complex by the tyk2 kinase (Fu 1992).

In order to investigate the physiological role of NRTKs during vertebrate development several NRTK genes have been mutated in mouse embryonic stem cells, and the phenotype of homozygous mice derived from these stem cells has been analyzed. Mice lacking either *fyn* or *lck* have phenotypes that affect the differentiation of immature T cells in the thymus (Appleby, Gross et al. 1992; Molina, Kishihara et al. 1992; Stein, Lee et al. 1992). These observations suggest that stimulation of the T cell receptor complex that occurs during thymocyte maturation requires functional *lck* and *fyn* genes. Although the numbers of mature T cells in both the *lck* and the *fyn* mutant mice is greatly reduced, mature T cells are observed in the peripheral blood. As expected, the response of these mutant T cells to antigen binding is reduced, however, the presence of the mutant T cells in

these mice suggests that there are additional mechanisms not dependent on *lck* or *fyn* involved in thymocyte maturation and in signaling through the T cell receptor. Two other NRTKs, *src* and *abl*, have also been mutated in embryonic stem cells and mice homozygous for the mutations have been generated (Schwartzberg, Stall et al. 1991; Soriano, Montgomery et al. 1991). Based on their ubiquitous expression pattern, and the ability of retroviral alleles of *src* and *abl* to transform cells in culture, these two tyrosine kinases were thought to play key roles in cell proliferation. The phenotypes of the homozygotes proved to be much less severe than what were expected. The *src⁻* mice suffer from osteopetrosis, which appears to be caused by a defect in osteoclast function. No other tissues are affected including those tissues like platelets and the brain that express high levels of *src*. Homozygous *abl* mutant mice survive to birth, but exhibit reduced viability and a depletion of certain populations of B and T cells. This phenotype is variable, despite the fact that the *abl* mutation is a null mutation. The unexpected phenotypes of the *src⁻* and *abl⁻* mice reveal a underlying problem with this type of genetic analysis, the problem of genetic redundancy. The phenotypes observed in the mutants reflect the lack of kinase activity in the tissues most sensitive to the loss of tyrosine kinase function, while the role of these kinases in other tissues is masked by the presence of redundant signal transduction pathways.

The well established genetic strategies for studying gene function during development in *Drosophila melanogaster* make *Drosophila* an ideal organism for studying the physiological function of NRTKs. The ability to isolate second site mutations that enhance the phenotype of NRTK mutants will help to identify genes involved in redundant signaling pathways. This

work will enable us to identify all the functions of NRTKs in various tissues.

Four NRTK homologues have been identified in *Drosophila*, *abl*, *src64B*,

src29A, and *fer* (Hoffman-Falk, Einat et al. 1983; Simon, Drees et al. 1985;

Gregory, Kammermeyer et al. 1987; Katzen, Monterras et al. 1991). Until

recently, mutant alleles had been identified in only the *Drosophila abl*. Much

like the mouse *abl* mutation, mutations in the *Drosophila abl* gene result in

a subtler phenotype than would have been predicted from the gene's

expression pattern. *abl* mutant flies die as pupae, but some adults eclose

with combinations of weaker alleles. These mutant adults have rough eyes

and die after a few days. Despite the fact that *abl* is expressed at high levels

in the developing central nervous system (CNS), the mutant flies show no

major disruptions in nervous system development or in the development of

any other tissues where abl is expressed. Although *abl* is necessary for

viability, other signaling pathways may compensate for loss of *abl* function

during the development of the CNS and other tissues in the *abl* mutant flies.

Further genetic analysis has identified mutations in several genes that

enhance the abl mutant phenotype (Gertler, Bennett et al. 1989; Gertler,

Doctor et al. 1990; Hoffmann 1991; Gertler, Hill et al. 1993). One of these

enhancers is called *disabled* (*dab*). *abl* mutant flies that are heterozygous for

mutations in the *dab* exhibit late embryonic lethality, and show a severe

disruption of the CNS. The characterization of the *abl* mutant phenotype in

the presence of one of the enhancers of *abl* has allowed researchers to identify

roles for the *abl* gene product that were not apparent in the *abl* mutant flies

because of redundant signaling pathways (Hoffmann 1991).

In this chapter, we report the isolation of mutations in the *fer* gene.

Previously, we reported that *fer* encodes a NRTK related to the *c-fps/fes* and

fer family of NRTKs. This report represents the first characterization of mutations in this family. The *fer* gene is expressed throughout *Drosophila* development with the highest expression during embryogenesis seen in the developing gut and somatic musculature. During the larval stages, *fer* expression is seen in the eye antennal disc behind the morphogenetic furrow in the developing ommatidia and in all the imaginal discs. Later, during pupal development, expression is seen in all the muscles and in the optic lamina of the brain. In adults, *fer* expression is limited to the gut, the retina, and the testes and ovaries. Characterization of the phenotype of the *fer* mutants has revealed that the mutations are semi-lethal. The adults that do eclose have defects that correlate with the sites of *fer* expression. The mutant flies have rough eyes that lack the normal number and spacing of the interommatidial bristles. The mechanosensory bristles on the head and thorax of the fly, the macrochaete, are also affected. Mutant adults often lack one or more of these bristles. The thoracic muscles of eclosed mutant adults show a disrupted structure and in pharate adults the structure of these muscles is severely disorganized. Other functions for *fer* may come to light when the study of mutations that interact with *fer* can be identified and characterized.

Results
Identification of a P element insertion into *fer*.

The region of the third chromosome where *fer* is located has not been very well characterized genetically. Very few mutations map to this region, and none of the deficiency chromosomes in the region remove *fer* (data not shown). Therefore a classical genetic screen to isolate mutations that are

uncovered by a deficiency chromosome for the region surrounding a gene of interest was not possible. Since I knew where *fer* was located on the third chromosome and the expression pattern of the gene during development, I sought to obtain enhancer trap P element insertions that mapped to this region and expressed ß-galactosidase (ß-gal) in a pattern similar to the expression pattern of *fer* mRNA. During larval development *fer* mRNA is detected in the eye antennal disc behind the morphogenetic furrow in the developing ommatidia (Katzen, Monterras et al. 1991). We obtained three enhancer trap lines from Dr. Gerry Rubin at UC-Berkeley that were generated in a screen to identify genes expressed in the eye disc behind the morphogenetic furrow. All three lines show a pattern of ß-gal expression in the eye antennal disc similar to the pattern seen for *fer* mRNA in the eye disc, and their P element insertions map to the same region on the right arm of the third chromosome that *fer* maps, 85D. Southern blot analysis of these lines showed that one line, E134, contained an insertion into the second intron of the *fer* gene (figure 2.1). The P element insertion site is approximately 1.4 kb downstream of exon 2 (figure 2.1). The other two lines do not have insertions anywhere in the *fer* locus (data not shown). E134 homozygous adults are wild type in phenotype, and express *fer* mRNA at wild type levels (data not shown). These observations are consistent with the idea that the P element insertion in line E134 does not disrupt the *fer* gene.

Isolation of mutations in the *fer* gene.

Since the P element that is inserted into the *fer* gene expresses the *white* gene, we can use the *white* gene as a genetic marker for the *fer* gene.

Figure 2.1
Map of the P element insertion site in Line E134
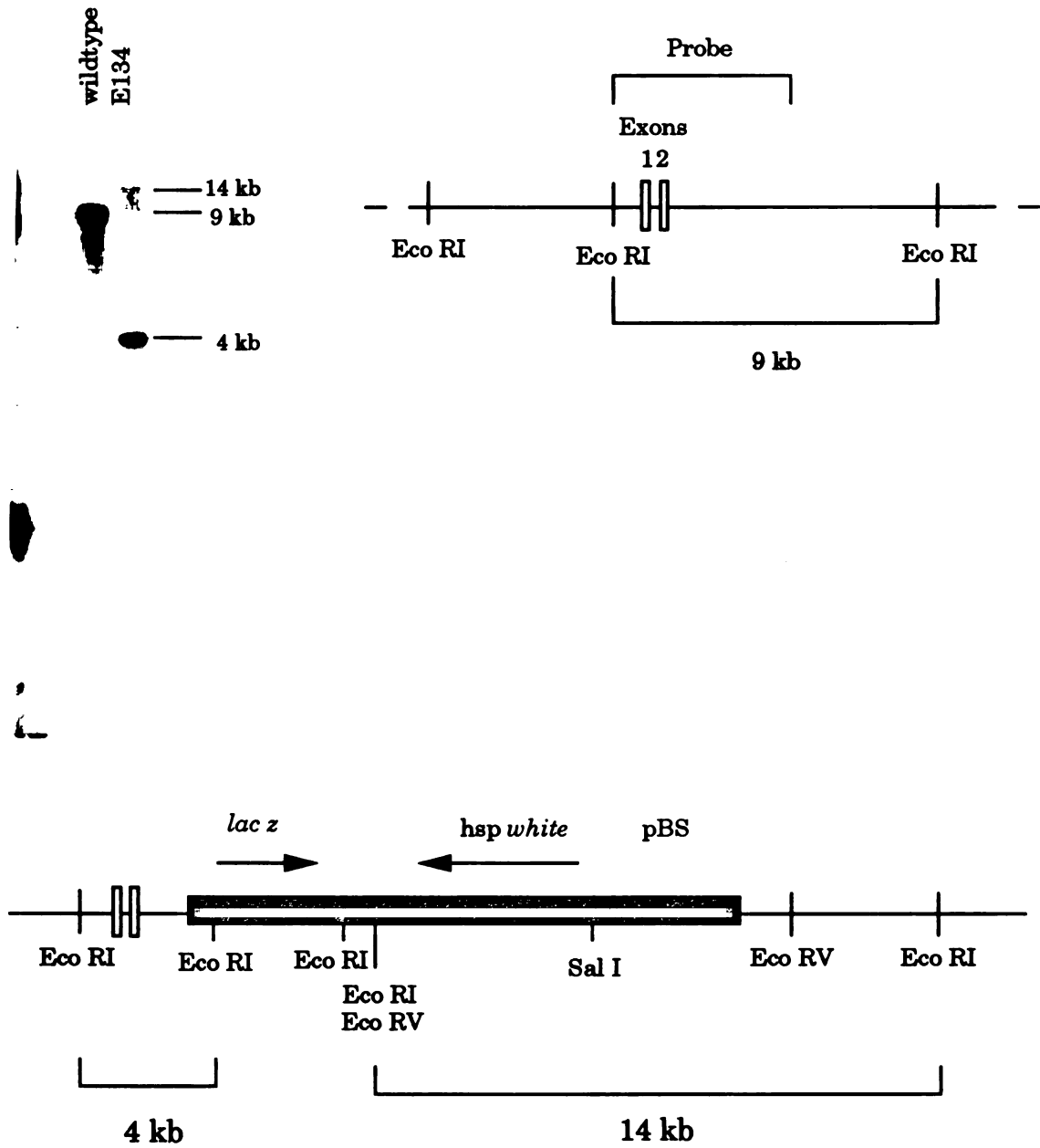
Legend figure 2.1:

Map of the Pelement insertion site in line E134.

The Southern blot is of an EcoRI digest of genomic DNA isolated from Line
E134 and wild type DNA. Theprobe used is indicated to the right of the blot.
A map of the P element insertion site is shown below.

By screening for mutations that disrupt *white* , we were able identify mutations that potentially would disrupt *fer*. In our initial mutagenic screen, we used X-rays as a mutagen in order to maximize the probability of inducing deletion and rearrangement mutations that would include both *white* and *fer*. We mutatgenized the E134 line with X-rays, and screened the progeny for loss of the *white* (figure 2.2). 36500 chromosomes were screened and 45 white eyed lines, 1 red eyed and 3 lines that showed variegated eyes were isolated. Three lines failed to establish permanant lines. All 46 of the mutant lines that we recovered carry a lethal mutation and were maintained over the TM3Sb balancer chromosome.

All the mutant lines were analyzed by Southern blot analysis for rearrangements or deletions of *fer* locus, using probes made to the cloned regions of the locus (data not shown). In addition, we tested all the mutant lines for rearrangements or deletions in the P element by probing Southern blots with a probe for the ß-gal gene (data not shown). Eight white eyed lines in these initial experiments appeared to have a rearrangement of the P element sequences. Only one of the mutant lines, E134^{X42} ,showed a rearrangement of *fer* locus 3' to the P element insertion site. Although, we might have expected to generate a large deletion of the P element insertion site and the surrounding genomic DNA, none of the original 46 mutated lines recovered from this screen contained a large deletion.

The eight white eyed lines that showed a rearrangement of the P element sequences and the variegated line E134^{X42} were characterized more carefully for mutations in *fer* by Southern blot analysis. Since the variegated eye phenotype exhibited by these lines indicates that they may contain a rearrangement that has moved the *white* gene of the P element to

Figure 2.2
X-ray Mutagenesis

X-rays

♂♂ w ; $\dfrac{\text{E134}}{\text{E134}}$ X ♀♀ w ; $\dfrac{\text{D}}{\text{TM3Sb}}$

♂ w ; $\dfrac{\text{E134}^*}{\text{D}}$

w ; $\dfrac{\text{E134}^*}{\text{TM3Sb}}$ X ♀ w ; $\dfrac{\text{D}}{\text{TM3Sb}}$

white eyed
mutants

w ; $\dfrac{\text{E134}^*}{\text{TM3Sb}}$ Establish lines
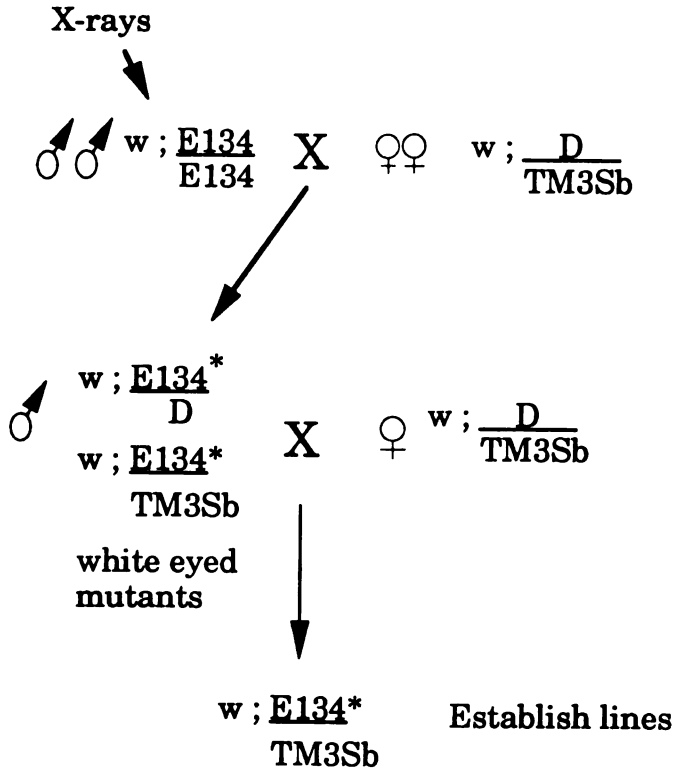
Results

36500 chromosomes screened

43 white eyed lines

3 variegated lines

3 lines failed to establish permanant lines

Legend Figure 2.2:

X-ray mutagenesis scheme.

Male E134 flies were irradiated with 4500 rads of X-rays. Potential mutants were isolated as shown.

heterochromatin, and this rearrangement may have rearranged the *fer* locus, the two other variegated mutant lines were further characterized (Spofford 1976). Subsequent analysis of the eight white eyed lines showed that the P element had been deleted and the wild type restriction fragment pattern had been regenerated (data not shown). It appears likely that the band detected by the ß-gal probe in the initial experiments was due to a contamination of the genomic DNA with plasmid DNA. I have mapped two rearrangement breakpoints in the E134^{X42} line. One breakpoint was mapped to a 9 kb restriction fragment near exon 3, and the second was mapped to a 226 bp interval in the alternate exon (figure 2.3). The analysis of the other two variegated lines, E134^{X8} and E134^{X44}, showed that in both lines the P element was intact and there were no other rearrangements or deletions in the *fer* locus, however (data not shown).

Based on the Southern blot analysis, it appeared that at least one line, E134^{X42} contained a potential *fer* mutation. Since I could not rule out that the other lines did not contain *fer* mutations, I intercrossed all eleven lines in order to group them into lethal complementation groups (table 2.1). The eleven lines fell into five lethal complementation groups. The largest group, group I, contained six members all of which are white eyed lines. The next largest group, group II, included E134^{X42} , the only line to show a rearrangement of the *fer* gene, and a second variegated line, E134^{X8}. The other three groups had only one member each.

The complementation analysis of the eleven lines did not simplify the identification of a *fer* mutation. Because we lacked a deficiency chromosome that removes the *fer* gene, the characterization of a loss of function complementation group was very difficult. The identification of two

Figure 2.3
Mapping rearrangements in Line E134^{X42}

Probes

E134^{X42}/TM3Sb
Wildtype

1

E134^{X42}/TM3Sb
Wildtype

2

probe 1

probe 2

P Element

Sites of rearrangement breakpoints
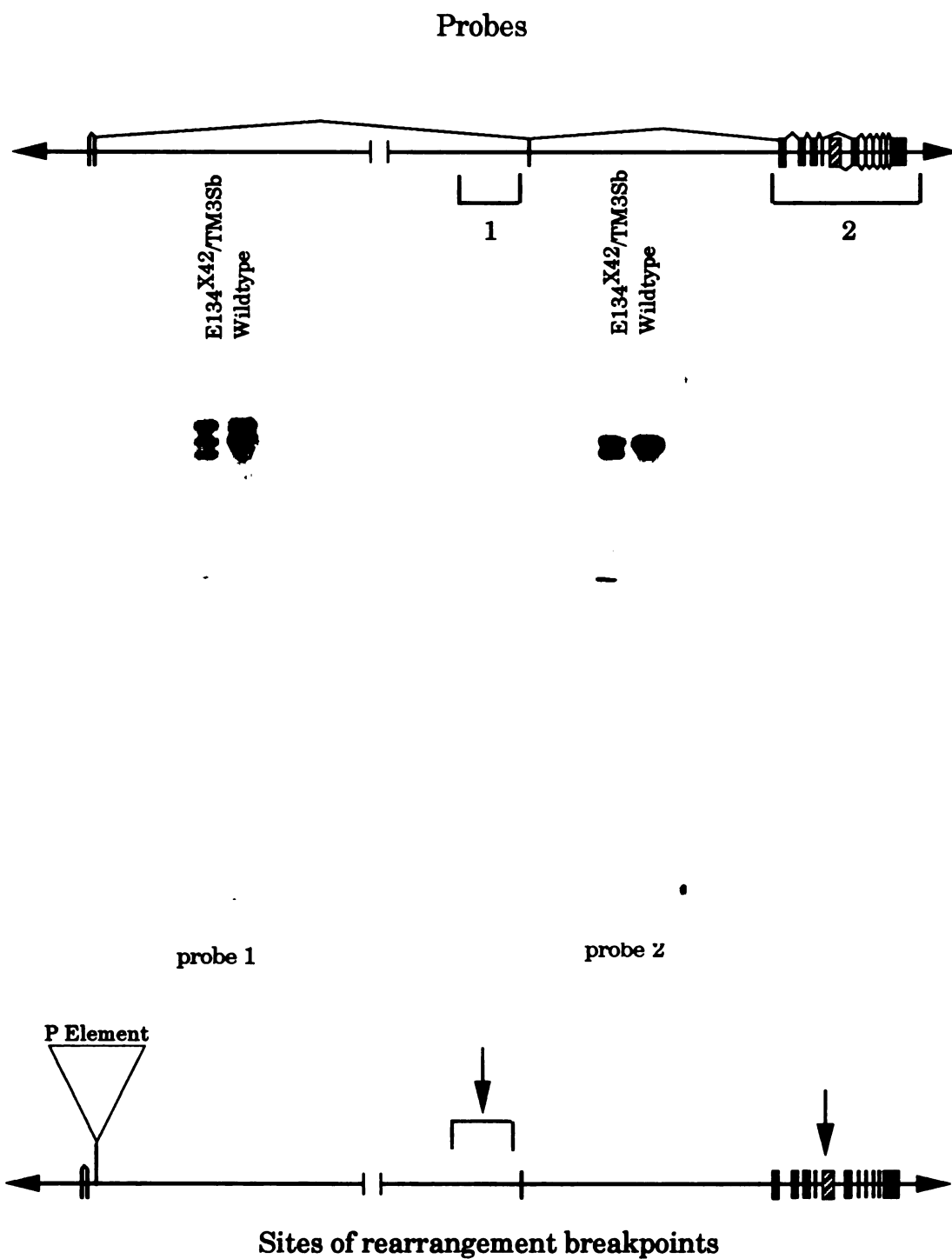
Table 2.1

Analysis of the mutant lines from the X-ray mutagenesis.

Complementation group	Members	Eye color	P element	Rearrangements in *fer*	p92.5fer
I	E134X7 E134X12 E134X15 E134X18 E134X27 E134X47	White	Absent	None	Yes
II	E134X8 E134X42	Variegated	Present	None detected in E134X8 2 Breakpoints in E134X42	? ~68 kd
III	E134X26	White	Absent	None	Yes
IV	E134X30	Red	Present	None	Yes
V	E134X44	Variegated	Present	None	Yes
The 35 other X-ray mutant lines		White	Absent	None	Not tested

Legend figure 2.3:

Mapping the rearrangements of the *fer* gene in line E134^{X42}.

At the top a schematic of the *fer* locus is shown with the positions of the two probes that detected rearrangements indicated. The left hand Southern blot is an ECORI-BamHI digest of genomic DNA probed with probe 1. The right hand Southern blot is a BamHI digest of genomic DNA and is probed with probe 2. At the bottom of the figure is a map of the sites of the rearrangement breakpoints.

breakpoints in *fer* in line E134^{X42} strongly suggested that group II was the *fer* mutant complementation group. Although the other member of this group, E134^{X8} did not have any detectable rearrangements in *fer,* the variegated eye phenotype implied that the E134^{X8} chromosome had sustained a rearrangement that had moved the *white* gene to heterochromatin. The breakpoints for this rearrangement must occur either outside the *fer* locus or in the regions of the locus that we have not yet cloned. Although, we cannot discount the possibility that all the other lines could contain undetectable mutations and therefore would also represent *fer* mutant alleles, we feel that since group II contained the only line that had a detectable rearrangement of the *fer* gene, this group was the best candidate for the *fer* lethal complementation group.

Characterization of the expression of *fer* mRNA and protein in complementation group II.

The identification of a rearranged *fer* gene in line E134^{X42} suggested that this chromosome might be defective for the production of *fer* mRNA and protein. Northern blots of RNA isolated from heterozygous and homozygous E134^{X42} flies were hybridized with a *fer* cDNA probe. For both the heterozygous and the homozygous E134^{X42} RNAs the *fer* probe detected a smear that was approximately the size of the 3.3kb *fer* mRNA (data not shown). From these data I was unable to determine whether the homozygous E134^{X42} produced an aberrant transcript. Since the analysis of the mRNA expression was not useful, Karin Immergluck analyzed line E134^{X42} for expression of p92.5^{fer}. Fortunately, E134^{X42} is only semi- lethal, and approximately 50% of the homozygous adults eclose and survive. These adults are fertile, and with careful maintenance a stock of homozygous flies

can be propagated. From this stock, homozygous E134^{X42} embryos were collected. Protein extracts derived from these embryos were run on SDS polyacrylamide gels and transferred to nitrocellulose. The blots were probed with antibodies raised against either the unique amino terminal domain or the SH2 domain of p92.5^{fer}. These Western blots revealed that the E134^{X42} does not make full length p92.5^{fer}. The SH2 antisera, however, did detect an ~ 68 kd protein that may represent a truncated mutant gene product. Karin has not been able to identify the gene product of the second form of *fer* mRNA, p45^{fer}, on western blots, and consequently we do not know whether E134^{X42} expresses p45^{fer}. It has not been determined whether line E134^{X8} expresses p92.5^{fer}. The absence of full length protein in the E134^{X42} line supports our assertion that the rearrangement observed in line E134^{X42} disrupts the *fer* gene, and that E134^{X42} in fact has a mutation in the *fer* gene.

In addition, Karin also analyzed the expression of p92.5^{fer} in the four other complementation groups. Since each of the complementation groups contains a lethal mutation, Karin was not able to analyze homozygous embryos from these lines. In order to alleviate this problem, she crossed each of the lines into the E134^{X42} background. The transheterozygous progeny were then mated to one another and the embryos were collected. Since E134^{X42} does not make full length protein and we presume that both mutant chromosomes will contribute equally to the protein derived from these embryos, Karin was able to use these embryos to determine whether the members of the four other complementation groups made full length *fer* protein. All nine of the lines that make up the four other complementation groups were positive on a western blot for full length *fer* protein. Because

these complementation groups do express full length *fer* protein, it is unlikely that they represent mutations in *fer*.

If the four other complementation groups are not *fer* mutations , then why were they isolated in the X-ray mutagenesis? Since the original E134 line was not isogenized prior to the X-ray mutagenesis, it is possible that a spontaneously occurring lethal mutation could be present in a small proportion of the stock. The mutant lines that make up the other complementation groups probably represent E134 chromosomes that have deleted the P element due the X-ray mutagenesis and carry a spontaneous lethal mutation. The breakpoints of X-ray induced mutations often occur at repeated sequences, therefore the apparent precise deletion of the P element in the white eyed stocks might have occurred because the P element ends are repeat sequences. The complementation groups that have only one member may have resulted from two mutagenic events on the third chromosome. One event deleted the P element sequences and the other event caused a second lethal mutation not in the *fer* gene. The second lethal would have to be linked to *fer*, since all the eleven lines that make up the five complementation groups were outcrossed to wild type flies to remove unwanted mutations.

Using P element mediated transformation to rescue the phenotype of complementation group II

Since the exact structure of the rearrangement that includes the *fer* gene in line E134^{X42} is not known, we must consider the possibility that other genes are also rearranged. If this is the case, the phenotype exhibited by E134^{X42} homozygotes and E134^{X42}/E134^{X8} transheterozygotes may not be due solely to a mutation in *fer*. These phenotypes might be caused either

by mutations in other genes or by a combination of mutations in *fer* and these other genes.

In order to confirm that complementation group II represents the *fer* complementation group, I attempted to rescue the phenotype of this group by introducing a wild type copy of the *fer* gene into the group II mutant lines via P element mediated transformation. Because the *fer* gene is very large, >50 kb, the frequency of transformation using a P element containing the entire *fer* gene would be too low to be practical. In order to get around this problem, a minigene was constructed. The minigene replaces the genomic sequence from exon 2 through exon 5 with cDNA sequences from these exons (figure 2.4). By removing introns 2, 3, and 4, I can eliminate >39 kb of the *fer* locus, and the resulting minigene is only 14 kb. The 5' end of the minigene construct contains approximately 6 kb of sequence upstream of the transcription start site, while the 3' end of the construct is approximately 1 kb downstream of the poly adenylation site in the *fer* gene. To facilitate the cloning of the cDNA fragment into the minigene, a new Xba1 site was introduced into the 5' untranslated sequence upstream of the ATG start codon located in exon 2. This new site allows me to monitor the expression of the minigene in the transformed flies.

A P element carrying the minigene, and called P[fer2345], was injected into Df(1) w^{67c23} embryos. One transformed line was obtained from about 1000 injected embryos. The P element insertion in this line maps to the second chromosome and shows no phenotype as a homozygote. Unfortunately, I was unable to detect expression of the *fer* minigene by reverse transcriptase PCR of RNA isolated from the transformed line. The

absence of transgene RNA suggested that the P element may have integrated in a location that is unfavorable for the expression of the transgene. This hypothesis is supported by the observation that the *white* gene marker of the P element is expressed at a low level in the eyes of these flies.

By crossing the P[fer2345] line to a line with a chromosome carrying a stable source of P element transposase, the D2/3 transposase line, the *fer* minigene P element can be induced to transpose to new sites in the genome. These new sites may be more favorable for the expression of the minigene. By inducing transposition, nine new lines, that expressed the white gene marker at a higher level were isolated. All of these lines map to the second chromosome, which is consistent with the idea that P elements transpose at higher frequency to nearby sites (Tower, Karpen et al. 1993). Five of the nine lines were crossed into the E134^{X8}/E134^{X42} background to test for rescue of the phenotype. All five failed to rescue the phenotype of the E134^{X8}/E134^{X42} flies. Analysis of the *fer* minigene expression in these five lines and the other four P[fer2345] lines revealed that none of the lines expressed the mini gene (figure 2.5). These experiments strongly suggest that the construction of the minigene has removed or destroyed some promoter or enhancer element that is essential for *fer* expression.

Isolation of a third member of complementation group II.

Since I was unable to rescue the phenotype of complementation group II with the P element containing the *fer* minigene construct, we must use other means to confirm that this group represents the *fer* complementation group. If we could isolate several new members of complementation group II, then we could determine whether all the members of this group have defects in the *fer* gene. A collection of a number of lines that all have mutations in

Figure 2.4
Construction of the minigene rescue P element.

P element

6 kb upstream
sequence
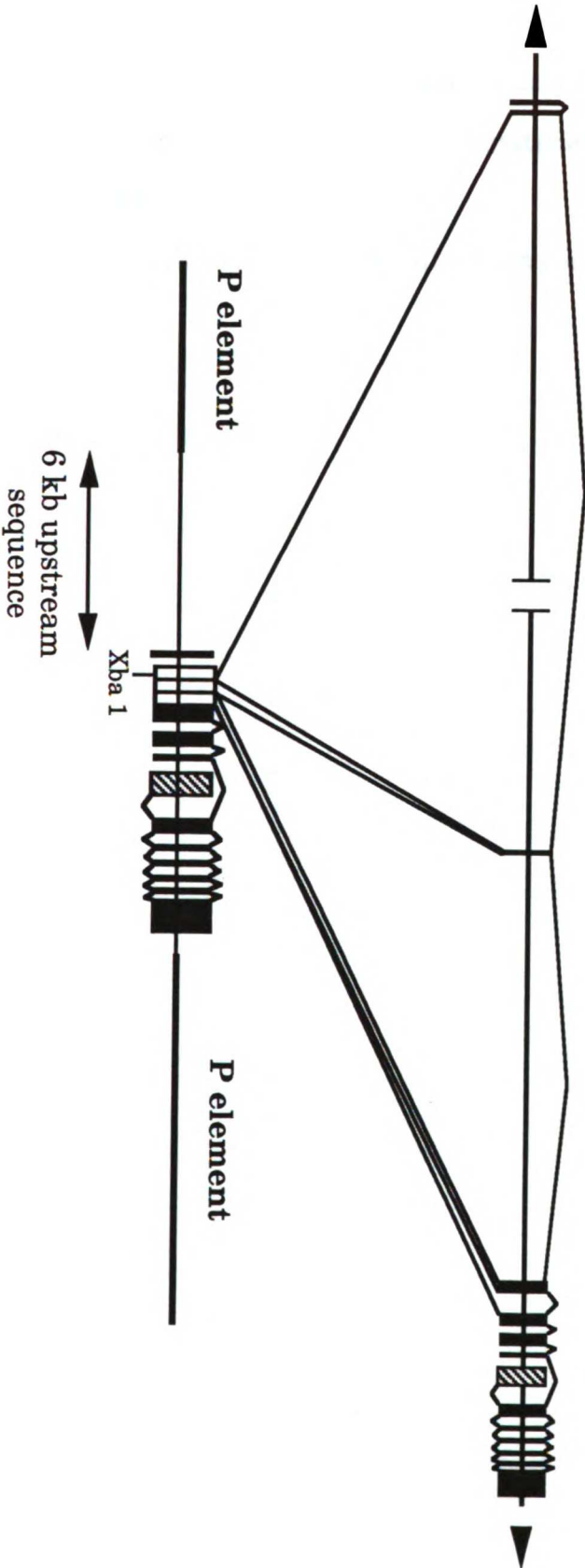
Xba 1

P element

Legend figure 2.4:

Diagram of the minigene rescue P element, P[2345fer].

The new Xba 1 site introduced during the construction of the P element is indicated in the figure.

See methods and materials for the details of its construction.

Figure 2.5
**Expression of the *fer* transgene in the P[2345fer]
transformed fly lines.**
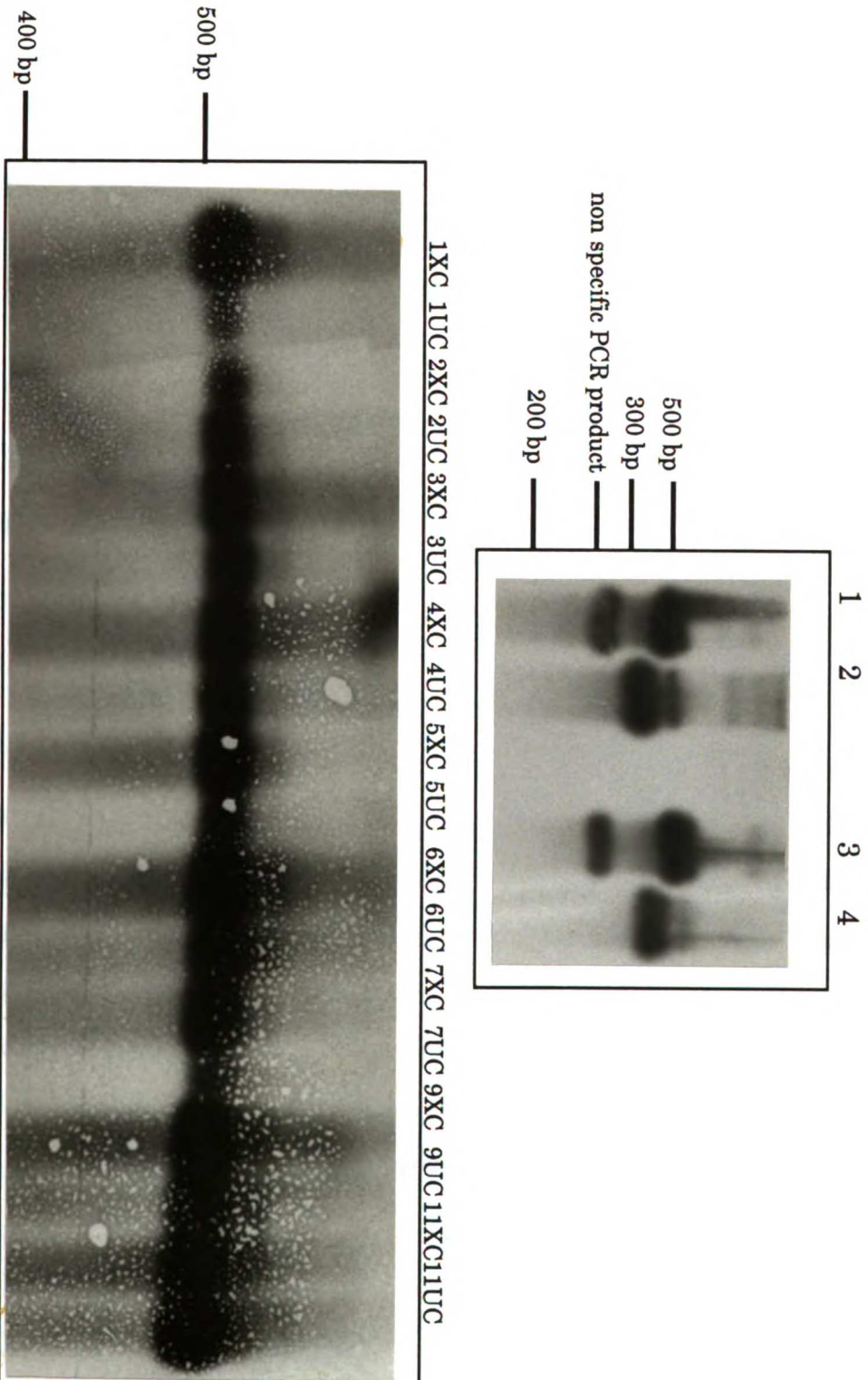
Legend figure 2.5:

RNA-PCR analysis to determine whether the rescue P element expresses the transgene.

The top panel shows the analysis of the original transformed line.

Lane 1 P[2345fer] cDNA used for RNA-PCR. PCR products uncut.

Lane 2 P[2345fer] cDNA used for RNA-PCR. PCR products cut Xba 1 (and PVU II to control for digestion).

Lane 3 Control 2-24 hour embryo cDNA used for RNA-PCR. PCR products uncut.

Lane 4 Control 2-24 hour embryo cDNA used for RNA-PCR. PCR products cut with Xba 1 (and PVUII to control for digestion).

The size of the expected bands are indicated:

uncut band 500 bp

PVUII cut band 300 bp

PVUII and Xba 1 cut band 200 bp.

Lower panel shows the analysis of the transformed lines isolated after the initial transformed line was induced to transpose. The lanes of the Southern are marked with the number of the line and whether the PCR products were cut with Xba 1 (C) or not digested with Xba 1 (UC).

The size of the expexted fragments are indicated:

uncut PCR product 500 bp

Xba 1 cut PCR product 400 bp

the *fer* gene and all exhibit the same phenotype would be strong evidence that this group is the *fer* complementation group. In order to isolate new members of complementation group II, we used the screen outlined in figure 2.6. This procedure involves screening f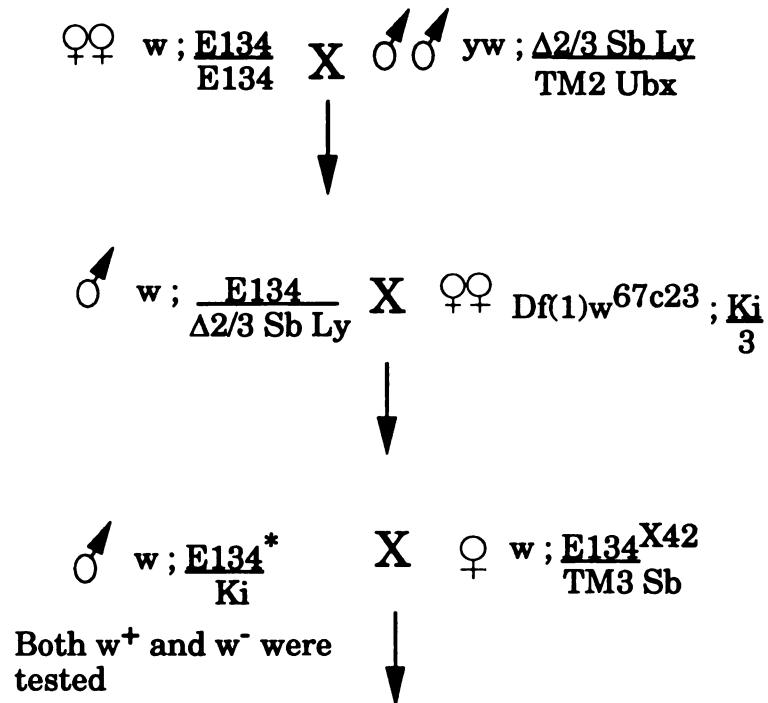or mutations induced by imprecise excision of the P element that failed to complement the lethality of $E134^{X42}$. All mutant lines that failed to complement $E134^{X42}$ were then either crossed with $E134^{X8}$ to test for complementation or the $E134^{X42}/E134^*$ flies were tested for expression of $p92.5^{fer}$. Deletion and rearrangement mutations in the DNA surrounding P element insertion sites occur at a reasonable frequency when P elements are induced to transpose (Daniels, McCarron et al. 1985).

The P element was excised by crossing line E134 to the D2/3 stable source of transposase. 681 excision lines were produced, and each line was crossed to $E134^{X42}$. One line, $E134^{P35.3}$, failed to complement both the $E134^{X42}$ and the $E134^{X8}$ lines. Southern blot analysis of line $E134^{P35.3}$ showed that the P element insertion site was rearranged (figure 2.7). Analysis of the rest of the *fer* gene shows no rearrangements upstream of the P element insertion site and no rearrangements in the restriction fragment that contains exons 4-13. The mapping of rearrangements in the genomic region that contains exon 3 and the two large introns was inconclusive and will have to be redone.

We next sought to determine whether the rearrangement of the *fer* gene observed in line $E134^{P35.3}$ disrupted the gene. Again Karin Immergluck analyzed the expression of $p92.5^{fer}$ in line $E134^{P35.3}$. Like the analysis of the lines that make up the other complementation groups, the analysis of $E134^{P35.3}$ was complicated by the fact that the $E134^{P35.3}$ chromosome is lethal as a homozygote. Once again this problem was alleviated by crossing

Figure 2.6
Imprecise excision mutagenesis

♀♀ w ; $\dfrac{E134}{E134}$ X   ♂♂ yw ; $\dfrac{\Delta2/3 \text{ Sb Ly}}{TM2 \text{ Ubx}}$

$\downarrow$

♂ w ; $\dfrac{E134}{\Delta2/3 \text{ Sb Ly}}$ X   ♀♀ Df(1)w^{67c23} ; $\dfrac{Ki}{3}$

$\downarrow$

♂ w ; $\dfrac{E134^*}{Ki}$ X   ♀ w ; $\dfrac{E134^{X42}}{TM3 \text{ Sb}}$

Both w$^+$ and w$^-$ were tested

$\downarrow$

All lines that failed to complement E134^{X42} were either tested for complementation with E134^{X8} or for p92.5^{fer} production in $\dfrac{E134^*}{E134^{X42}}$ embryos.

Results

681 lines were tested

1 line E134$^{P35.3}$ failed to complement both E134^{X42} and E134^{X8}.

E134$^{P35.3}$ does not make full length p92.5^{fer}.

Legend figure 2.6:

The imprecise excision mutagenesis scheme.

In the second cross of the scheme, individual E134/D2/3 males were mated with ten females. The potential mutant progeny were from each of these crosses were kept separate to insure that the mutations induced were independent events.

E134$^{P35.3}$ into the E134^{X42} background. 10 -15% of the E134$^{P35.3}$/E134^{X42} transheterozygotes eclose and survive. The transheterozygotes are then mated to one another and the embryos are collected. Since we already had determined that the E134^{X42} line does not make full length protein, and we presume that both of the mutant chromosomes will contribute equally to the protein derived from these embryos, Karin was able to use these embryos in order to ascertain whether E134$^{P35.3}$ makes full length protein. Western blots of embryo protein extracts derived from the E134^{X42}/E134$^{P35.3}$ transheterozygotes were probed as described earlier with either the anti-amino terminal domain or the anti-SH2 domain antisera. No full length *fer* protein was detected with either antiserum. Since the E134^{X42} chromosome produces a truncated protein, this protein was detected during the western blot analysis of the E134$^{P35.3}$/E134^{X42} embryos. We cannot rule out the possibility that E134$^{P35.3}$ also makes a truncated protein of a similar molecular weight as that seen in the E134^{X42} line. These data provide compelling evidence that line E134$^{35.3}$ also contains a mutation in the *fer* gene.

Although I was unable to rescue the phenotype of the complementation group II with the P[fer2345] transgene, the evidence is very compelling that this complementation group is the *fer* mutant complementation group. We have isolated three independent lines that fail to complement one another. Two of these lines, E134^{X42} and E134$^{P35.3}$, certainly have mutations in the *fer* gene. This is demonstrated by the rearrangements of the *fer* gene observed in these lines and the failure of these lines to express full length p92.5 ^{fer}. In addition, all the different combinations of mutant chromosomes within group II produce the same phenotype. On the basis of this evidence, I

conclude that complementation group II represents the *fer* complementation group. The members of this group are renamed, fer^{X8}, fer^{X42}, and fer$^{P35.3}$. **The phenotype of the *fer* mutant alleles.**

The *fer* complementation group was identified as a lethal complementation group. However not all the allelic combinations in the group are completely lethal (figure 2.8). X42 is the weakest allele in the group. Approximately 50% of the expected X42 homozygotes survive to adults. When this allele is crossed to either the X8 or the 35.3 allele the number of mutant flies is severely reduced with only 34% of the mutant adults surviving. Both the X8 and the 35.3 alleles are completely lethal as homozygotes. In crosses between X8 and 35.3, I have observed only one X8/35.3 mutant fly .

The lethal periods for the X8 and the X42 *fer* alleles were determined as diagrammed in figure 2.9. In all combinations of the X8 and X42 alleles, I did not detect any significant embryonic lethality. When the X8 allele was crossed to itself, the homozygous larvae that were produced failed to develop through to the pupal stage. This observation suggests that the lethal period for the X8 allele is during the late larval stage. Although some X42 homozygotes survive to adults, the mutant progeny that fail to survive appear to die as pupae. The mutant progeny produced by crossing the X8 and X42 alleles, have a lethal period that is intermediate between the lethal periods of the two alleles as homozygotes. X8/X42 mutant progeny survive through the larval stage, but very few of them survive the pupal stage and eclose as adults. The lethal period of the 35.3 allele has not yet been determined.

Figure 2.7
Mapping rearrangements in Line E134$^{P35.3}$
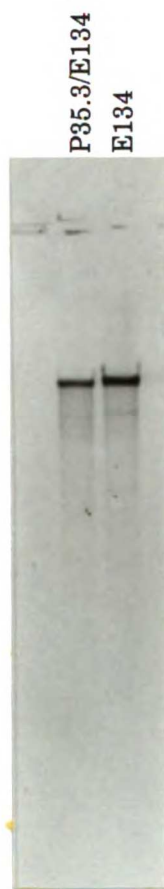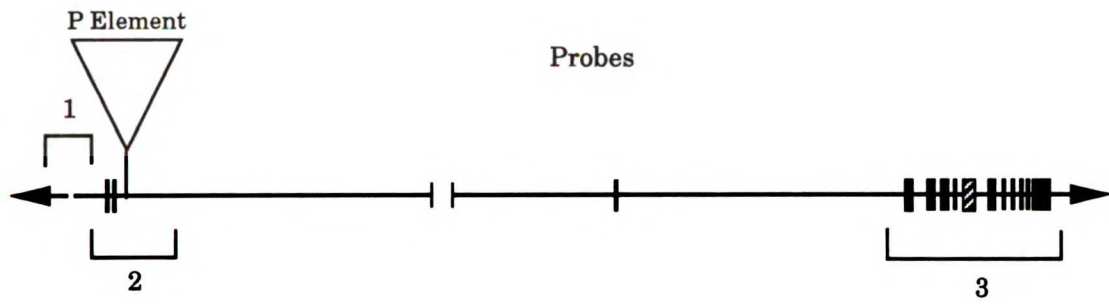
Probe 1

Probe 2

Probe 3

Legend figure 2.7:

Mapping rearrangements in the *fer* locus in line E134$^{P35.3}$.

At the top is a schematic of the *fer* locus with the positions of the different probes indicated. The left hand panel is a Southern blot of an EcoRI digest of genomic DNA and was probed with probe 1. The center panel is a Southern blot of an EcoRI digest of genomic DNA probed with probe 2. The right hand panel is a Southern blot of a BamHI-EcoRI digest of genomic DNA.

Initial characterization of the phenotype of the *fer* mutants has been limited to the characterization of defects in the surviving mutant adults. I have detected abnormalities in three tissues of the mutant progeny, the eye, the macrochaete of the head and thorax, and the thoracic indirect flight muscles. The eye and macrochaete phenotypes are observed with all three alleles, while the thoracic muscle phenotype has only been analyzed in the X8 and X42 alleles.

The wild type eye is a regular array of hexagonal ommatidia with each ommatidium having three bristles protruding from alternate vertices of the hexagon (figure 2.10). Each ommatidium is made up of 14 cells, 8 photoreceptors, 4 cone cells, and 2 primary pigment cells (Cagen and Ready 1989). The individual ommatidium are then linked together to form the regular array observed in wild type eyes by shared interactions with secondary and tertiary pigment cells and the cells that make up the bristles. The *fer* mutant eye phenotype, a roughening of the surface of the eye, was first identified in the X8/X42 adults that survived to eclose. The phenotype is much weaker in the X42/X42 homozygotes, while the X42/P35.3 adults exhibit the stronger eye phenotype associated with the X8/X42 adults.

Scanning electron microscopy (SEM) of wild type and mutant eyes has revealed the nature of the rough eye phenotype (figures 2.10-2.13). In the weakest representative of this phenotype, the X42 homozygotes, the eye is approximately wild type in appearance. Closer inspection of the eye, however, reveals that some of the interommatidial bristles are missing. Other bristles seem to be mislocalized to adjacent vertices of the hexagon and in some cases two bristles are seen from a single vertex. In addition to the

Figure 2.8
Survival of the *fer* mutant adults and the timing of the lethal period.

	E134X8	E134X42	E134P35.3
E134X8	0% Larval lethal	34% Pupal lethal	< 2.9% not determined
E134X42		50% pupal lethal	25% not determined
E134P35.3			0% not determined

The numbers in the table represent: the number of mutant progeny observed / the number of mutant progeny expected X 100

Legend figure 2.8:

Table of the percent surviving mutant adults observed with the different mutant allele combinations. The lethal period for the allele combinations that have been determined are also indicated.

Figure 2.9

Determination of the lethal periods for fer^{X42} and fer^{X8}

$$\left. \begin{array}{ccc} \dfrac{fer^{X42}}{TM6B} & \mathbf{X} & \dfrac{fer^{X42}}{TM6B} \\[2ex] \dfrac{fer^{X42}}{TM6B} & \mathbf{X} & \dfrac{fer^{X8}}{TM6B} \\[2ex] \dfrac{fer^{X8}}{TM6B} & \mathbf{X} & \dfrac{fer^{X8}}{TM6B} \end{array} \right]$$

Collected embryos and allowed them to hatch on molassus plates. Counted the number of hatched larvae.

↓
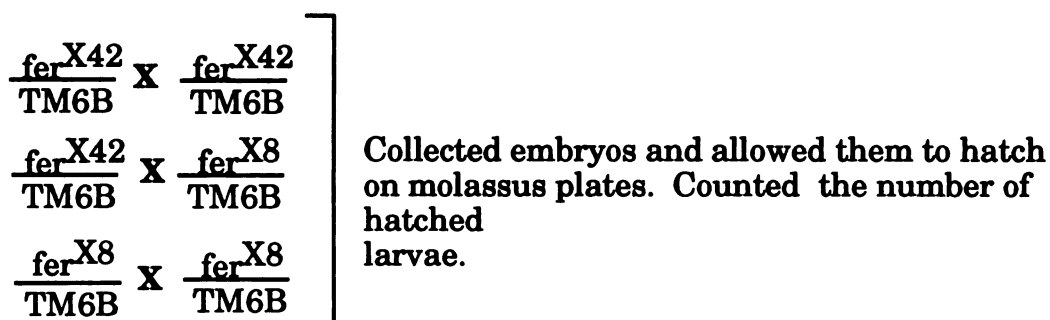
Picked all the *Tb*$^+$ larvae and transfered them to vials. Determined the number of larvae that formed pupae.

↓

Allowed the pupae to develop and counted the number of adults that eclosed.

Legend figure 2.9:

Diagram of the procedure for determining the lethal period of the different allele combinations. Between 30 and 50 mutant progeny were tested at each stage of development for lethality in order to determine the lethal period of the mutant allele combination.

bristle phenotype, a few of the ommatidia are not hexagonal in shape. This observation suggests that there may be a defect in the assembly of cells that make up the ommatidium (figure 2.11). In X8/X42 and P35.3/X42 adult flies, the eye phenotype is more severe (figures 2.12-2.13). Under the dissecting scope the eyes look rougher than in the X42 homozygotes. The SEM experiments show that there are a greater number of missing and mislocalized bristles. Also, more of the ommatidia appear to be abnormally shaped.

Many different mutations have been identified that exhibit a rough eye phenotype (Lindsley and Zimm 1992). Often sections cut through the mutant eyes revealed that the eyes had defects in the number and arrangement of the retinal cells. We examined sections of X8/X42 eyes in order to determine whether the *fer* mutations caused a similar defect in the assembly of cells in the ommatidia. These sections showed that the number of photoreceptor cells was correct, however, the arrangement of the cells was not as regular as the arrangement observed in the control eyes (figure 2.14).

Macrochaete are the large mechanosensory bristles on the head and thorax of the adult fly (Hartenstein and Posakony 1989). The number of macrochaete is constant from fly to fly and they are arranged in an invariant bilaterally symmetric pattern. Macrochaete are made up of four cells, a neuron, a glial like cell called a thecogen, a bristle secreting cell called the tricogen and a cell that forms a socket for the bristle called a tormogen. Only the tricogen and the tormogen are visible on the exterior of the fly.

In the X42 homozygotes and in the X42/X8 and X42/P35.3 transheterozygotes, one or two macrochaete are missing. The location of the missing macrochaete varies among different mutant flies. This phenotype is

Figure 2.10
Scanning Electron microscopy of
control $\underline{fer^{X8}}$ eyes
TM6B
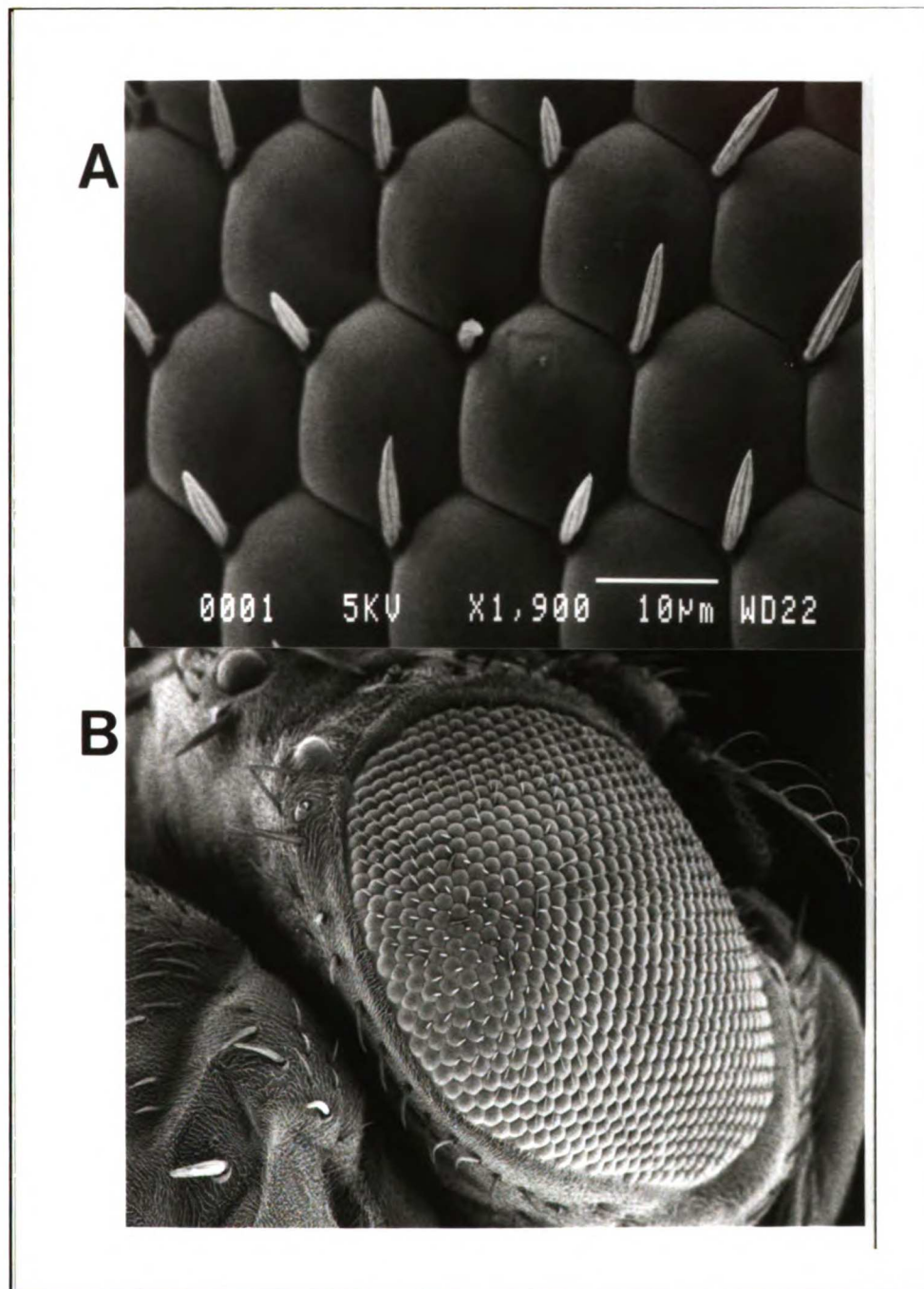
Legend figure 2.10:

Scanning Electron microscopy of control flies.

      A. Magnification is 1900X

      B. Magnification is 190X.

Figure 2.11
Scanning Electron microscopy of
$$\frac{fer^{X42}}{fer^{X42}} \text{ eyes}$$
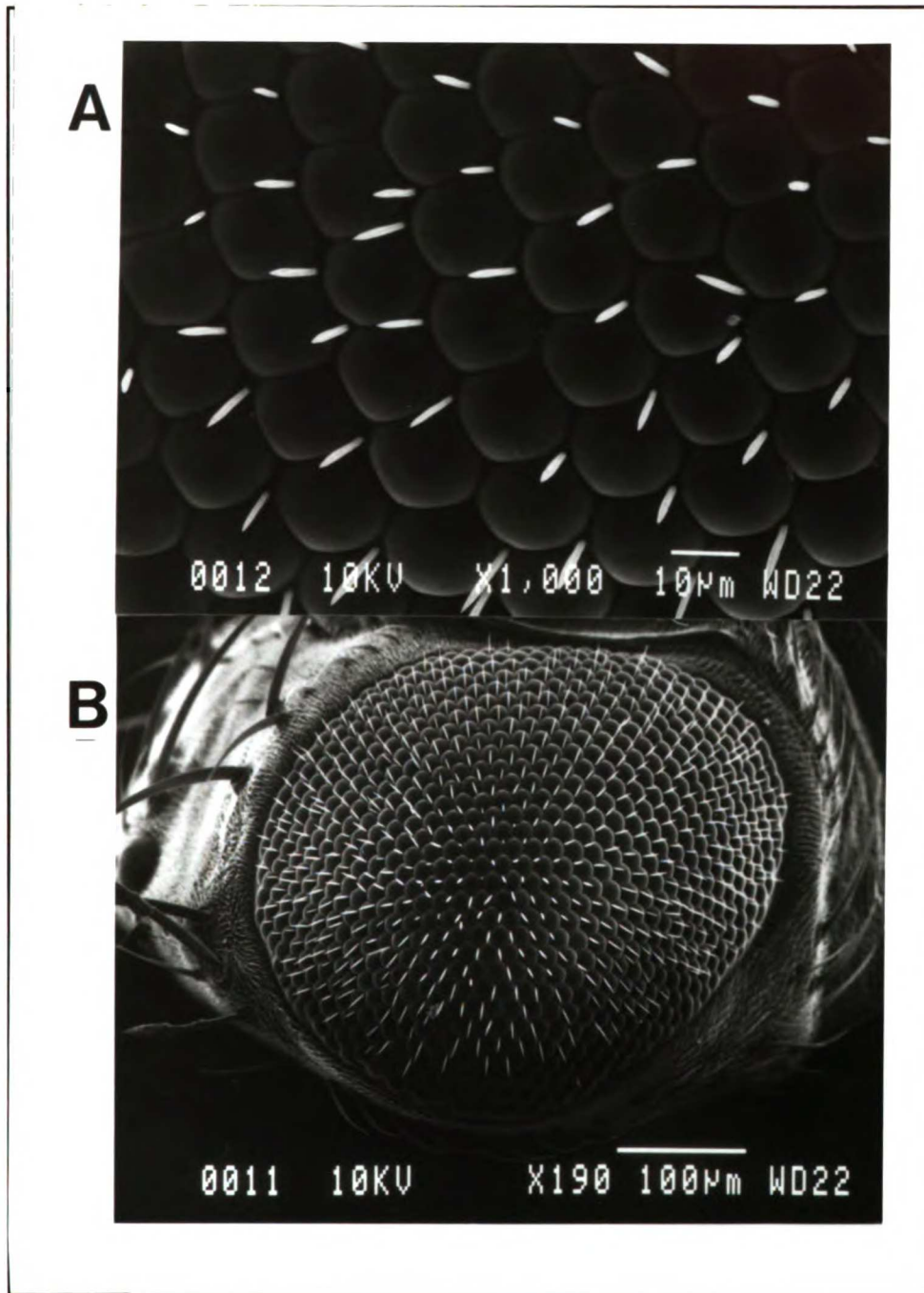
Legend figure 2.11:

Scanning Electron microscopy of fer^{X42} homozygous flies.

    A. Magnification is 1900X

    B. Magnification is 190X.

Figure 2.12
Scanning Electron microscopy of
$\frac{fer^{X8}}{fer^{X42}}$ eyes

Legend figure 2.12:

Scanning Electron microscopy of fer^{X8}/ fer^{X42} flies.

    A. Magnification is 1900X

    B. Magnification is 190X.

Figure 2.13
Scanning Electron microscopy of
$\frac{fer^{P35.3}}{fer^{X42}}$ eyes
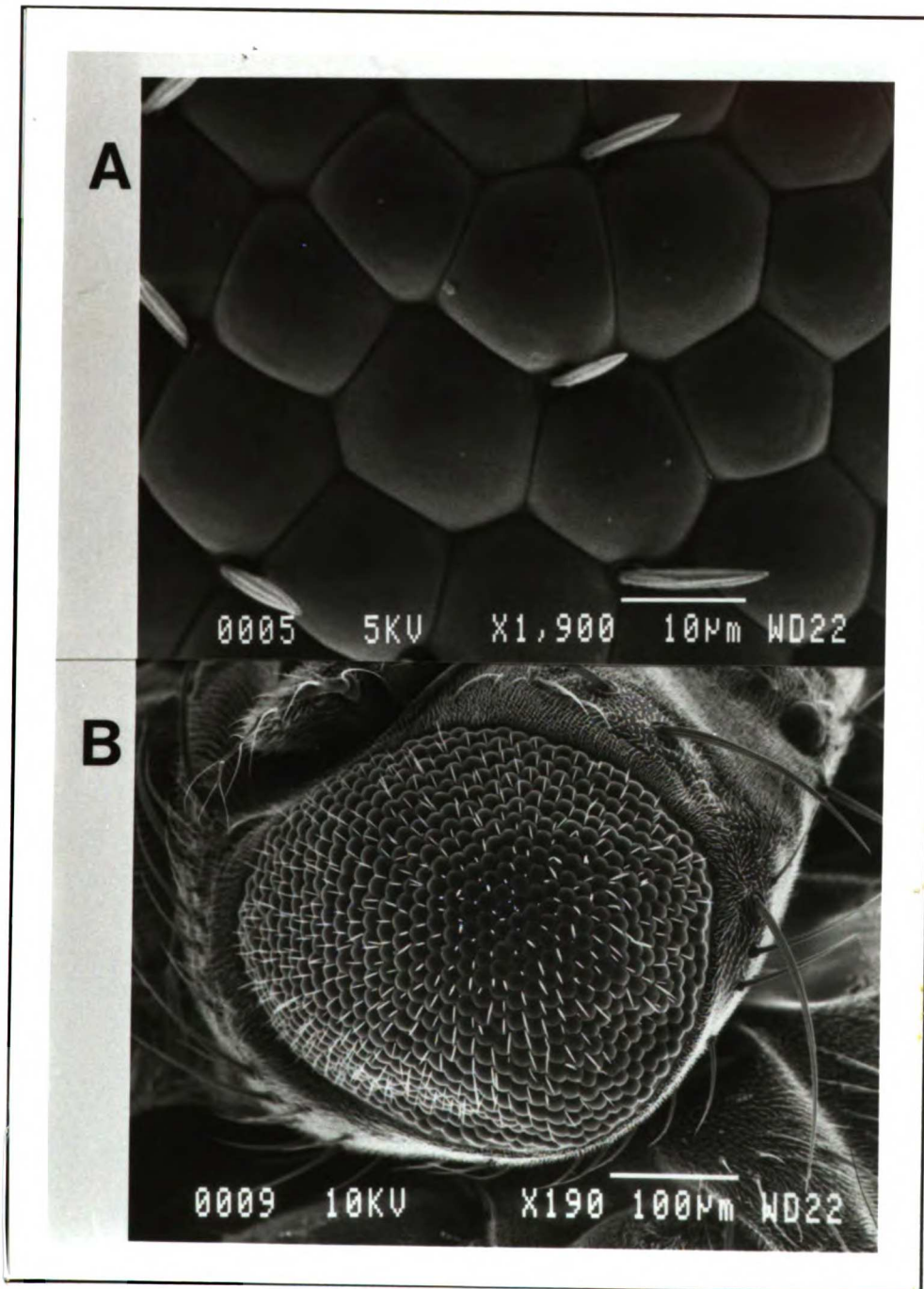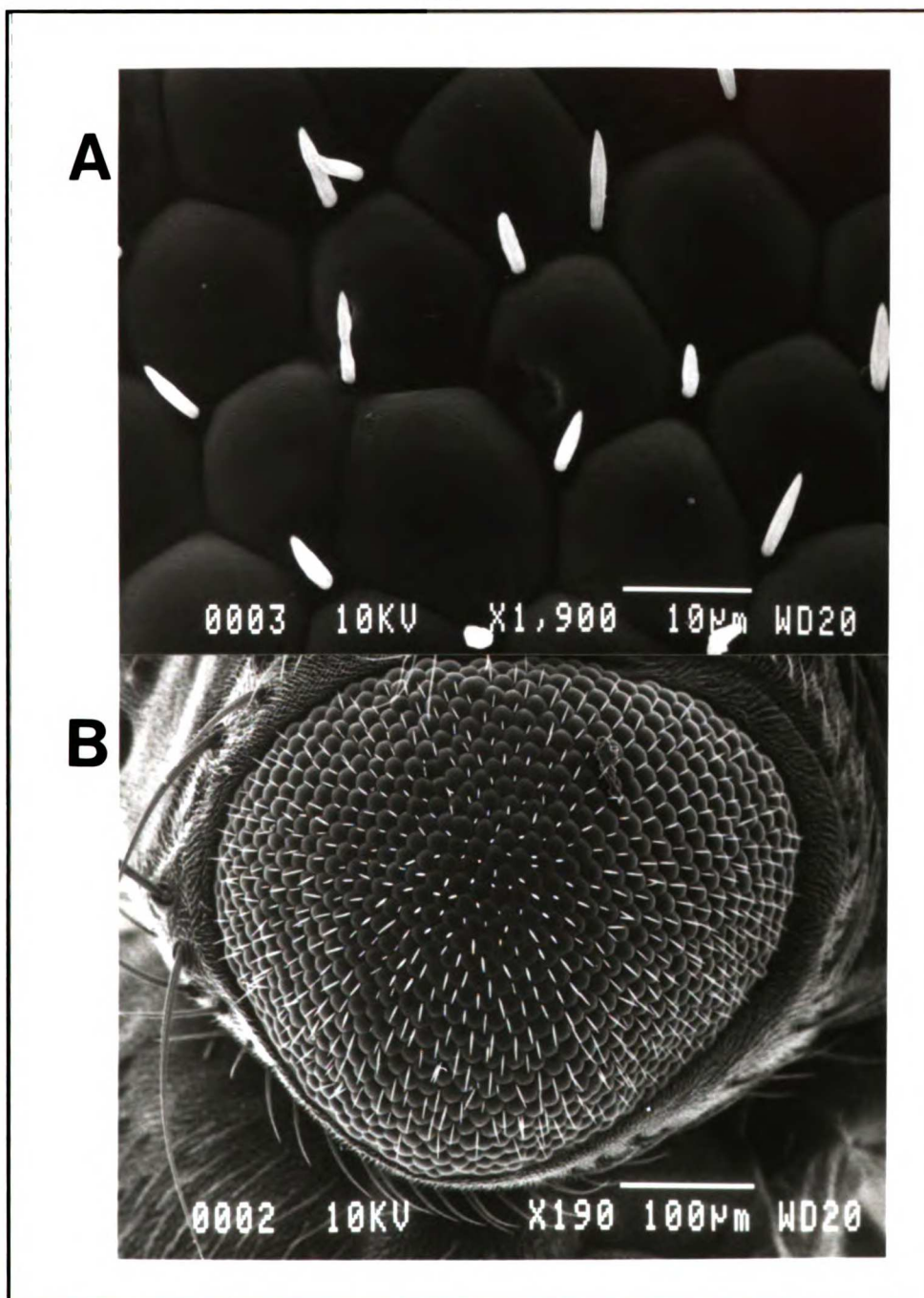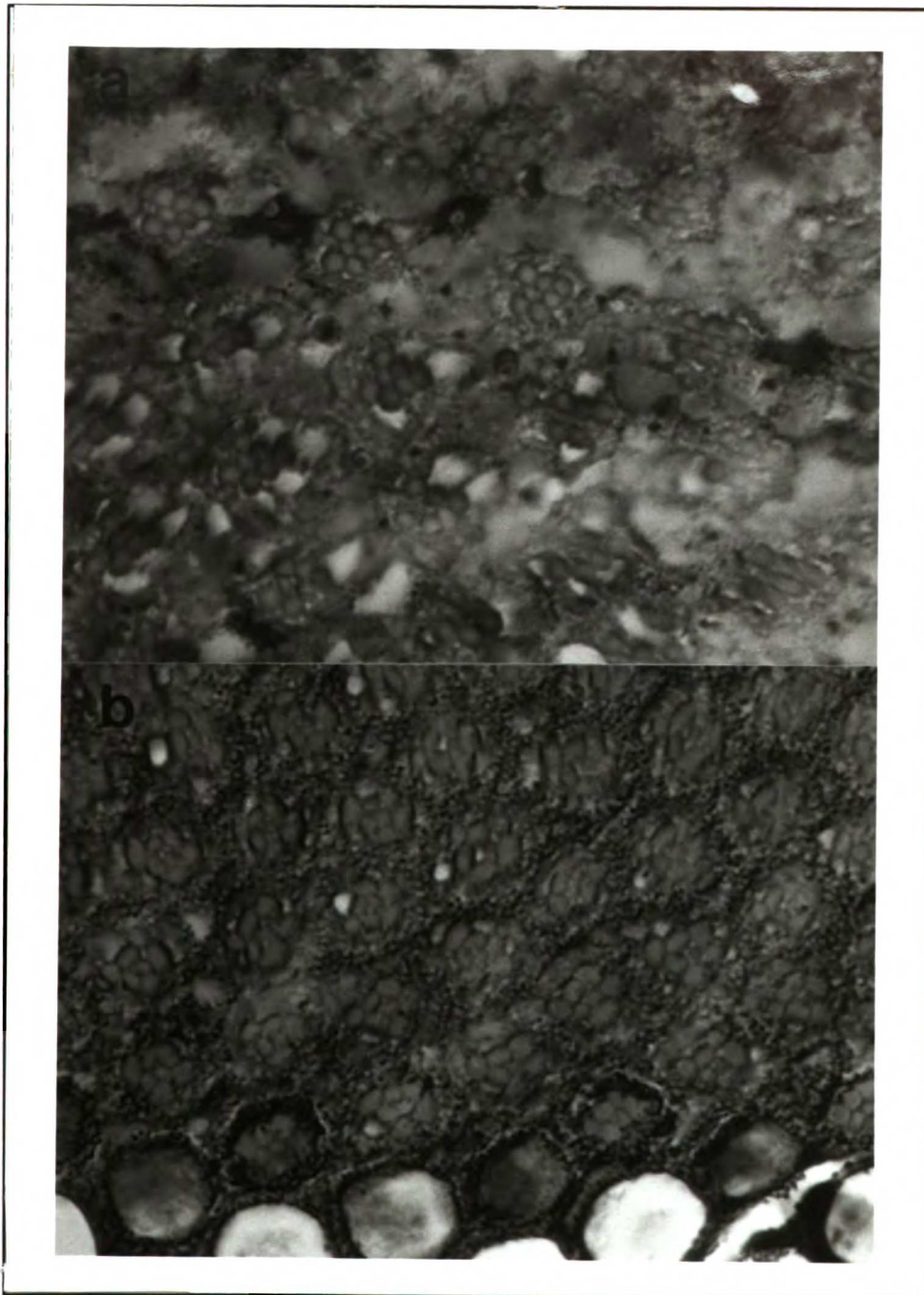
Legend figure 2.13:

Scanning Electron microscopy of fer$^{P35.3}$/ fer^{X42} flies.

    A. Magnification is 1900X

    B. Magnification is 190X.

Figure 2.14
Sections through
$\dfrac{fer^{X42}}{TM3Sb}$ and $\dfrac{fer^{X8}}{fer^{X42}}$ eyes

Legend figure 2.14:

Tangential sections through control eyes (a), and fer^{X8}/fer^{X42} eyes.

Magnification is 100X.

not 100% penetrant, and the penetrance increases when the flies are kept at 27º C (Table 2.2). The penetrance of the phenotype is also dependent upon the combination of alleles in the mutant adults. X42 homozygotes show decreased penetrance as compared to the X42/X8 and X42/P35.3 allele combinations. SEM of the mutant thoraxes revealed that the expressivity of the phenotype can vary among different flies, but it does not vary among the different allele combinations.

Some of the mutant macrochaete have a smaller bristle with a smaller socket around it (Figure 2.15). Other mutant macrochaete have lost the bristle entirely while still retaining the socket (data not shown). In the most extreme examples of the mutant phenotype, both the bristle and the socket are missing. In this case, the macrochaete is replaced with a small bulge in the cuticle (figure 2.16). I have not determined whether the neuron and the thecogen are affected in these mutant macrochaete.

The macrochaete phenotype observed in the *fer* mutants is similar to the phenotype observed in weaker alleles of the *Hairless* (*H*) mutation. *H* mutant adults also show a range of mutant phenotypes in the macrochaete which include short bristles, loss of bristles with a duplication of the socket, and total loss of both the bristle and the socket (Bang, Hartenstein et al. 1991; Bang and Posakony 1992).

Since *fer* message is expressed in all the thoracic muscles during the pupal stage of development, I investigated the effects of *fer* mutations on the development of these muscles. The indirect flight muscles of the thorax of the fly provide the force for flight. These muscles are both fibrillar and tubular in structure. The fibrillar muscles are categorized by their patterns of fasciculation and their attachment sites. The two major groups of fibrillar

Table 2.2
Penetrance of the macrochaete phenotype of
***fer* mutations**

	$\dfrac{fer^{X8}}{fer^{X42}}$	$\dfrac{fer^{X42}}{fer^{X42}}$
Room temperature (~20°C)	<10%	50%
27°C	30%	100%

Numbers reflect the percentage of mutant adults that
are missing one or more macrochaete.
The macrochaete phenotype has not
been quantified for the $fer^{P35.3}$ allele.

Figure 2.15
Scanning Electron microscopy of the
small bristle macrochaete phenotype of
$$\frac{fer^{X42}}{fer^{X42}} \text{ flies}$$
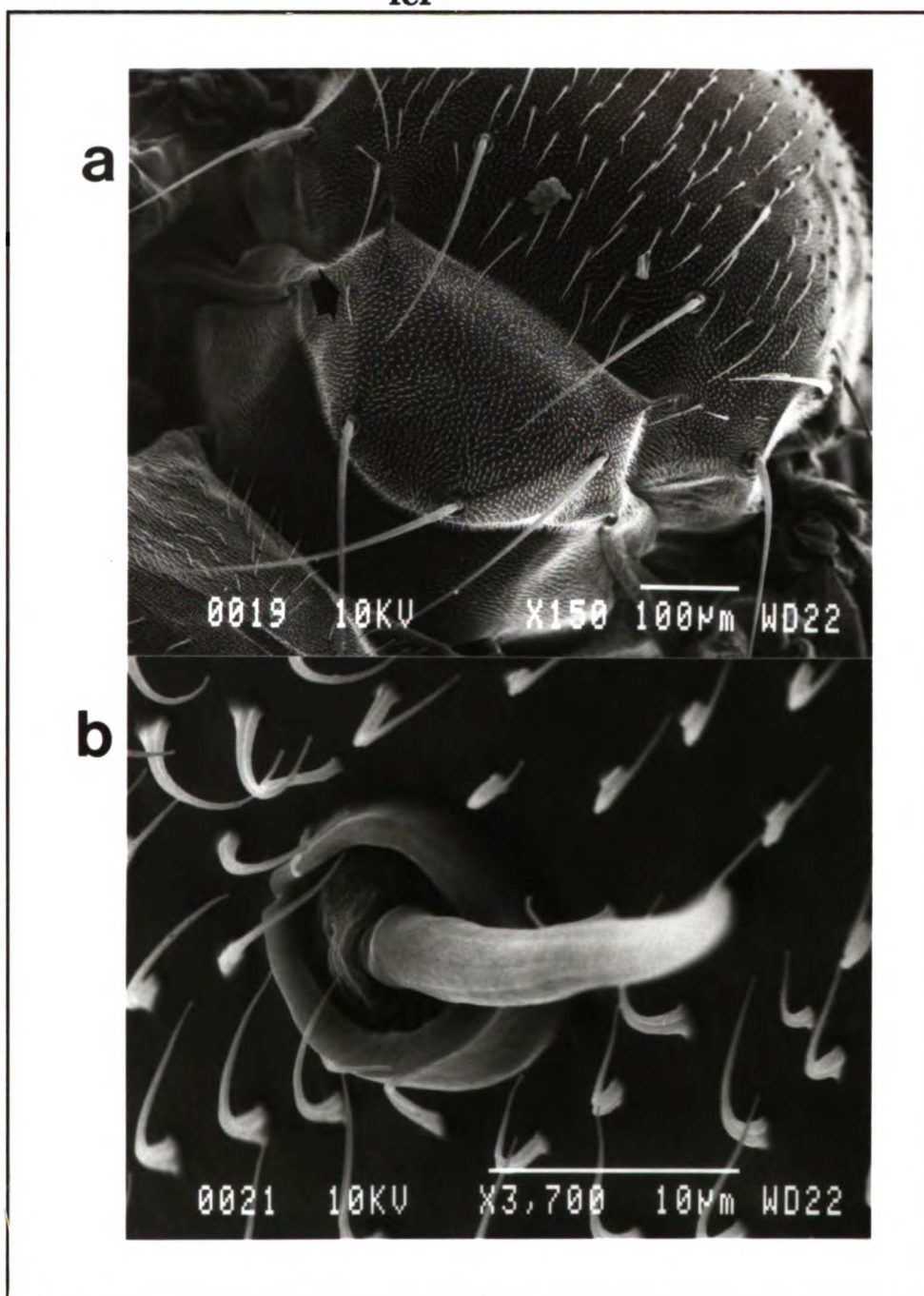
Legend figure 2.15:

Scanning Electron microscopy of the short bristle macrochaete phenotype of *fer* mutants.

Top panel magnification is 190X.

Bottom panel magnification is 3700X.

Figure 2.16
Scanning Electron microscopy of the
missing macrochaete phenotype of
$$\frac{fer^{X42}}{fer^{X42}} \text{ flies}$$
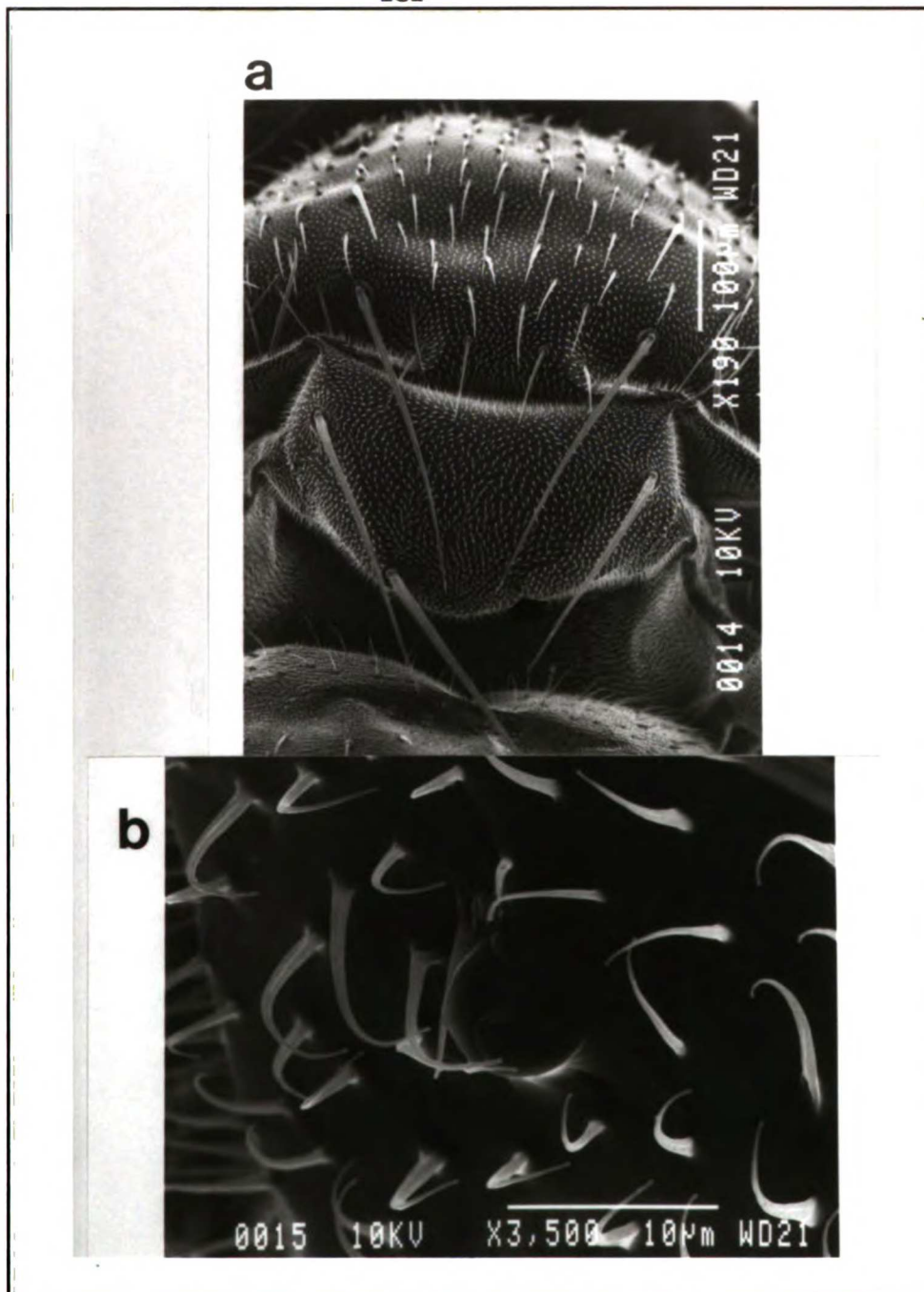
Legend figure 2.16:

Scanning Electron microscopy of the loss of bristle macrochaete phenotype of

fer mutants.

Top panel magnification is 190X.

Bottom panel magnification is 3500X.

muscles present in the thorax are the dorsal longitudinal muscles (DLMs) and the dorsal ventral muscles (DVMs). A third major muscle in the thorax is the tergal depressor of the throcanter (TDT). This muscle is a tubular muscle that is involved in the jump reflex in addition to serving indirectly during flight (Crossley 1978; Fernandez, Bate et al. 1991). Mutations that affect the development of the thoracic muscles exhibit a range of phenotypes that include abnormal wing position, inability to fly, and an inability to jump in response to a light stimulus (Deak 1977; Koana and Hotta 1978; Deak, Bellamy et al. 1982).

In all the combinations of *fer* alleles that produce adult progeny, none showed an abnormal wing position. X42 homozygous adults were tested for their ability to fly in standard flight tests (Koana and Hotta 1978). These flies showed no defects in their flight ability as compared to heterozygous flies (figure 2.17). I have not been able to obtain large enough numbers of X42/X8 or X42/P35.3 flies to test their ability to fly. The jump reflex of the fly in response to a light stimulus is also an indicator of the function of the thoracic muscles. In qualitative experiments, X42 homozygotes were able to jump in response to a light stimulus (Costello and Wyman 1986). I have not determined whether this jump response is quantitatively different from wild type.

The structure of the thoracic muscles in the *fer* mutants was investigated by analyzing sections cut through thoraxes that had been silver stained to highlight the muscles (Deak 1977; Deak, Bellamy et al. 1982; De La Pompa, Garcia et al. 1989). Longitudinal sections cut through the control heterozygous adults revealed the wild type pattern of muscles in the thorax. The pattern is bilaterally symmetric with a DLM, three sets of DVMs, and a

Figure 2.17
Flight test of $\dfrac{fer^{X42}}{fer^{X42}}$ flies
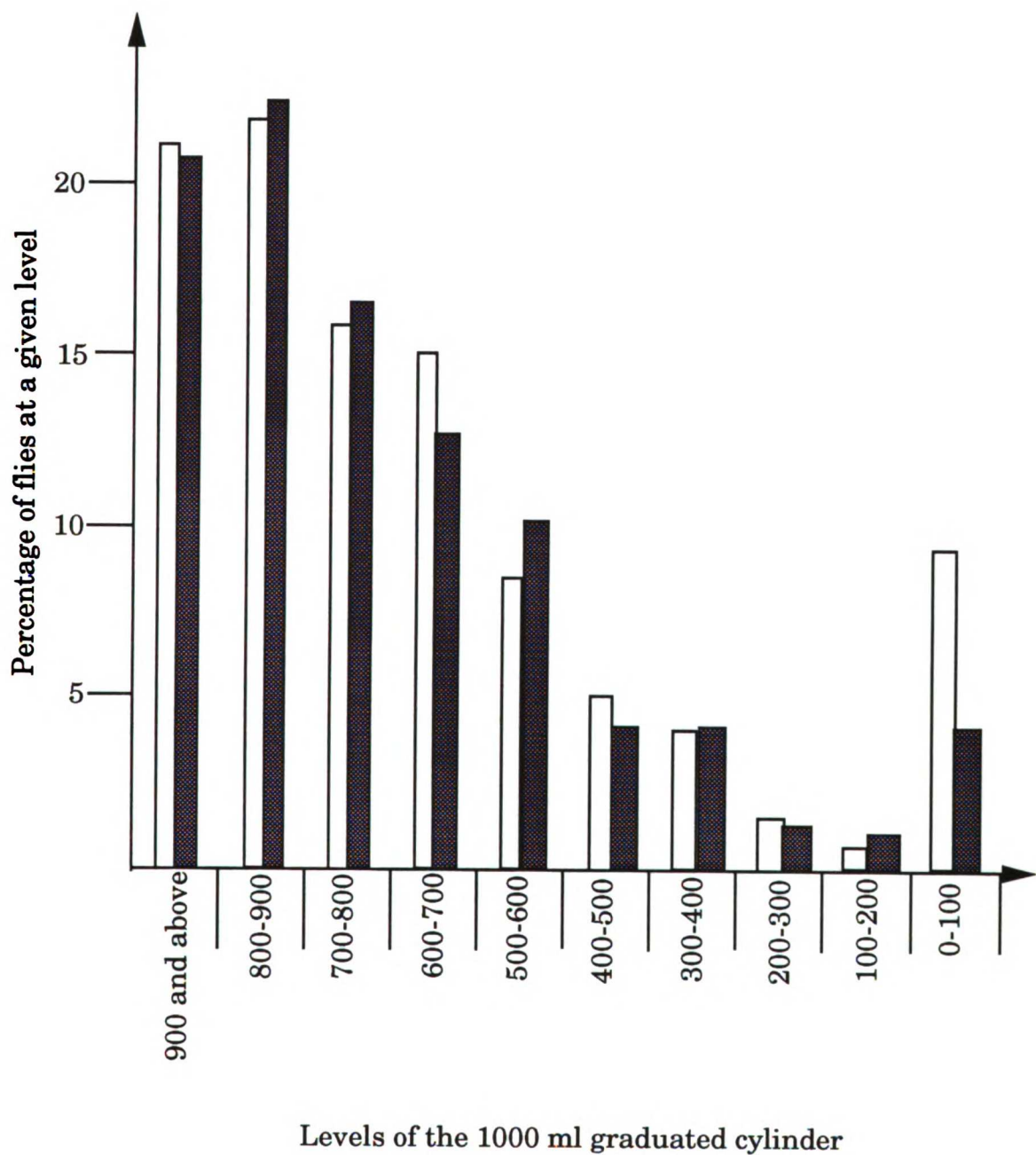
Legend figure 2.17:

Flight tests for fer^{X42} homozygous adults and control flies.

406 fer^{X42} flies and 484 control flies were tested.

Figure 2.18
Silver stained thoracic muscle sections
of
control adults
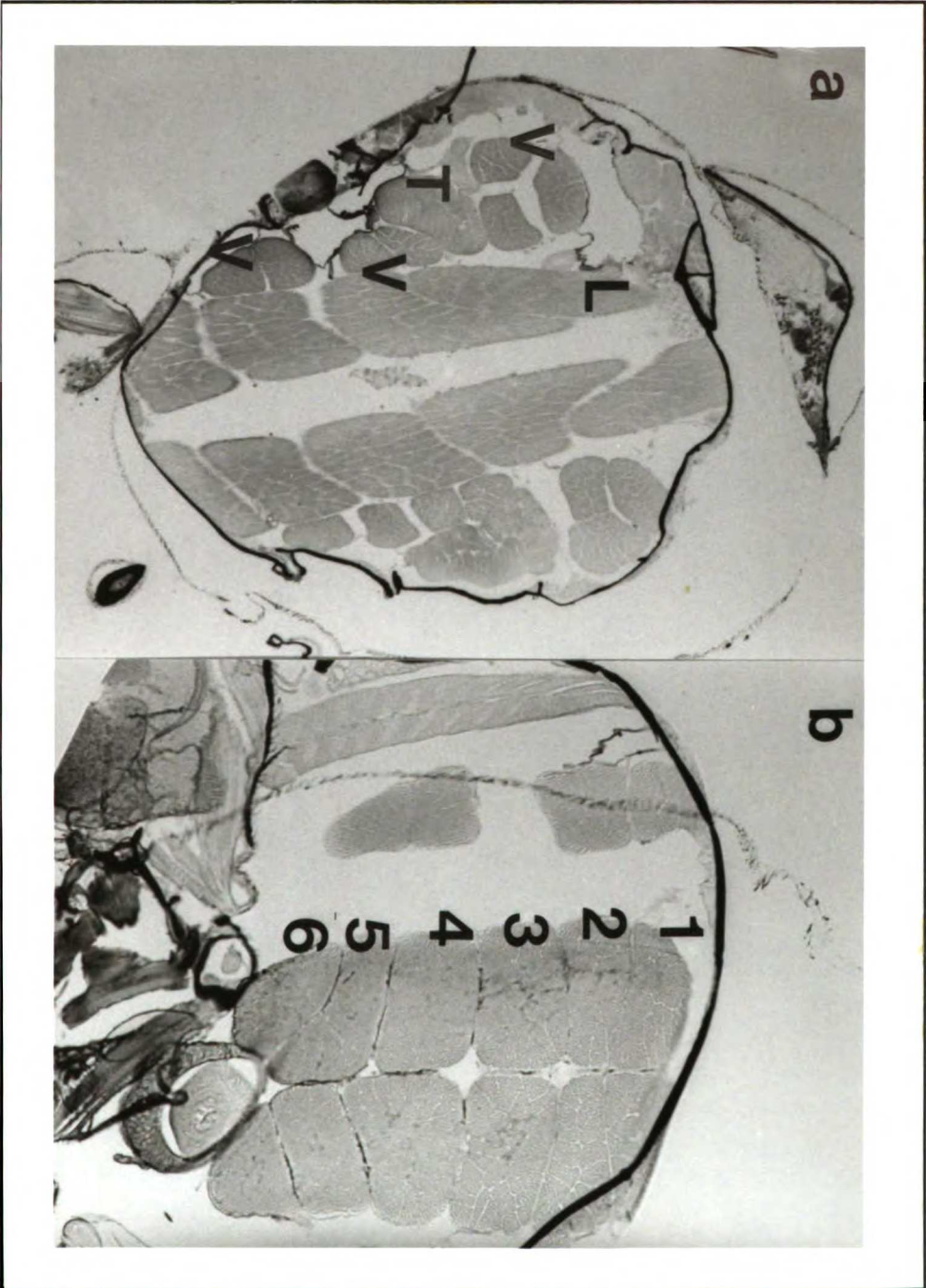
Legend figure 2.18:

Silver stained sections of control adult thoraxes.

A. Longitudinal section that shows the three major indirect flight muscle groups. Abbreviations: dorsal longitudinal muscle, DLM; dorsal ventral muscle, DVM; and tergal depressor of the throcanter, TDT. Magnification 40X

B. A frontal section that shows the six fibers of the DLMs. Magnification 40X

Figure 2.19
Silver stained thoracic muscle sections
of mutant fer$\frac{X42}{}$ adults
fer^{X42}
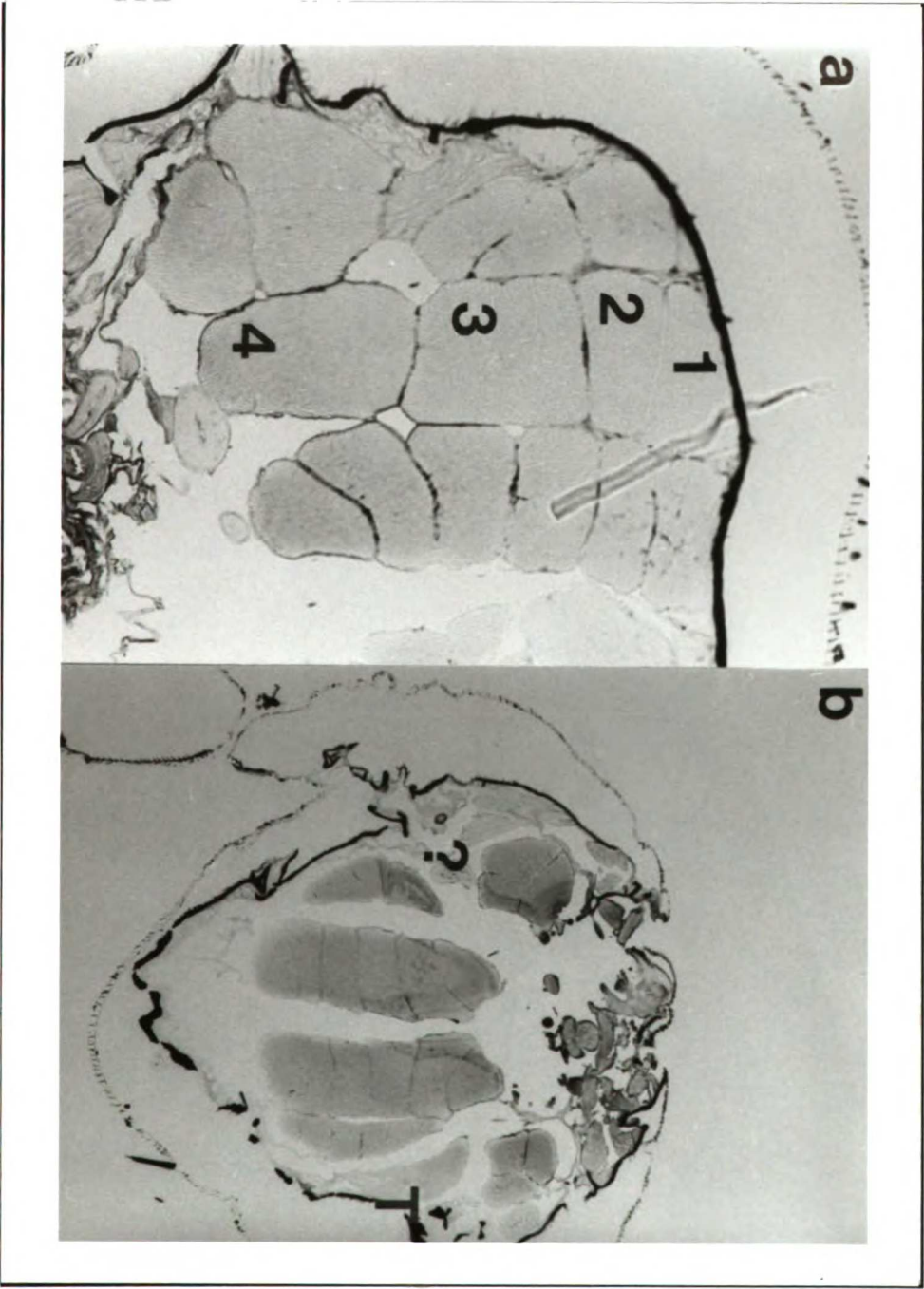
Legend figure 2.19:

Silver stained sections through homozygous mutant fer^{X42} thoraxes.

    A. Frontal section that shows the abnormal fasciculation of one of the DLM muscles. This DLM contains only four fibers. Magnification 40X

    B. Longitudinal section that shows that the left side TDT muscle is missing (as indicated by the ?). This specimen was serially sectioned and the TDT muscle was absent in all sections. Magnification 40X

144

Figure 2.20
Silver stained thoracic muscle sections
of mutant $\underline{fer^{X42}}$ adults
fer^{X42}
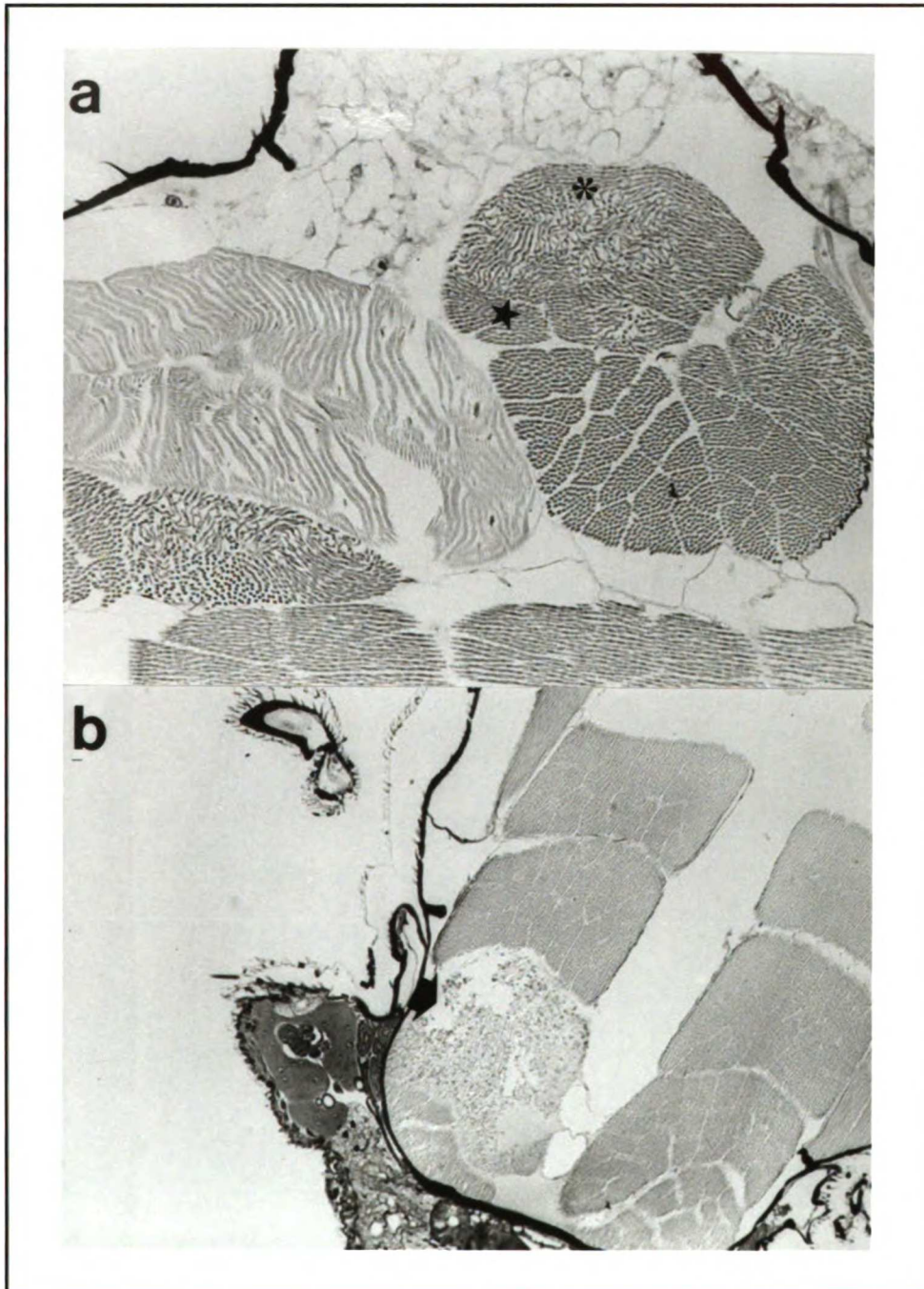
Legend figure 2.20:

Siver stained sections of homozygous fer^{X42} adult thoraxes.

A. Longitudinal section that shows a disruption of the patterning of the fibers in a DVM. The star points out a normal fiber pattern, while the * points out an abnormal pattern. Magnification is 100X.

B. Logitudinal section that shows a breakdown of the myofibrils in the DLM. The arrow points to the affected region. Magnification 40X

Figure 2.21
Silver stained thoracic muscle sections
of
control pharate adults
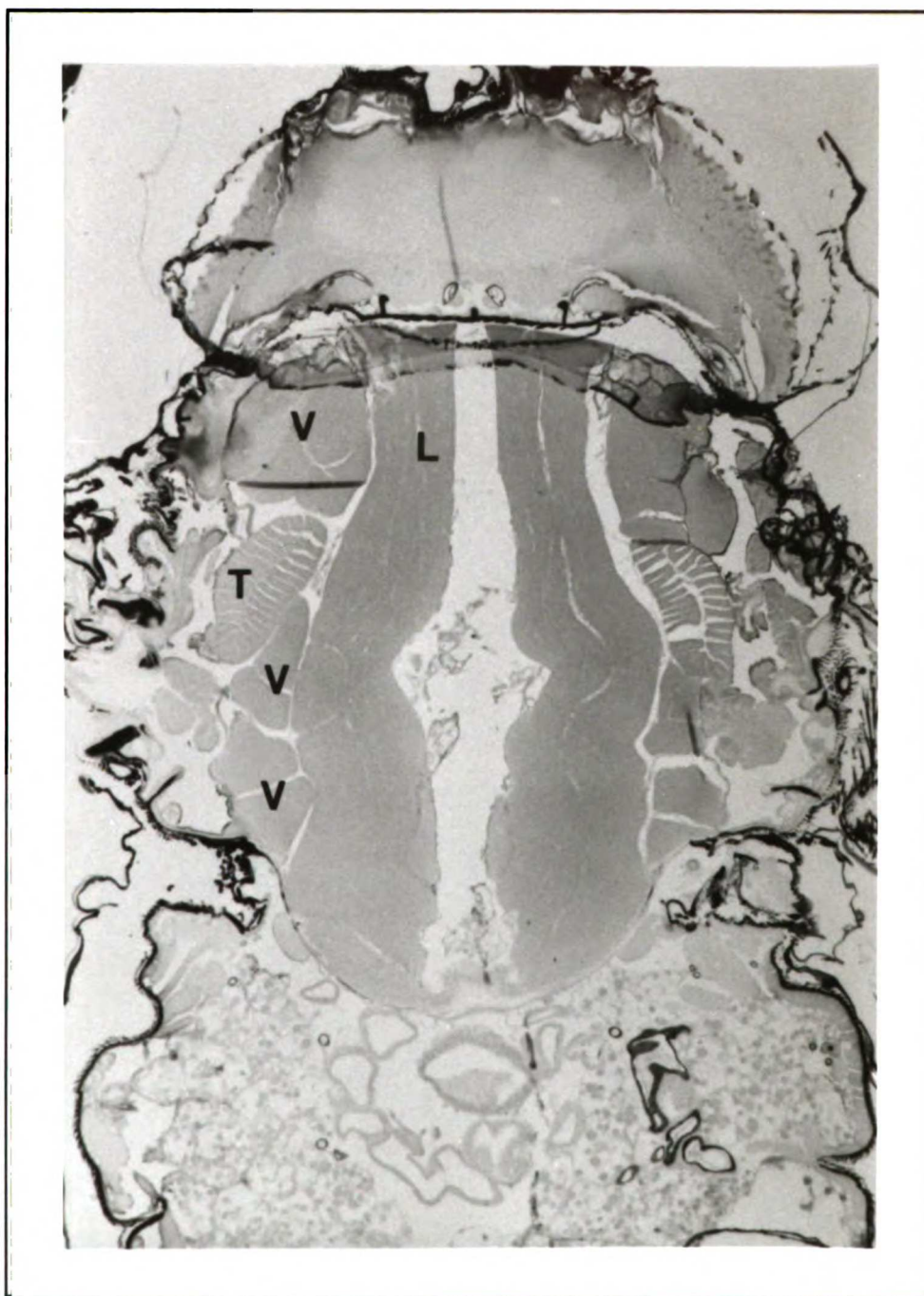
Legend figure 2.21:

Longitudinal sections of silver stained control pharate adults. Magnification 40X.

TDT on each side of the thorax (Figure 2.18A). Frontal sections of the control adults showed that DLM is made up of six fibers (figure 2.18B) (Crossley 1978). In X42 homozygous adults, the pattern of thoracic muscles was approximately wild type, but upon closer examination several defects were revealed. In some of the mutant flies, the regular structure of the fibers appeared to be disrupted. This defect varied from a subtle irregularity in the myofibrils to a more gross disruption in the fiber, and was not limited to any particular muscle type (figure 2.20). In frontal sections, it also appeared that some of the muscles were abnormally fasciculated. In one extreme case the TDT muscle of the mutant fly was missing entirely (figure 2.19). Crosses between X42 and X8 do not produce very many mutant progeny, so I turned to analyzing the development of the thoracic muscles in late pupal stage pharate adults. The pattern of the thoracic muscles in the control late pupae was essentially the same as that seen in the control adults (figure 2.21). However, when X42/X8 late pupae were examined the sections revealed that the pattern of thoracic muscles was severely disrupted. All the muscles were affected. I observed abnormal fasciculation, decrease in the size of some of the muscles, and in some cases the complete loss of a muscle (figure 2.22). In addition, there seemed to be an accumulation of particulate lymph in the mutant thoraxes. This accumulation has also observed by others studying mutations that affect muscle development (De La Pompa, Garcia et al. 1989). The gross disruption of muscle development observed in the X42/X8 pharate adults very likely contributes to the pupal lethality in this allele combination.

Discussion

Because the first NRTKs were isolated as retroviral oncogenes, it was initially hypothesized that they would participate in the regulation of cell

Figure 2.22
Silver stained thoracic muscle sections
of mutant $\frac{fer^{X8}}{fer^{X42}}$ pharate adults
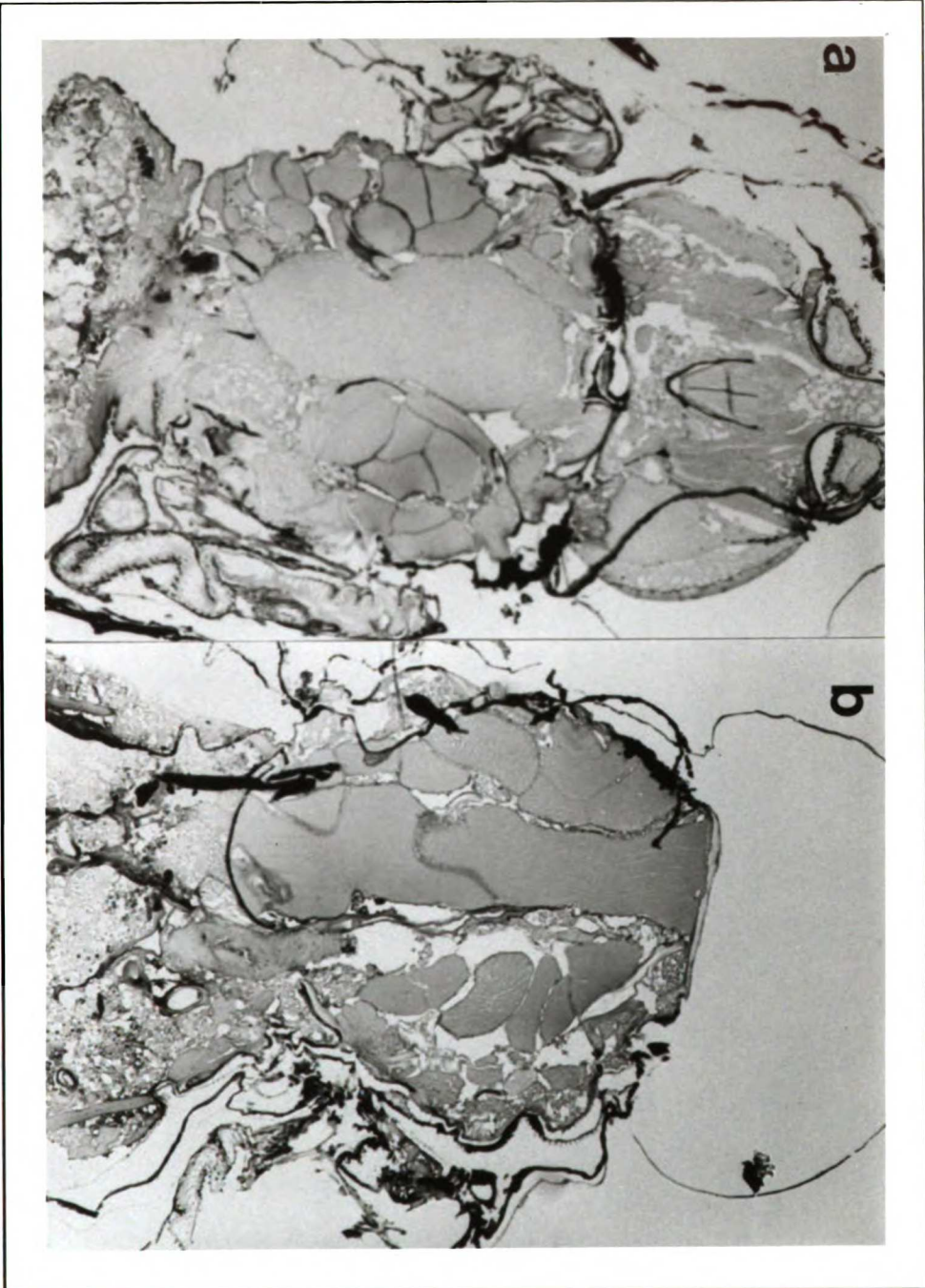
Legend figure 2.22:

Longitudinal sections through silver stained mutant fer^{X8}/fer^{X42} pharate adults.

A and B show two examples of the mutant thoraxes of pharate adults. Magnification 40X.

proliferation. The subsequent observation that several endogenous NRTKs are expressed in post mitotic cells suggested that NRTKs might instead play a role in the regulation of terminal differentiation. This idea has been supported by the analysis of the phenotypes associated with mutations in several NRTKs (Henkemeyer, Gerteler et al. 1987; Soriano, Montgomery et al. 1991; Tybulewicz, Crawford et al. 1991; Appleby, Gross et al. 1992; Molina, Kishihara et al. 1992; Stein, Lee et al. 1992). The primary defect in these mutants is not in the regulation of cell proliferation, but rather the defect is in the terminally differentiated functions. Unfortunately, the phenotypes observed in these mutations were weaker than those that were predicted by the expression patterns of the genes, and not all the tissues that expressed a particular NRTK were affected in the mutant animals. These data suggested that the function of another gene might be compensating for the loss of NRTK activity in the mutants (Hoffmann 1991). This problem of genetic redundancy has hampered the investigation of the function of NRTKs during development. The well established genetic strategies available in *Drosophila*, however, provide methods to analyze the function of NRTKs during development, and to identify redundant genes that can compensate their function.

Identification of *fer* mutations

We have isolated mutations in the *fer* gene of *Drosophila melanogaster*. These mutations represent the first mutations in a member of the *c-fps/fes* family of NRTKs. Since the three alleles in the *fer* complementation group are all rearrangements, we must address the question of whether or not the phenotype associated with this group is due solely to *fer* mutations or if mutations in other genes contribute to the

phenotype. Rescue of the mutant phenotype with a P element containing the *fer* gene would have been the most straight forward method to address this question. Unfortunately, we were unable to rescue the mutant phenotype exhibited by the *fer* mutations because the *fer* minigene P element construct failed to express *fer* mRNA. Nevertheless, we feel that we have compelling evidence to support the hypothesis that the phenotype of the *fer* complementation group is due to mutations in *fer*. In the first place, the analysis of *fer* protein expression in the X42 and P35.3 mutant alleles shows conclusively that these alleles have mutations in *fer*. Since the three alleles are independently derived, and molecular analysis has revealed that the alleles do not contain the same mutations, it is unlikely that these three alleles would have an additional mutation in the same second gene that is responsible for the phenotype of the *fer* mutants. Second, the defects in the development of the eye, the macrochaete, and indirect flight muscles that define the phenotype attributed to the *fer* complementation group are exhibited by multiple combinations of mutant alleles. Third, the defects observed in the *fer* mutant flies occur in tissues that express *fer* during their development. On the basis of this evidence , we are confident that the phenotype exhibited by the *fer* complementation group is due to the mutations in the *fer* gene.

We cannot say for certain whether any of the three *fer* alleles we have identified are null mutations. Although the X42 allele fails to make full length p92.5^{fer} protein, anti *fer* antisera recognizes a smaller protein in homozygous X42 embryo extracts. This protein could represent a truncated *fer* gene product that may retain some activity. The presence of this truncated protein coupled with the weaker phenotype exhibited by the X42

homozygotes when compared to either of the transheterozygotes with X8 or P35.3 is consistent with the idea that X42 is not a null allele. The P35.3 allele also does not make full length *fer* protein, however, because the expression of p92.5^{fer} in P35.3 was assayed in the X42 background we cannot rule out the possibility that this allele also produces a truncated protein. However, the more severe phenotype associated with the P35.3 allele in transheterozygotes with X42 and X8 suggests that it may be a null mutation. Although further characterization of the X8 allele is necessary, including an analysis of the protein expression, the severe phenotype of the transheterozygotes between X8 and X42 or P35.3 suggests that X8 could also be a null mutation. Before we can definitively state that any of these alleles are null alleles, we must characterize whether second *fer* gene product is expressed in these alleles.

The lack of a deficiency chromosome that removes the *fer* gene has hampered the analysis of the null phenotype of *fer* mutations. Interestingly, we did not recover any large deletions that removed the *fer* gene in the X-ray screen, even though the dosage of X-rays was sufficient to induce such mutations. This observation can be explained by the fact that *fer* is linked to the testes specific ß-tubulin gene, *β2t*. A deficiency chromosome for this region that includes *β2t*, called Df(3R) ß2t, is haploinsufficient and must be maintained over a duplication for the region (Kemphues, Raff et al. 1980; Kemphues, Raff et al. 1983). Any large deletions for the region including *fer* and ß2t that we may have induced during the X-ray mutagenesis would not have been recovered because of this haploinsufficient region linked to *β2t* and *fer*.

Since the expression of *fer* is entirely zygotic in origin, the phenotype exhibited by the *fer* mutations should reflect a loss of *fer* gene function during development. So what does the phenotype of the *fer* mutants tell us about the function of *fer* during *Drosophila* development? Although *fer* and other members of the *c-fps/fes* family of NRTKs can be mutated to become oncogenic, our current information concerning the phenotype of the *fer* mutant flies does not reveal a general role for *fer* in cell proliferation. Instead like many other mutations in NRTKs, mutations in *fer* appear to affect the terminal differentiation.

I have only characterized the phenotypes of the mutant adults that have eclosed and the X42/X8 pharate adults. None of the three tissues that show defects in *fer* mutants are completely abnormal in all the mutant flies. Since I cannot state with certainty that any of the *fer* alleles are null alleles, the incomplete phenotypes observed in the mutant flies may be due to residual *fer* activity. However, based on the results from the characterization of NRTK mutants in mice and flies, it is possible that the function provided by the *fer* gene product both in the affected tissues and in the tissues that express *fer* but do not show any mutant phenotype may be compensated for by another NRTK or another gene product (Hoffmann 1991). Alternatively, the low expressivity of the mutant phenotype may indicate that *fer* is involved in fine tuning a signaling process, and loss of *fer* function therefore may not totally disrupt signal transduction.

The role of *fer* in macrochaete development

The phenotypes I observe in the macrochaete of the *fer* mutant flies can be explained by a requirement for *fer* function at two points during macrochaete development. The macrochaete of the thorax develop from the

monolayer of cells that make up the wing disc epithelium. Within this monolayer of cells, a cluster of cells forms at the site where a macrochaete will later develop. One cell in this cluster will then become the sensory organ precursor cell (SOP), the other cells will be inhibited from taking on the SOP fate by a process termed lateral inhibition. After the SOP has formed, it divides twice and the four progeny cells will differentiate to form the four cells that make up the macrochaete (Hartenstein and Posakony 1989).

The determination of the SOP defines the first point where a requirement for *fer* can result in the phenotype observed in *fer* mutants. The phenotype of *Hairless*, *H*, mutations is similar to the macrochaete phenotype of *fer* mutants. *H* is required for the determination of the SOP, and the loss of *H* function results in a change of fate by the cell that would have become the SOP (Bang, Hartenstein et al. 1991; Bang and Posakony 1992). *fer* may also be involved in the determination of SOP fate. Alternatively, *fer* may play a role in regulating the proliferation of the SOP that results in the four progeny cells

The second point during macrochaete development that may require *fer* function is the differentiation of the SOP into the four cells that make up the macrochaete. Once again, the analysis of mutations in *H* has revealed that it is required for the proper development of the tricogen, which makes the bristle, and the tormagen, which makes the socket. The bristle-less double socket and short bristle phenotypes observed in weak *H* alleles are a result of this requirement for *H* function (Bang and Posakony 1992). Since *fer* also exhibits a range of phenotypes similar to that observed in weak *H* alleles, *fer* may also function during the development of the tricogen and tormogen.

Since our analysis of this phenotype is limited to characterizing the external morphology of the mutant macrochaete, we can not say definitively that the defects observed in the *fer* mutants phenocopies the defects observed in the *H* mutants. In order to determine which step of macrochaete development is disrupted in the *fer* mutants we must characterize the development of the macrochaete in *fer* mutant flies. By staining pupal wing discs with antibodies that recognize the SOPs, we can determine whether the SOPs are formed correctly in *fer* mutants. In addition antibody staining of mutant macrochaete on *fer* mutant adult thoraxes will determine which of the four cells that make up the macrochaete are affected by the loss of *fer* function. Once we know how *fer* mutations affect the differentiation of the cells that make up the macrochaete, we will have a better idea which step or steps of macrochaete development require *fer* function.

fer mutations cause defects in eye development

The simplest explanation for the defect in the number and regular spacing of the interommatidial bristles and the roughening of the eye observed in the *fer* mutants is that this phenotype is a reiteration of the macrochaete phenotype in the eye. The interommatidial bristles are formed in a manner similar to the macrochaete (Cagen and Ready 1989). Early in bristle development a single cell becomes a bristle mother cell. This cell divides twice to form the four cells that will make up the bristle. Unlike the macrochaete, however, the bristle cells must be precisely arranged within the complex lattice of cells that make up the compound eye. Because the ordered structure of the eye is determined by the local cell-cell interactions, any disruption in the normal pattern of differentiation can cause a disruption in the precise organization of cells in the compound eye. Consequently, the

rough eye phenotype associated with *fer* mutants may result from an abnormal arrangement of cells that would have made contacts with the missing bristle cells. We do not know which step of bristle development is affected in the *fer* mutants.

Alternatively, the eye phenotype could be due to a defect much earlier in the development of the eye. Mutations that affect the development of the photoreceptors can also cause defects in the development of the other cell types in the eye. Since sections of the *fer* eyes show the normal number of photoreceptor cells, it appears that the differentiation of photoreceptor cells during early eye development is normal. However the bristle loss and the rough eye phenotype observed in *fer* mutants, could still be due to defects in the subsequent development of the cone cells or pigment cells which in turn would lead to misdevelopment of the cells that make up the bristles (Cagan and Ready 1989). In this case, the eye defect in *fer* mutants would be caused indirectly by the earlier requirement for *fer* function in the cone cells or pigment cells.

In the future , we will need to identify at which point during eye development *fer* function is required. Staining of larval and pupal eye discs with antibodies that recognize different cell types in the eye and staining of pupal discs with cobalt sulfide to highlight the apical surface of the cells would help identify the abnormalities that cause the bristle loss and the rough eye phenotype of the *fer* mutants.

Even though the phenotype of *fer* mutants appears to primarily affect the development of the eye bristles, *fer* mRNA is detected in all cells behind the morphogenetic furrow in the developing eye, and the E134 enhancer trap line expresses ß-gal in all cells behind the furrow. *fer* therefore may play an

additional role during eye development that may be masked by the function of other genes. Indeed this appears to be the case, as will be described in the next chapter of this thesis, mutations in at least two other genes enhance the eye phenotype of *fer* mutant flies. These observations suggest that *fer* may play a wider role in the development of the eye than is indicated by the *fer* mutants.

fer mutations also affect the development of the indirect flight muscles

It is easy to propose a comparable function for the *fer* gene product in the development of the macrochaete and the compound eye based on the similar phenotypes of *fer* mutants in these two tissues. It is not obvious how the function of *fer* during indirect flight muscle development could relate to the function for *fer* during macrochaete and eye development. The indirect flight muscles of the thorax are made up of three muscle groups, the DLMs, the DVMs, and the TDTs. Although all these muscle groups express *fer* during their development, the DLMs develop in a manner distinct from that of the DVMs and the TDTs. The pattern for DLM development is derived from a set of larval muscles that are not histolyzed during pupal development (Fernandez, Bate et al. 1991). Myoblasts derived from the wing disc adepithelial cells fuse with these persistent larval muscles to form the DLMs. The abnormalities observed in the development of the DLMs in the X42/X8 pharate adults may be due to defects in the development of the larval muscles that are used as a pattern for DLM development. We will need to examine the effect of *fer* mutations on muscle development during embryogenesis in order to determine whether this is the case.

Unlike the DLMs, the DVMs and the TDTs do not use larval muscles as a pattern for their development. These muscles appear to develop de novo by a process that may involve the migration of a muscle precursor cell to the appropriate position to which myoblasts fuse to form the muscle (Fernandez, Bate et al. 1991). DVM and TDT formation is thought to be similar to the development of muscles during embryogenesis. Defects such as the loss of a muscle that was observed for one TDT in a *fer* mutant fly, could result from a defect in the muscle precursor cell that prohibited its fusion with myoblasts.

The observation that the *fer* mutants affect all three muscle types suggests that the mutation may affect myoblast function. The severe abnormalities in the DLMs of the X42/X8 pharate adults may be caused by the combination of defects during embryonic myogenesis in the larval muscles that will be used as patterns for DLM formation and defects in the myoblasts derived from the wing disc (Fernandez, Bate et al. 1991). In order to further characterize the effects of *fer* mutations on myogenesis in the fly, we will need to investigate more thoroughly the development of the indirect flight muscles in the *fer* mutants. By using antibodies raised against muscle myosin and against indirect flight muscle actin (Actin 88F) to stain pupal thoraxes, we will be able to identify which aspect of myogenesis is disrupted.

The nervous system has been shown to exert an influence on the development of muscles, and it is well established that denervation can lead to muscle degeneration (Gutmann 1976; Lawrence and Johnston 1986). The posterior dorsal motor neuron (PDMN) innervates the fibers of the DLM in a very characteristic pattern (Ikeda, Koenig et al. 1980; Costello and Wyman 1986). It is important for us to also examine whether the PDMN is affected in the *fer* mutants.

The identification of mutations in a member of the *c-fps/fes* family of NRTKs and the preliminary characterization of their phenotype provide the initial steps necessary to understand the function of these genes during growth and development. In the next chapter, I will present some preliminary evidence that shows that heterozygous mutations in two other genes reveal a greater role for *fer* in the development of the eye. I will also discuss some ideas about other mutations that may interact with the *fer* mutations.

Chapter 3

Genetic interactions between

fer mutations and mutations that interact with mutations in

Drosophila abl and *sevenless* tyrosine kinases.

Abstract

The mechanism by which receptor and non-receptor tyrosine kinases transmits signals has been analyzed by both genetic and biochemical experiments. Several downstream components of the signaling pathway have been cloned. In addition, genetic analysis of the signaling pathways of the *sevenless* and *torso* receptor tyrosine kinases and the *abl* non-receptor tyrosine kinase in *Drosophila melanogaster* has identified several mutations that enhance or suppress the phenotypes of mutations in these three genes.

In order to characterize the *Drosophila fer* signaling pathway, I have started to analyze the genetic interactions between mutations in *fer* and mutations *abl,* two enhancers of the *abl* mutant phenotype, *disabled* and *failed axon connections*, and a suppressor of the *abl* phenotype, *enabled.* Preliminary results showed that only the *disabled* mutation interacted with *fer* mutations causing an enhanced eye phenotype. In addition, mutations in the *Son of sevenless* also enhance the eye phenotype suggesting that a *ras* mediated signaling pathway may function downstream of *fer*. A *torpedo* allele of the *Drosophila EGF receptor* was also tested but showed no interaction with the *fer* mutations.

Introduction

Protein tyrosine kinases (PTKs) have been shown to mediate signals that induce cells to proliferate and differentiate. The mechanism by which a signal transmitted by a PTK causes a cellular response is not well understood. Biochemical experiments performed in vertebrate tissue culture cells have identified a number of proteins that either physically interact with PTKs or are phosphorylated by PTKs *in vitro* and *in vivo*. However, by using only biochemical methods, it is often difficult to determine what function these proteins perform during PTK mediated signaling.

The identification of PTK genes in *Drosophila* and the characterization of mutations in these genes have provided us with the opportunity to genetically analyze PTK function during development (Hoffmann 1991). By isolating second site mutations that enhance or suppress the phenotype of PTK mutations, gene products that genetically interact with PTKs will be identified. This strategy of enhancer and suppressor analysis has been used very successfully in identifying gene products that function downstream of the *seenless (sev)* and *torso (tor)* receptor tyrosine kinases (RTKs) (Simon, Bowtell et al. 1991; Doyle and Bishop 1993).

Several genes encoding enhancer and suppressor mutations have been cloned (Nishida, Hata et al. 1988; Rogge, Karlovich et al. 1991; Rubin 1991; Simon, Bowtell et al. 1991; Perkins, Larsen et al. 1992; Doyle and Bishop 1993; Tsuda, Inoue et al. 1993). The gene products encoded by some of these genes have been shown to correspond to proteins initially isolated as proteins that interact with RTKs using biochemical techniques on tissue culture cells. Similarly, other genes identified in suppressor-enhancer analysis in *Drosophila* and *C. elegans*, have subsequently been shown to interact

biochemically with RTKs in vertebrate tissue culture cells (Rubin 1991;

Sternberg and Horvitz 1991; Clark, Stern et al. 1992; Rubin and al. 1992).

The excellent correlation between the gene products identified in tissue

culture cells and those identified by suppressor-enhancer analysis illustrates

the power of this type of genetic analysis for the study of RTK function.

The identification of genes that genetically interact with non-receptor

tyrosine kinases, NRTKs, has proved to be more difficult. The normal

cellular functions of only a few NRTKs have been characterized (Gassmann,

Guttinger et al. 1992; Straus and Weiss 1992). Biochemical analysis of

NRTK mediated signaling has identified only a few proteins that physically

interact with NRTKs. Unfortunately, the genetic analysis of NRTK function

during development has revealed that the phenotypes of mutations in NRTKs

in both mice and *Drosophila* were less severe than the phenotypes that would

have been predicted by the expression patterns of the genes (Henkemeyer,

Gerteler et al. 1987; Schwartzberg, Stall et al. 1991; Soriano, Montgomery et

al. 1991; Appleby, Gross et al. 1992; Molina, Kishihara et al. 1992; Stein, Lee

et al. 1992). It appears that other gene products may compensate for the loss

of NRTK activity in the mutants. In order to use a genetic analysis to

identify genes that interact and may be downstream of an NRTK, the

redundant signaling pathways that obscure part of the function of the NRTK

must be removed. In *Drosophila*, it is possible to use genetics to identify

redundant signaling pathways as well as to identify genes that interact with

NRTKs.

In order to determine whether the loss of *fer* activity in the *fer* mutant

is compensated for by the activity of another NRTK, I tested the effect of a

mutation in the *Drosophila abl* gene on the phenotype of the *fer* mutants. In

addition I also tested two mutations that enhance the *abl* phenotype, *disabled (dab)* and *failed axon connections (fax)*, and one mutation that suppresses the *abl* phenotype, *enabled (ena)* (Gertler, Bennett et al. 1989; Gertler, Doctor et al. 1990; Hoffmann 1991; Gertler, Hill et al. 1993). Since the ras gene product had been shown to function downstream of the *v-fps* gene product as well as several RTKs including *sev* and *tor*, I tested the effects of the *Son of sevenless (Sos)* mutation on the *fer* mutant phenotype. *Sos* encodes a guanine nucleotide exchange factor for the *ras* protein and acts as a positive regulator of *ras* function (Simon, Bowtell et al. 1991; Bonfini, Karlovich et al. 1992). Mutations in *Sos* block *ras* mediated signaling, therefore any interactions between *Sos* and *fer* would imply that *ras* may function downstream of *fer*. The final mutation that I tested for interactions with *fer* mutations is the *torpedo (top)* mutation. *top* is an allele of the *Drosophila EGF receptor (DER)* gene (Clifford and Schupach 1989). *DER* is expressed in a tissue distribution similar to *fer* and mutations in *DER* affect the development of both the macrochaete and the compound eye in a manner similar to *fer* mutations.

Preliminary results have shown that *dab* and *Sos* enhance the *fer* eye phenotype. These observations suggest that *fer* may play a wider role in the development of the compound eye than was evident from the analysis of the *fer* mutant eyes. The enhancement of the *fer* eye phenotype by the *Sos* mutation suggests that the *Sos-ras* mediated signaling pathway may also be involved in *fer* signaling. This work is the first to identify gene products that functionally interact with a member of the *c-fps/fer* family of NRTKs and should help in the further characterization of the mechanism by which these kinases function in normal cellular processes.

Results and Discussion

Interactions between the *fer* mutation and the *abl* mutation and the *fer* mutation and the mutations that enhance or suppress the *abl* mutation.

Since mutations in *Drosophila abl* are the only other mutations in an NRTK that have been characterized in *Drosophila*, I wanted to determine whether mutations in this gene would affect the phenotype of *fer* mutations. I also decided to examine whether two mutations isolated as haploinsufficient enhancers of the *abl* lethal phenotype, *dab* and *fax*, and the one mutation isolated as a haploinsufficient suppressor of the *abl* mutant lethality, *ena*, would affect the *fer* mutant phenotype. The *dab* and *fax* mutant chromosomes that I received from Mike Hoffman contain *abl* mutations, and they will be referred to as *abl-dab* and *fax-abl*. The four mutations *abl*, *ena*, *abl-dab,* and *fax-abl* were crossed into the *fer* mutant background as described in figure 3.1. These mutations were then assayed for their effect as heterozygotes in a X42/X8 *fer* mutant background. Three aspects of the *fer* mutant phenotype were assayed in the mutant combinations; lethality, the effect on macrochaete development and the effect on the development of the compound eye. Mutations in *abl*, *fax-abl*, and *ena* did not have any significant effect on the *fer* mutant phenotype (figure 3.2).

The presence of the *abl-dab* mutations in an X42/X8 background did have an effect on the *fer* phenotype. The *abl-dab* mutations appeared to slightly suppress the lethality seen in the *fer* mutant (figure 3.2). The macrochaete phenotype of the *fer* mutant was not affected by the *abl-dab* mutations, but the eye phenotype was enhanced. Scanning electron microscopy on the *abl-dab* heterozygotes in the *fer* mutant background,

Figure 3.1
Construction of the strains containing *ena, abl, fax-abl,* and *abl-dab* mutations in the fer^{X8} mutant background

A. *abl, fax-abl,* and *abl-dab* in the fer^{X8} background:

$$\male\male \ \frac{\text{Df(3L) st j7 Ki roe p}^p}{\text{TM6B}} \quad \text{X} \quad \female\female \ \frac{\text{fer}^{X8}}{\text{TM3Sb}}$$

$$\female\female \ \frac{\text{Df(3L) st j7 Ki roe p}^p}{\underset{\text{Ki}\female}{\text{fer}^{X8}}} \quad \text{X} \quad \male\male \ \text{th st ri in p}^p$$

$$\male \ \frac{\text{Df(3L) st j7 fer}^{X8}}{\underset{\text{st, Ki}^+ \male}{\text{th st ri in p}^p}} \quad \text{X} \quad \female \ \frac{\text{fer}^{X8}}{\text{TM3Sb}}$$

$$\frac{\text{Df(3L) st j7 fer}^{X8}}{\text{TM3Sb}}$$
$$\text{Sb flies}$$
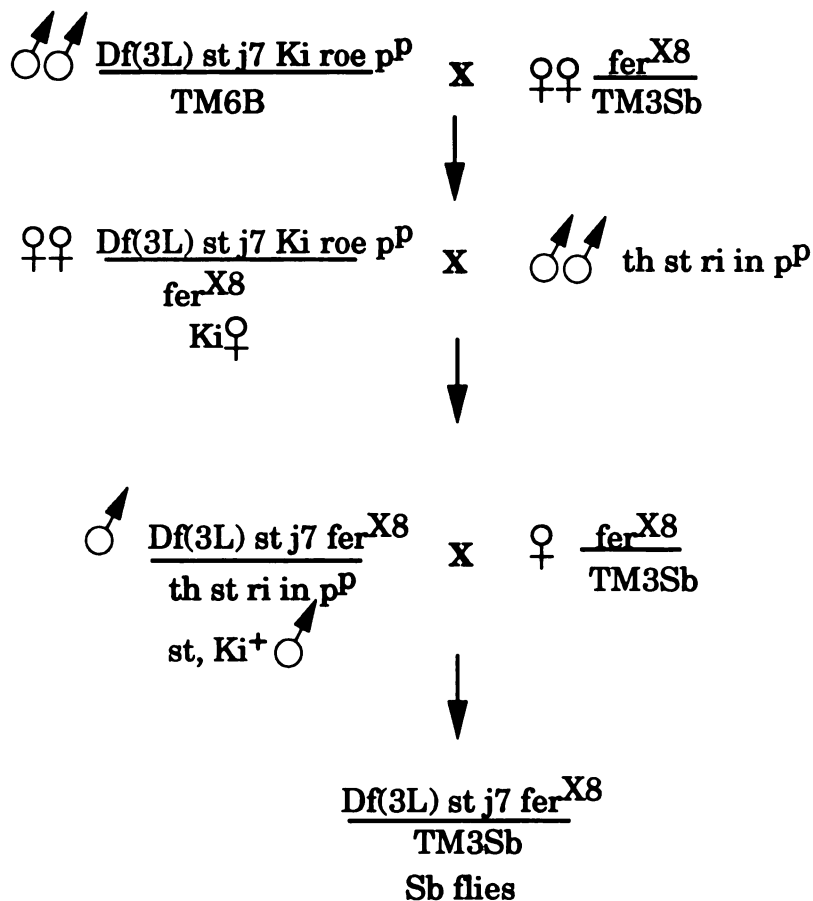
The *fax-abl/fer^{X8}* and the *abl-dab/fer^{X8}* were constructed in a similar manner except that the starting strain was different.

For *fax-abl* $\dfrac{\text{fax}^{M34}\ \text{Df(3L) st j7 Ki roe p}^p}{\text{TM6B}}$ was used

For *abl-dab* $\dfrac{\text{Df(3L) st j7 dab}^{M2}\ \text{Ki roe p}^p}{\text{TM6B}}$ was used

Figure 3.1 continued

B. Construction of $\dfrac{\text{ena}^{210}}{\text{CYO}} \; ; \; \dfrac{\text{fer}^{X8}}{\text{TM6B}}$

$\male\male \; \dfrac{\text{ena}^{210}}{\text{CYO}} \; ; \; \dfrac{\text{TM2}}{\text{TM6B}}$ X $\female\female \; \dfrac{+}{+} \; ; \; \dfrac{\text{fer}^{X8}}{\text{TM3Sb}}$

$\downarrow$

$\male \; \dfrac{+}{\text{CYO}} \; ; \; \dfrac{\text{fer}^{X8}}{\text{TM6B}}$ X $\female \; \dfrac{\text{ena}^{210}}{\text{CYO}} \; ; \; \dfrac{\text{TM2}}{\text{TM6B}}$

CYO;Tb $\male$ $\downarrow$

$\male \; \dfrac{+}{\text{CYO}} \; ; \; \dfrac{\text{fer}^{X8}}{\text{TM6B}}$ X $\female \; \dfrac{\text{ena}^{210}}{\text{CYO}} \; ; \; \dfrac{\text{TM2}}{\text{TM6B}}$

$\dfrac{\text{ena}^{210}}{\text{CYO}} \; ; \; \dfrac{\text{fer}^{X8}}{\text{TM6B}}$

CYO;Tb $\male$ $\downarrow$
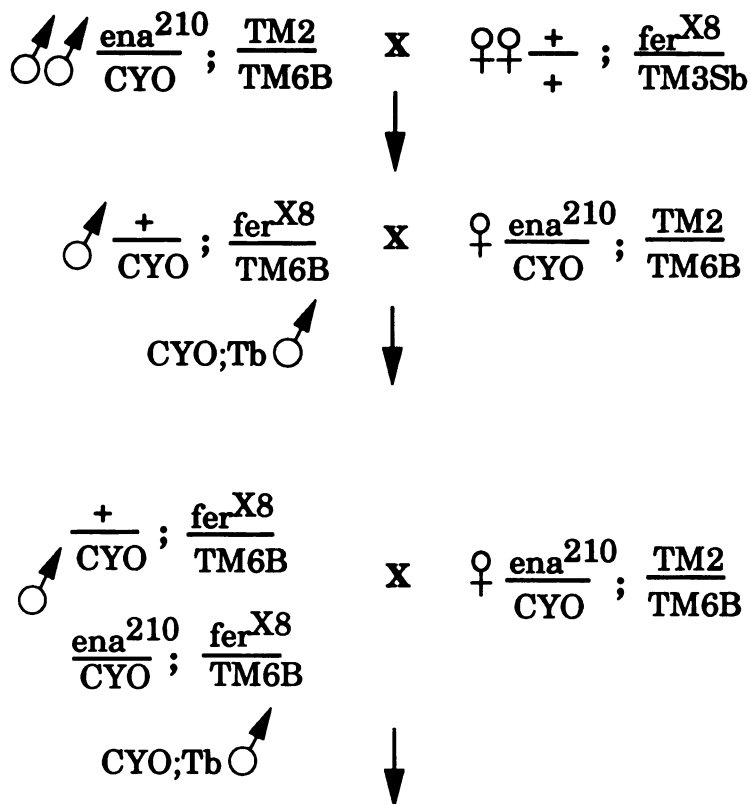
If all progeny were CYO then the stock is $\dfrac{\text{ena}^{210}}{\text{CYO}} \; ; \; \dfrac{\text{fer}^{X8}}{\text{TM6B}}$

Legend figure 3.1:

Construction of the strains that carry mutations in *abl, fax-abl, abl-dab*, and

ena in the fer^X8 mutant background.

Df(3L) st j7 is a deficiency that removes the *abl* gene, but not *dab*.

Figure 3.2
The effects of the *abl*, *fax-abl*, *abl-dab*, and
ena on the $\underline{fer^{X8}}$ mutant phenotype
fer^{X42}

A. The crosses:

$$\frac{Df(3L)\ st\ j7\ fer^{X8}}{TM3Sb} \quad \textbf{X} \quad \frac{fer^{X42}}{TM3Sb}$$

$$\frac{Df(3L)\ st\ j7\ dab^{M2}\ fer^{X8}}{TM3Sb} \quad \textbf{X} \quad \frac{fer^{X42}}{TM3Sb}$$

$$\frac{fax^{M34}\ Df(3L)\ st\ j7\ fer^{X8}}{TM3Sb} \quad \textbf{X} \quad \frac{fer^{X42}}{TM3Sb}$$

The number of Sb versus Sb$^+$ progeny were compared.

$$\frac{ena^{210}}{CYO};\frac{fer^{X8}}{TM6B} \quad \textbf{X} \quad \frac{fer^{X42}}{TM3Sb}$$

The number of CYO$^+$; Sb$^+$ versus CYO ; Sb$^+$ progeny were compared.

B. The results:

|	Surviving adults	Eye Phenotype	Macrochaete phenotype
$\dfrac{Df(3L)\ st\ j7\ fer^{X8}}{fer^{X42}}$	~30%	unaffected	unaffected
$\dfrac{ena^{210}}{CYO};\dfrac{fer^{X8}}{fer^{X42}}$	10%	unaffected	unaffected
$\dfrac{fax^{M34}\ Df(3L)\ st\ j7\ fer^{X8}}{fer^{X42}}$	20%	unaffected	unaffected
$\dfrac{Df(3L)\ st\ j7\ dab^{M2}\ fer^{X8}}{fer^{X42}}$	71%*	enhanced	unaffected

Legend figure 3.2:

All crosses were done in two ways: Male of strain 1 X Female strain 2 and

Female of strain 1 X Male of strain 2.

(*abl-dab* X42/X8) revealed that the defect in the development of the interommatidial bristles is more wide spread than in the *fer* mutations and that more of the ommatidia were abnormally shaped (figure 3.3). As I described in the previous chapter, *fer* mutations result in a loss of the normal number and spacing of the interommatidial bristles and in a roughening of the eye due to the abnormal shape of some of the ommatidia. *abl* mutations are known to result in a disruption of eye development different from that observed in *fer* mutant adults, with defects in photoreceptor development and in the structure of the normal ommatidial array. I sought to determine whether the *abl-dab* X42/X8 flies exhibited some of the defects observed in the *abl* mutant adults. Sections cut through the *abl-dab* X42/X8 eyes showed that all of the photoreceptor cells are present (figure 3.4). This result shows that the enhanced eye phenotype is not caused by a defect in photoreceptor cell development as is seen in *abl* mutant flies but rather may be due to an enhanced defect in the development of the cells that make up the bristle group or in the development of the cone and pigment cells that could subsequently affect bristle and ommatidia assembly.

This result is very provocative, but the enhancement of the *fer* eye phenotype has only been observed with one *fer* mutant allele combination. Since all the *fer* alleles are rearrangements, it is important for these results to be repeated with other allele combinations in order to rule out any interactions involving other genes that might be rearranged in the *fer* mutant chromosomes. In addition it must be determined whether the enhanced eye phenotype in due solely to the *dab* mutation or if it requires both the *abl* and the *dab* mutations. Since the *abl* X42/X8 flies were normal, I have concluded that a mutation in *dab* is necessary for this interaction with *fer*. However, I

Figure 3.3
Scanning Electron microscopy of
$\underline{Df(3L) \, st \, j7 \, dab^{M2} \, fer^{X8}}$ eyes
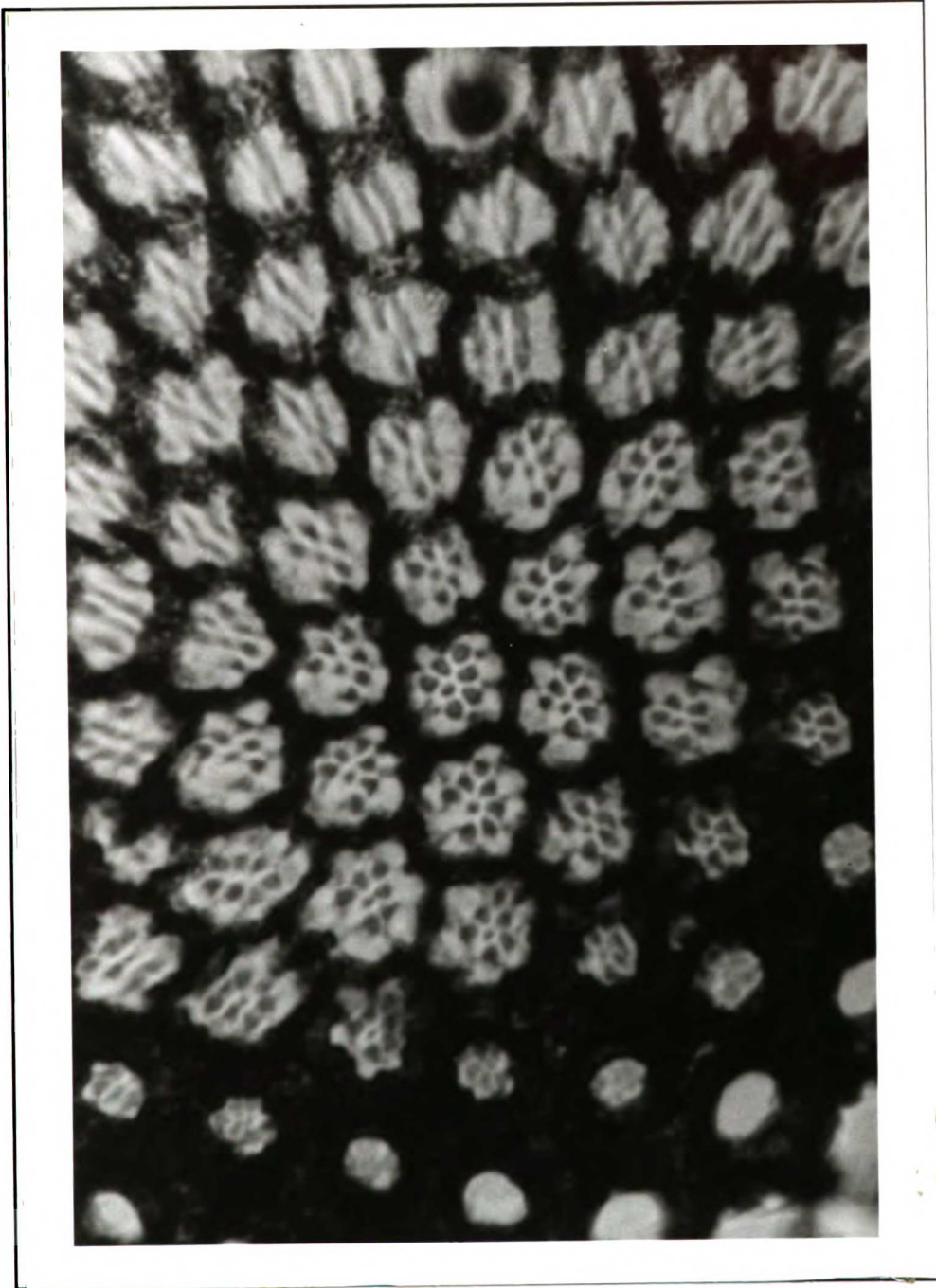## fer^{X42}
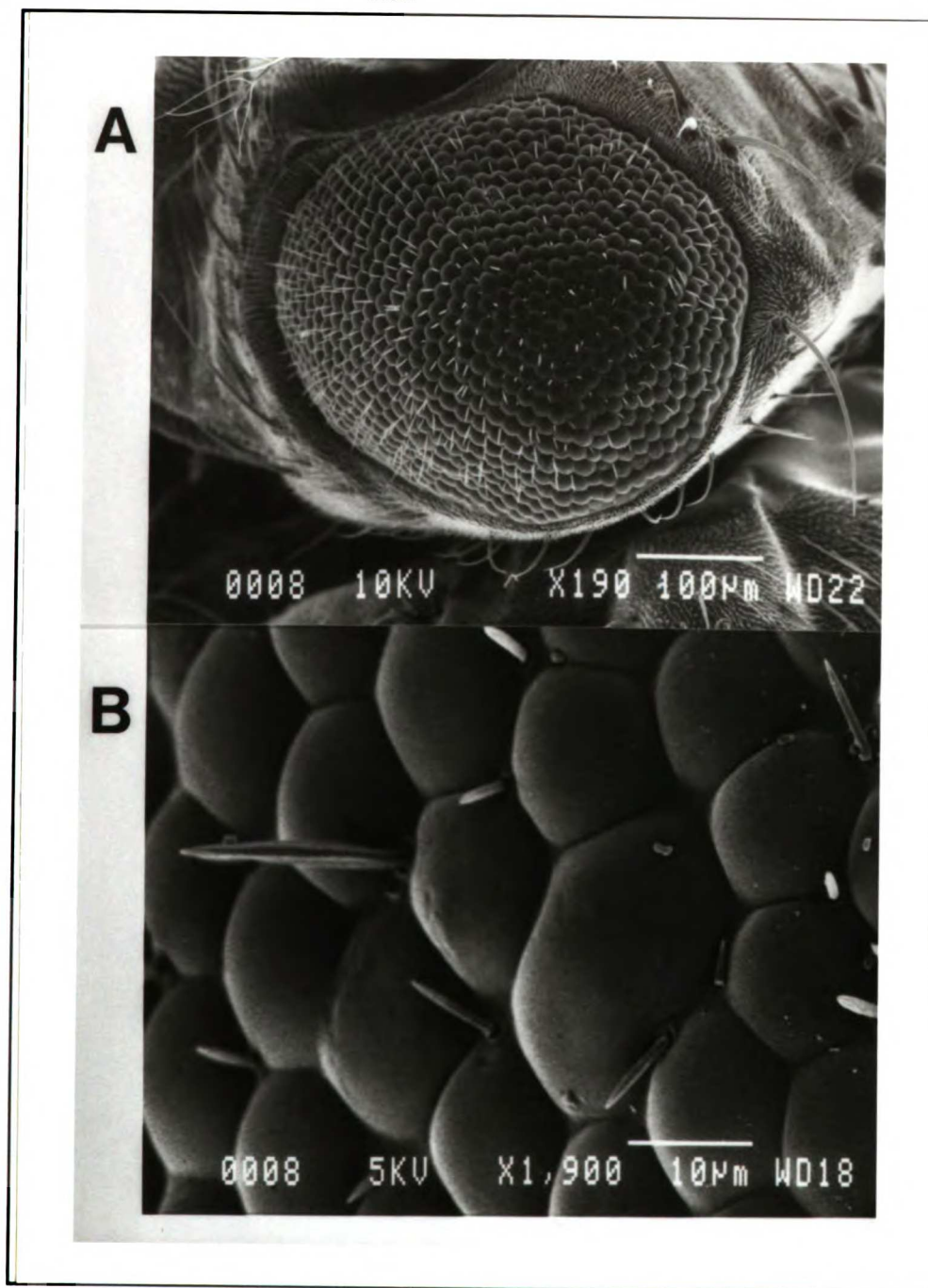
Legend figure 3.3:

Scanning electron microscopy of abl-dab X8/ X42 flies.

    A. Magnification is 190X

    B. Magnification is 1900X

174

Figure 3.4

Section through a $\dfrac{\text{Df(3L) st j7 dab}^{M2}\text{ fer}^{X8}}{\text{fer}^{X42}}$ eye

Legend figure 3.4:

Tangential section through the eye of aa abl-dab X8/X42 fly.

Magnification is 100X.

cannot be certain that the *dab* mutation alone is sufficient for this interaction. In order to determine whether an *abl* mutation is also necessary, a chromosome that contains the *abl* rescue transposon, tnabl, will be crossed into the *abl-dab* X42/X8 flies. Once the requirement for the *abl* mutation has been addressed, it will be important to show that other alleles of *dab* (or *abl-dab*) also show this enhancement of the *fer* eye phenotype.

Based upon the enhanced eye phenotype observed in the *abl-dab* X42/X8 flies several models could explain the function of these genes during the development of the eye. If *abl* is found to be required for the *abl-dab* interaction with *fer*, then it would suggest that an *abl-dab* dependent signaling pathway is acting during the development of the interommatidial bristles. *abl* and *dab* may function in a pathway that is separate from the *fer* dependent signaling pathway or they may act as a component of the *fer* pathway itself.

Alternatively, the enhancement of the *fer* eye phenotype observed in the *abl-dab* X42/X8 flies may require only a mutation in *dab*. The *dab* gene product may function downstream in the *fer* dependent pathway in addition to its already characterized role in the *abl* dependent signaling pathway. According to this hypothesis, in the *abl-dab* X42/X8 flies the decreased *dab* activity causes a further decrease in a *fer* dependent signal. Because the *fer* dependent signal is reduced, more of the cells in the developing eye now fail to receive enough signal to complete normal eye development which leads to an enhancement of the eye phenotype. If this model is correct, then *dab* is a component of two separate NRTK signaling pathways. This process may be similar to the way RTKs signal, where a single gene product may act downstream of multiple RTKs.

It is important to note that the extent of the function of the *dab* gene product during eye development has not been fully characterized. Therefore, *dab* may also function in a signaling pathway that is independent of both *abl* and *fer* during eye development. If this pathway were functionally redundant to the *fer* dependent pathway, then the disruption of this pathway in the *abl-dab* X42/X8 flies might uncover additional requirements for *fer* function during eye development which would lead to an enhancement of the rough eye phenotype in the *abl-dab* X42/X8 flies.

Once the interaction between the *abl-dab* mutation and the *fer* mutation has been confirmed using multiple *fer* alleles and multiple alleles of *dab* or *abl-dab,* then the exact nature of the enhanced eye phenotype exhibited by the mutant flies should be characterized in more detail. Larval and pupal eye discs from double mutants should be stained with antibodies that recognize the different cell types in the developing eye in order to identify which cell types are affected in the *abl-dab* X42/X8 flies. In addition, mosaic analysis of both the *abl-dab* X42/X8 mutants and the *fer* mutants alone would help to identify which cells require *fer* function in the developing eye and which cells are sensitive to the dosage of (*abl-*) *dab* in the *fer* mutant eye. Finally, biochemical analysis will be necessary to determine which of the possible signaling pathways are affected by the *abl-dab* mutations in the *fer* mutant background.

Interactions between the *fer* mutations and the *Son of sevenless* mutation.
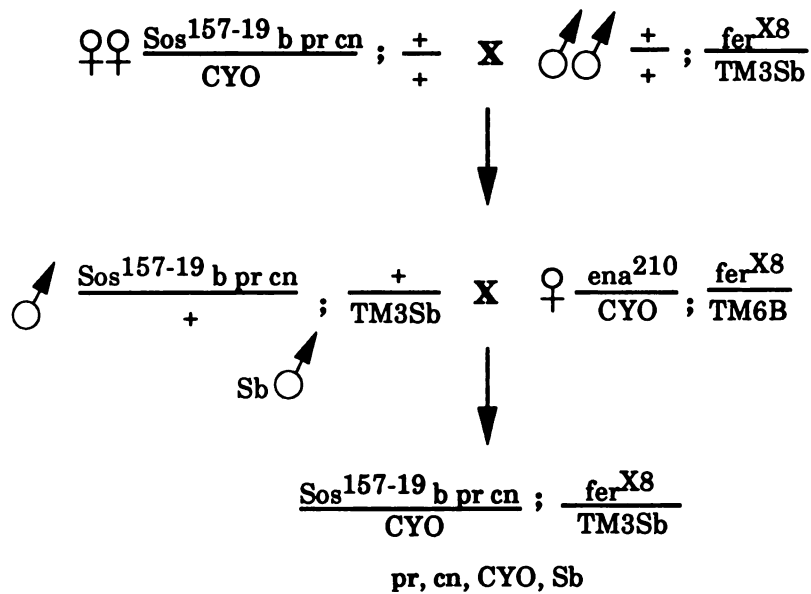
Sos was first identified as a dominant suppressor of a weak loss of function *sev* allele, and was subsequently shown to also enhance the phenotype of a temperature sensitive loss of function *sev* mutation at the

permissive temperature (Rogge, Karlovich et al. 1991; Simon, Bowtell et al.

1991). Molecular analysis of *Sos* revealed that the gene encodes a protein

that is similar to *cdc 25* of *S. cerevisiae*. *cdc25* acts as a positive regulator of

ras function by stimulating the exchange of GDP for GTP on p21^{ras}

(Robinson, Gibbs et al. 1987). The identification of *Sos* has supported the

hypothesis that all RTKs signal through a *ras* dependent signaling pathway.

Indeed further genetic characterization has shown that *Sos-ras* also functions

in the *torso* and *DER* signaling pathways (Simon, Bowtell et al. 1991; Doyle

and Bishop 1993). The requirement for *Sos-ras* function in several different

RTK signaling pathways is consistent with the observation that mutations in

both *ras* and *Sos* are lethal. Although there is substantial evidence that *ras*

may function downstream of mutated oncogenic NRTKs in vertebrate cells,

there very little evidence that normal cellular NRTKs signal through a *ras*

mediated pathway. In fact, the *Sos* mutation does not seem to interact with

the *abl* mutations in *Drosophila* (Mike Hoffmann personal communication).

This result suggests that unlike the signaling mechanism observed with

RTKs, the *ras* dependent signaling pathway does not appear to function

downstream of all normal cellular NRTKs.

Since it had been shown that *Sos* and *ras* were required for normal eye

development in *Drosophila*, I wanted to investigate whether *Sos*, and by

inference the *ras* dependent signaling pathway, interacted with the *fer*

dependent pathway during eye development. I crossed the *sos*$^{157-19}$ mutant

allele into the *fer* mutant background, and tested the effect of a heterozygous

Sos mutation on the phenotype of a *fer* mutant. The *Sos* mutation was

crossed into three different *fer* mutant allele combinations, X42/X8, X42/X42,

and X42/35.3 (Figure 3.5). The *Sos-fer* mutant flies were analyzed for the

Figure 3.5

Construction of the strains with the Sos^{157-19} mutation in the *fer* mutant background

1.

$$\female\female \ \frac{Sos^{157-19} \text{ b pr cn}}{CYO} \ ; \ \frac{+}{+} \qquad X \qquad \male\male \ \frac{+}{+} \ ; \ \frac{fer^{X8}}{TM3Sb}$$

$$\downarrow$$

$$\male \ \frac{Sos^{157-19} \text{ b pr cn}}{+} \ ; \ \frac{+}{TM3Sb} \qquad X \qquad \female \ \frac{ena^{210}}{CYO} \ ; \ \frac{fer^{X8}}{TM6B}$$

$$Sb\ \male$$

$$\downarrow$$

$$\frac{Sos^{157-19} \text{ b pr cn}}{CYO} \ ; \ \frac{fer^{X8}}{TM3Sb}$$

pr, cn, CYO, Sb

2.

$$\male\male \ yw \ ; \ \frac{Bc \ Elp}{CYO} \ ; \ \frac{Ki}{TM3Sb \ Ser} \qquad X \qquad \female\female \ \frac{+}{+} \ ; \ \frac{fer^{X42}}{fer^{X42}}$$

$$\downarrow$$

$$\male \ yw \ ; \ \frac{+}{CYO} \ ; \ \frac{Ki}{fer^{X42}} \qquad X \qquad \female \ \frac{Sos^{157-19} \text{ b pr cn}}{CYO} \ ; \ \frac{fer^{X8}}{TM3Sb}$$

$$\male \ yw, \ CYO, \ Ki$$

$$\downarrow$$

$$\frac{Sos^{157-19} \text{ b pr cn}}{CYO} \ ; \ \frac{fer^{X42}}{TM3Sb}$$

pr, cn, CYO, Sb
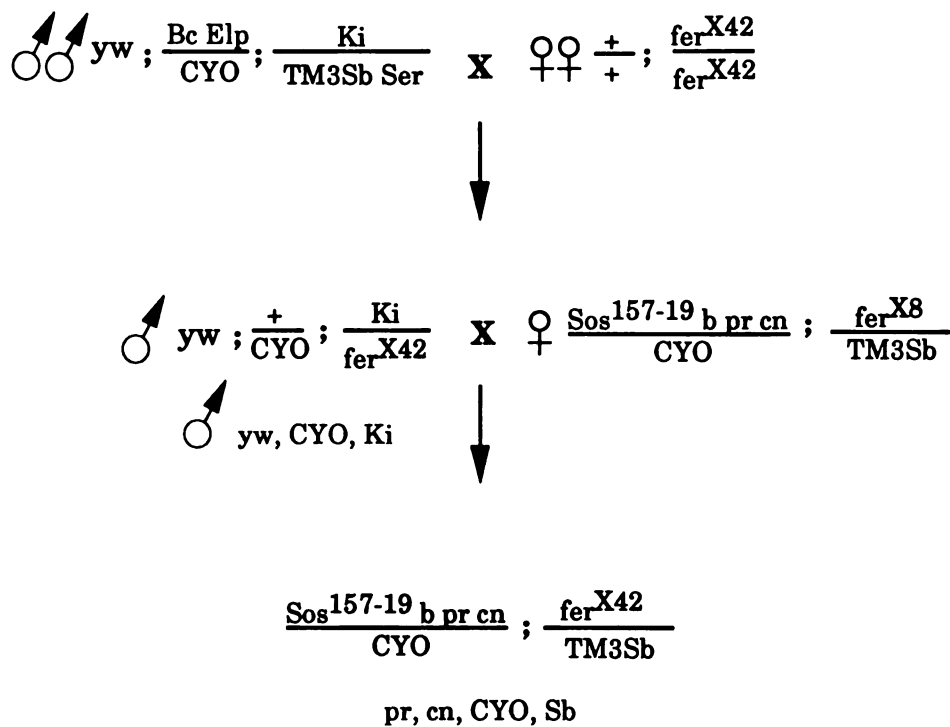
Legend figure 3.5:

The construction of strains containing the Sos[157-19] mutant allele in the fer[X8] and the fer[X42] mutant backgrounds.

effects of the *Sos* mutation on the lethality of the *fer* mutations and on the development of the compound eye. The lethality of the *fer* mutations was not affected in any of the three classes of *Sos-fer* mutants (Figure 3.6). In addition, the defect in macrochaete development normally observed in *fer* mutant adults did not seem to be altered. The rough eye phenotype observed in the *fer* mutant adults was, however, enhanced.

One of the classes of *Sos-fer* mutant adults, *Sos-X42/X8*, developed eyes that were markedly rougher than eyes of either the *fer* mutants or the *abl-dab* X42/X8 flies (Figure 3.7). The eyes in the *Sos-*X42/X8 appeared to be smaller than wild type and much more disorganized. SEM showed that when these eyes were compared to those of the *fer* mutants, many of the ommatidia were abnormally shaped and many more of the interommatidial bristles were missing or mislocalized. The *Sos-*X42/X42 adults did not show any significant enhancement of the rough eye phenotype (Figure 3.8). We have shown that the X42 allele is not a protein null, instead this allele appears to produce a truncated form of the *fer* gene product. X42/X42 mutant flies exhibit a weak eye phenotype, and the activity of the *fer* in these mutant eyes may be sufficient that a decrease in *Sos* activity does not enhance the phenotype. The effect of an *Sos* mutation on the development of the eye in the *Sos-*X42/P35.3 flies is presently under investigation.

The enhanced rough eye phenotype of the *Sos-*X42/X8 flies was initially characterized by sectioning the mutant eyes. Although the quality of these sections was not very good, I could identify several ommatidia that contained fewer than the normal seven photoreceptors (Figure 3.9). Thus the decrease in *Sos* activity caused by the heterozygous mutation in *Sos* of the *Sos-*X42/X8 flies has uncovered a role for *fer* in the development of the photoreceptor cells.

Figure 3.6
The effects of the $Sos^{157\text{-}19}$ mutation on the *fer* mutant phenotype

A. The crosses:

$$\frac{Sos^{157\text{-}19}\,b\,pr\,cn}{CYO}\;;\;\frac{fer^{X8}}{TM3Sb}\quad\mathbf{X}\quad\frac{fer^{X42}}{TM3Sb}$$

$$\frac{Sos^{157\text{-}19}\,b\,pr\,cn}{CYO}\;;\;\frac{fer^{X42}}{TM3Sb}\quad\mathbf{X}\quad\frac{fer^{X42}}{TM3Sb}$$

B. The results:

	Surviving Adults	Eye phenotype
$\dfrac{Sos^{157\text{-}19}\,b\,pr\,cn}{+}\;;\;\dfrac{fer^{X8}}{fer^{X42}}$	16%	enhanced
$\dfrac{Sos^{157\text{-}19}\,b\,pr\,cn}{+}\;;\;\dfrac{fer^{X42}}{fer^{X42}}$	78%	unaffected

Legend figure 3.6:

The effects of the Sos^{157-19} mutation on the phenotype of fer mutations.

All crosses were done in two ways: Male strain 1 X Female strain 2 and

Female strain1 X male of strain 2.

Figure 3.7

Scanning Electron microscopy of $\dfrac{Sos^{157\text{-}19}\,b\,pr\,cn}{+}$; $\dfrac{fer^{X8}}{fer^{X42}}$ eyes
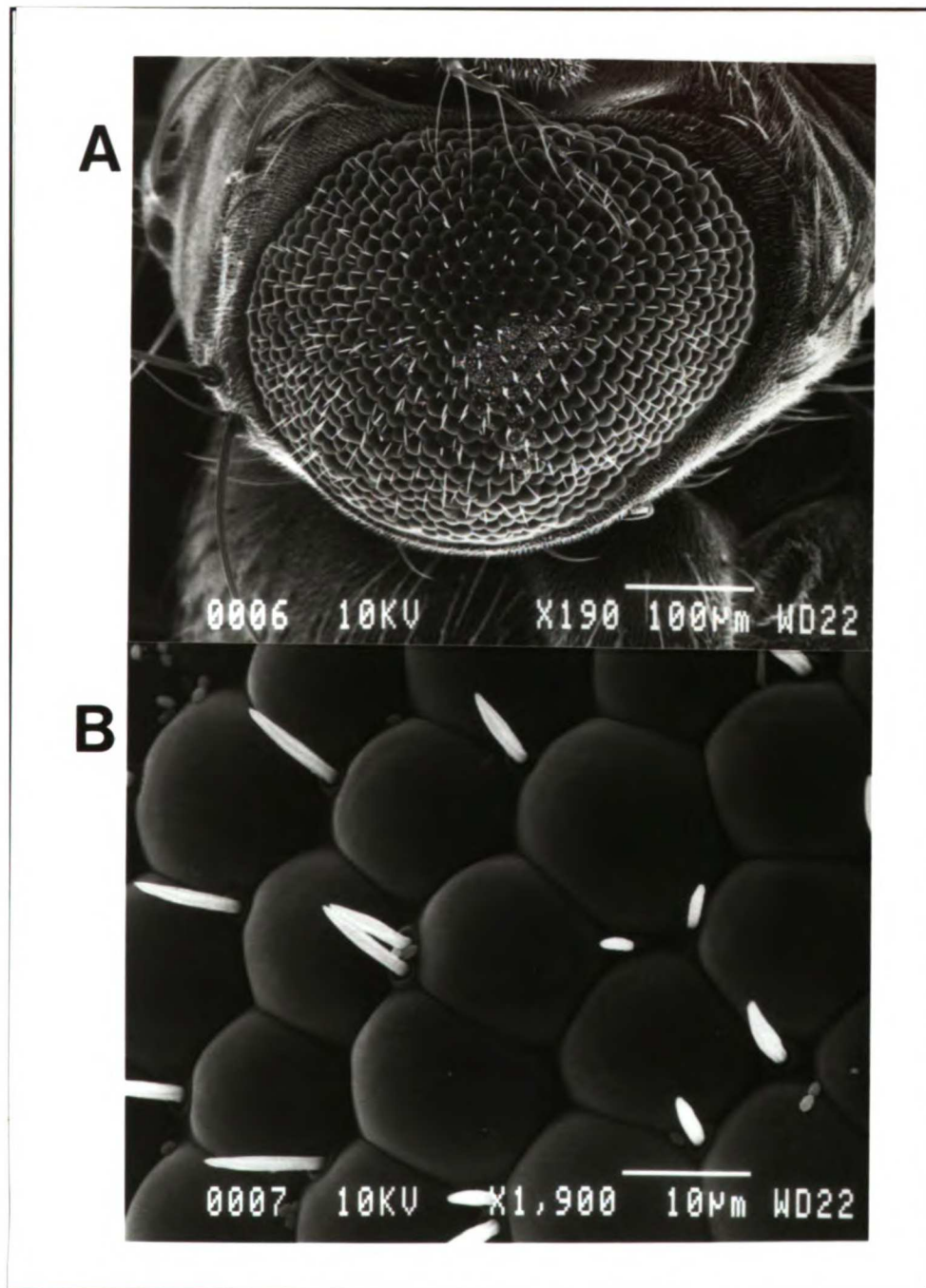
Legend figure 3.7:

Scanning electron microscopy of Sos^{157-19} ; fer^{X8}/fer^{X42} mutant eyes.

    A. Magnification is 190X

    B. Magnification is 1900X

Figure 3.8

Scanning Electron microscopy of $\dfrac{Sos^{157\text{-}19}\ b\ pr\ cn}{+}$; $\dfrac{fer^{X42}}{fer^{X42}}$ **eyes**
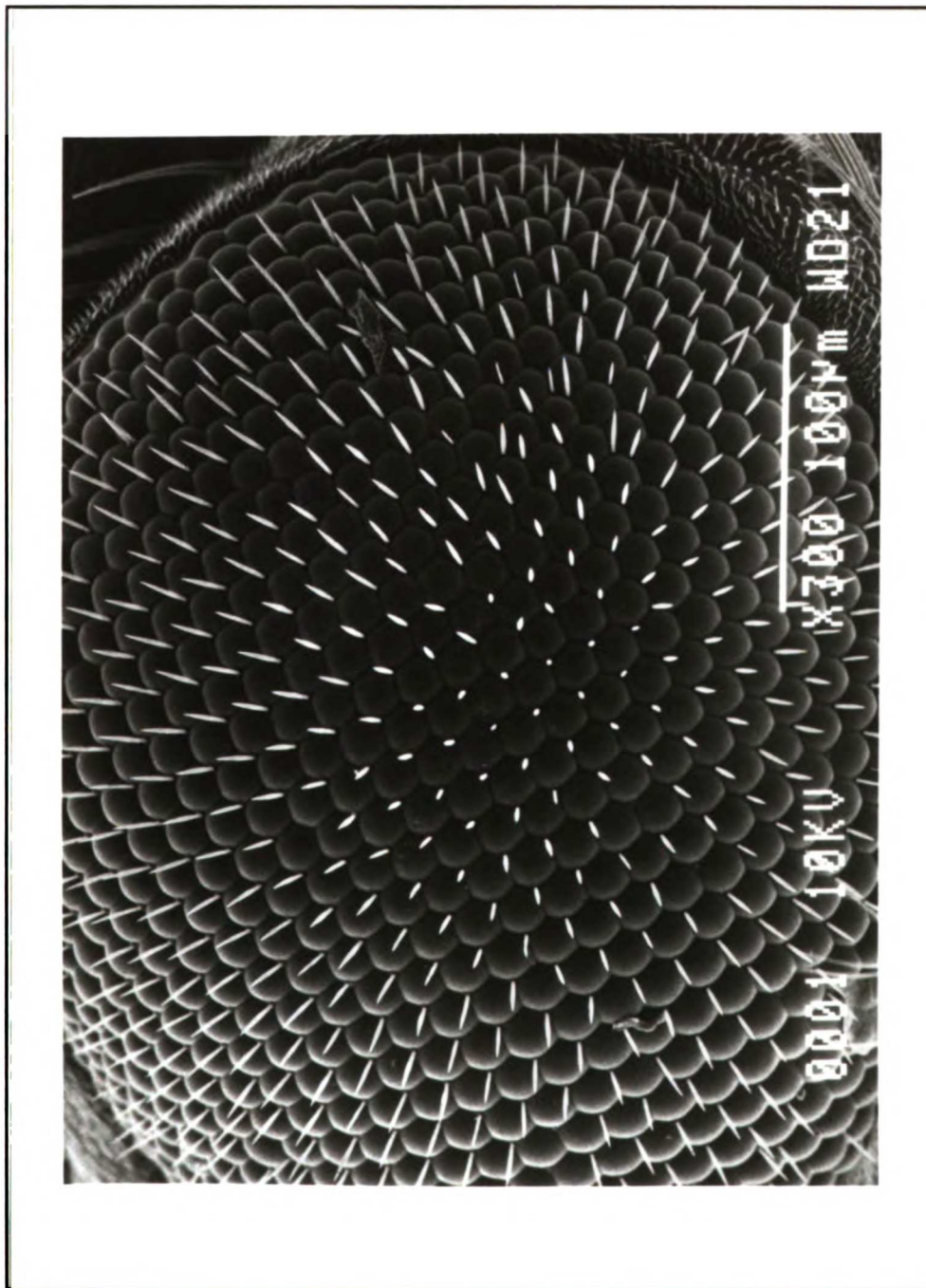
Legend figure 3.8:

Scanning electron microscopy of Sos^{157-19} ; fer^{X42}/fer^{X42} mutant eyes.

Magnification is 300X.

Although *fer* is expressed in the developing photoreceptors, the *fer* mutant phenotype did not reveal any requirement for *fer* function in the development of the photoreceptor cells. This requirement may be compensated for by a redundant signaling pathway that requires *Sos-ras*. Two RTKs, *sev* and *DER,* have been shown to play an important role in the development of the photoreceptor cells and in the correct assembly of the ommatidia in the eye (Baker and Rubin 1989; Rubin 1991; Baker and Rubin 1992). Genetic experiments have demonstrated that *ras* and *Sos* function downstream of both of these RTKs. *fer* may function either in parallel with one of these RTK mediated pathways or as a component of one of these pathways.

It is also possible that *fer* functions in a different manner during eye development. The level of *fer* dependent signaling activity necessary for normal photoreceptor development may be low enough that a mutation in *fer* does not affect photoreceptor development. The additional mutation in one copy of *Sos* may reduce the *fer* dependent signal to a level that now is unable to support normal photoreceptor development. These data are consistent with the hypothesis that *Sos-ras* acts downstream of *fer*. If this model is true, then these results represent strong evidence that the *ras* mediated signaling pathway can also function downstream of a normal cellular NRTK.

This model could also provide some insight into the mechanism of transformation by *v-fps*. In fibroblasts, proliferation can be induced by several growth factors that act through a *ras* mediated signaling pathway (Smith, DeGudicibus et al. 1986). Expression of *v-fps* in these cells might cause the hyper stimulation of the *ras* dependent pathway that results in over proliferation of the cells. The stimulation of the *ras* mediated pathway

Figure 3.9

Sections through $\dfrac{Sos^{157-19}\ b\ pr\ cn}{+}$; $\dfrac{fer_X8}{fer_X42}$ eyes
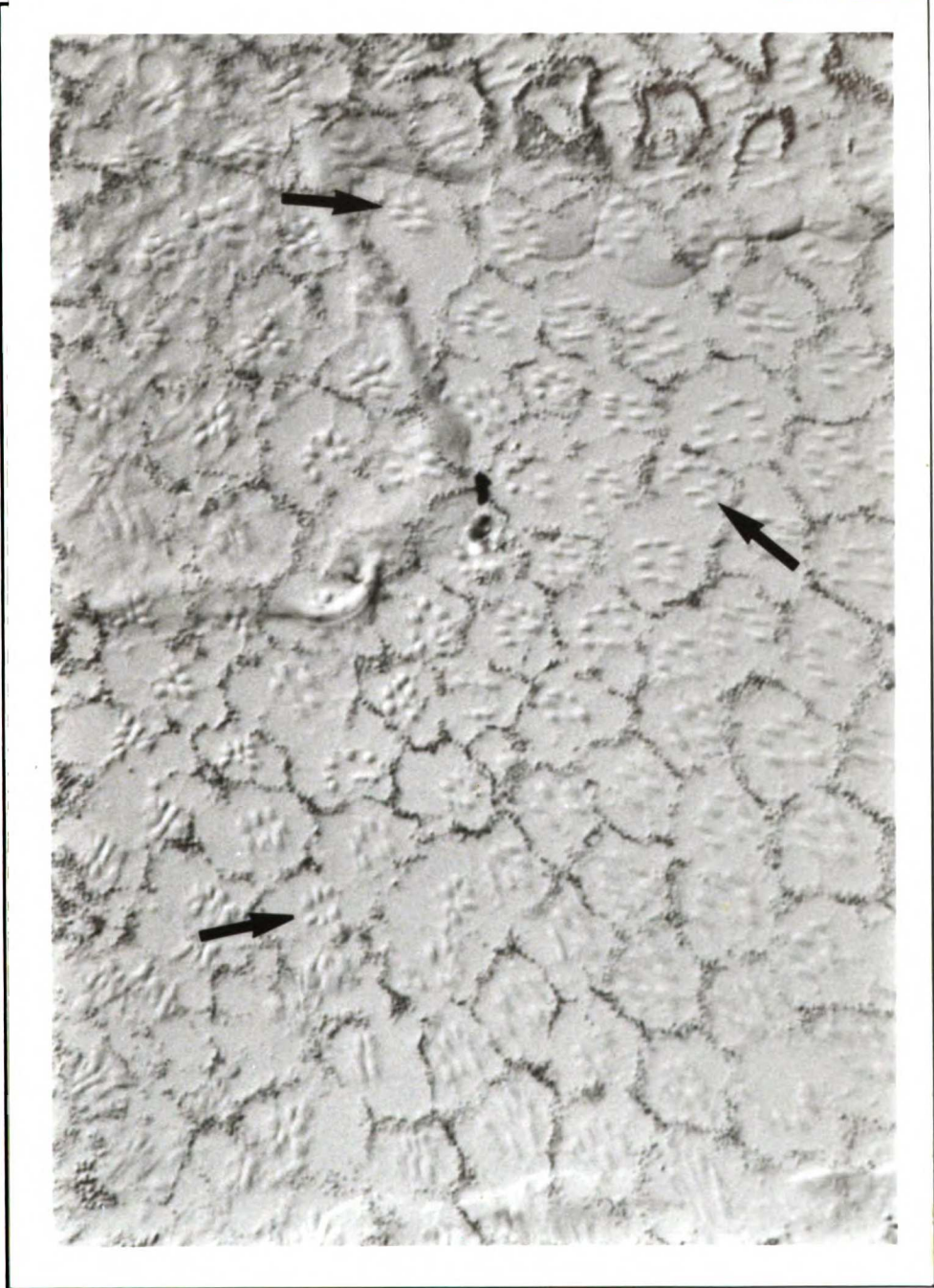
Legend figure 3.9:

Tangential section through a mutant $Sos^{157\text{-}19}$; fer^{X8}/fer^{X42} eye.

Magnification is 100X.

The arrows point out ommatidia that contain only six photoreceptor cells.

would not be a new function for *fps*, since it appears from the results in *Drosophila*, that *fer* normally acts through a *ras* dependent pathway.

The enhanced rough eye phenotype of the *Sos-fer* flies must be characterized in greater detail. In order to determine exactly which cells are affected by the addition of the an *Sos* mutation in a *fer* mutant background, our analysis should include the staining of larval and pupal eye discs with antibodies that recognize the different cell types in the developing eye . *Sos* was originally identified in a screen for suppressers and enhancers of mutations in RTKs. Several other mutations were also identified in this screen, and it would be interesting to see if these mutations also interact with *fer* mutations. In addition the mutations in the RTKs themselves should also be tested. If *fer* mutations suppress or enhance mutations in the *sevenless* then that result might suggest that *fer* is a component of the *sev* signaling pathway.

Work in progress: Interactions between mutations in *fer* and a *torpedo* allele of the *Drosophila EGF receptor* homologue.

One interpretation of the interaction between *fer* and *Sos* is that *fer* interacts with an RTK mediated signaling pathway that is dependent on *Sos-ras* function. In order to investigate this possibility I have started to test whether *fer* interacts with the *Drosophila EGF receptor* homologue, *DER*. Several pieces of evidence suggest that a mutation in *DER* is a good candidate for a mutation that might interact with a *fer* mutation. Genetic experiments have revealed a requirement for a *Sos-ras* mediated signaling activity in the *DER* pathway (Simon, Bowtell et al. 1991). *DER* activity is known to be required for normal eye development. A gain of function allele of *DER* called *Ellipse* (*Elp*) affects the formation of the ommatidial preclusters,

and causes a great reduction in the number of ommatidia (Baker and Rubin 1989; Baker and Rubin 1992). As a result *Elp* flies have a disorganized eye. Weak loss of function *DER* alleles, called *torpedo* alleles, also cause defects in eye development (Clifford and Schupach 1989). Flies homozygous for torpedo alleles develop rough eyes that have irregularly shaped ommatidia and abnormally distributed interommatidial bristles. In addition these flies also exhibit defects in macrochaete development, with some macrochaete severely reduced in size, missing altogether, or duplicated (Clifford and Schupach 1989). Mutations in *fer* affect eye development and macrochaete development in a manner very similar to *torpedo* mutations. A comparison of the expression pattern of the two genes during development reveals that *fer* and *DER* are coexpressed in several tissues (Katzen, Kornberg et al. 1991; Katzen, Monterras et al. 1991). Both of the genes are expressed in all the imaginal discs including the eye disc, in the follicular epithelium of the ovary, and in the ventral midline of the CNS during embryogenesis.

In order to investigate a potential interaction between *DER* and *fer* mutations , I constructed a strain that carried the *DER torpedo* allele *top^{CJ}* and the X8 allele of *fer*. The *top^{CJ}* allele is a weak hypomorphic allele that is homozygous viable, exhibits a weak eye roughening, shows a consistent loss of the ocellar macrochaete, and homozygous females produce eggs with fused dorsal appendages and ventralized embryos (Clifford and Schupach 1989). The reason that I chose the *top^{CJ}* allele was that I felt that I could easily test whether *fer* mutations enhanced or suppressed the weak phenotype exhibited by *top^{CJ}*. Double heterozygote flies, *top^{CJ}/+*;X8/TM3Sb do not exhibit any characteristics of the *top^{CJ}* or *fer* phenotypes. These flies were mated to: *top^{CJ}*/CYO flies to determine the effect that a decrease in *fer* activity caused

by the a single *fer* mutation would have on the phenotype of a homozygous *top^{CJ}* fly; and to X42/TM3Sb flies to determine the effect of a single *top^{CJ}* mutation on the phenotype of a homozygous *fer* mutant (Figure 3.10).

The heterozygous *fer* mutation did not affect the viability of the homozygous *top^{CJ}* progeny. Nor did it affect the weak rough eye phenotype (Figure 3.11) or the loss of the ocellar bristles. In collaboration with Helen Doyle, I have investigated whether the oogenesis defect exhibited by the *top^{CJ}* mutation was affected in the *top^{CJ}/top^{CJ}*;X8/+ flies. The oogenesis defect was not enhanced or suppressed by the presence of a heterozygous *fer* mutation. The X42/X8 *fer* mutant allele combination causes significant lethality, and the heterozygous *top^{CJ}* mutation did not change the extent of the lethality of the X42/X8 flies. Unfortunately I have only recovered one *top^{CJ}*/+;X42/X8 fly, SEM of this fly's eyes shows that the rough eye phenotype of the *fer* mutants may be slightly suppressed. However, since this observation is based on only one fly, we will need to examine more *top^{CJ}*/+;X42/X8 flies before we can reach any conclusions.

From these early data, it appears that, *top^{CJ}* does not interact with *fer*. However, the *top^{CJ}* *DER* allele may not have been the best choice for this analysis. Recent experiments have shown that *top^{CJ}* does not suppress the phenotype of the gain of function *Elp* alleles, therefore the decrease in *DER* function in the eye of *top^{CJ}* flies may be minimal (Baker and Rubin 1992). If we want to use the eye phenotype of *fer* as an indicator of an interaction between *fer* and *DER*, then we might want to test stronger alleles of *DER* in combination with *fer* alleles for their effects on the *fer* rough eye phenotype.
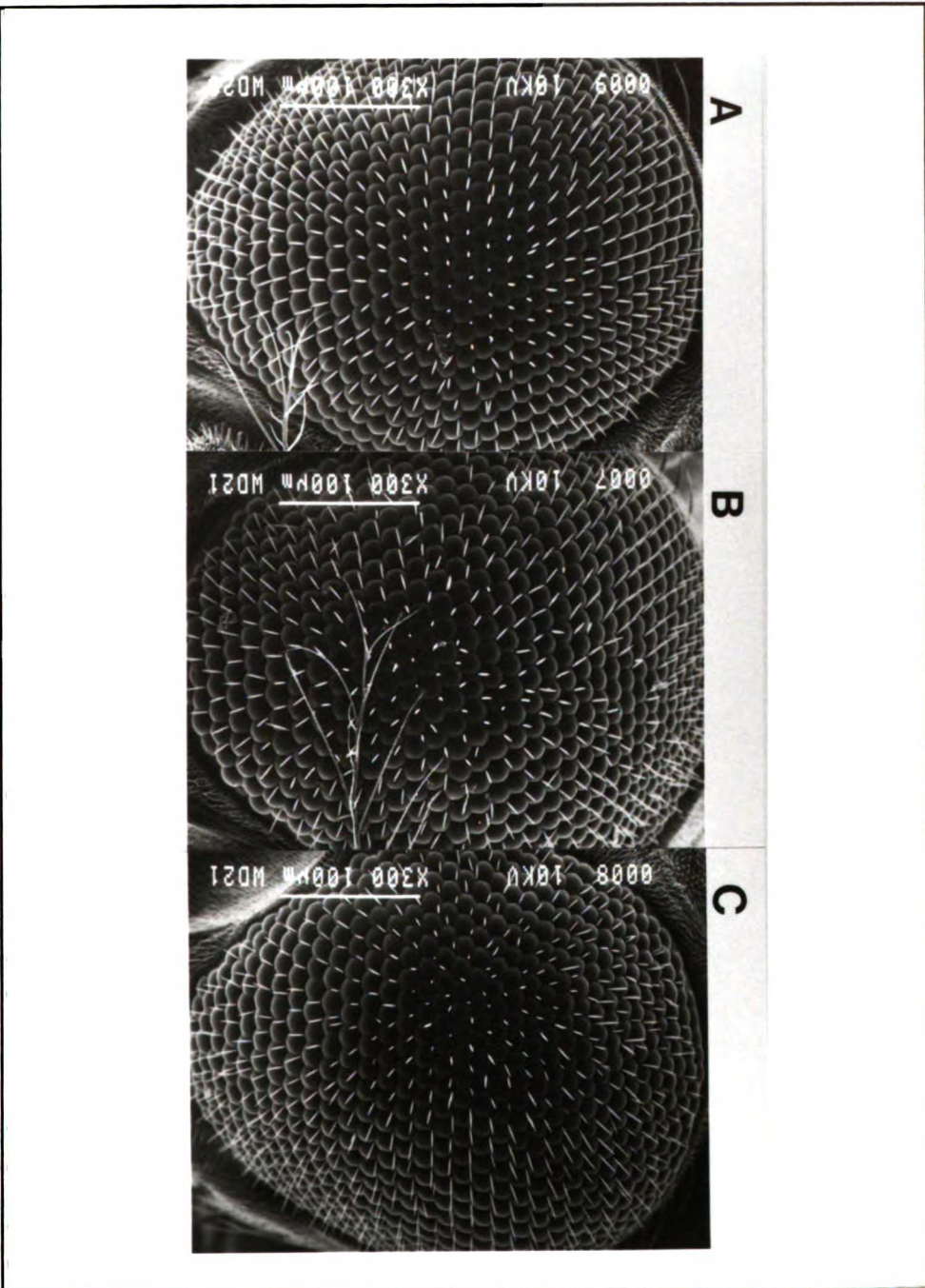
Figure 3.10

Construction of $\dfrac{\text{top}^{CJ}\,\text{cn bw}}{\text{CYO}}$; $\dfrac{\text{fer}^{X8}}{\text{TM3Sb}}$ strain

A.

$\male\male\,\dfrac{\text{top}^{CJ}\,\text{cn bw}}{\text{CYO}}$; $\dfrac{+}{+}$ **X** $\female\female\,\dfrac{+}{+}$; $\dfrac{\text{fer}^{X8}}{\text{TM3Sb}}$

$\downarrow$

$\male\,\dfrac{\text{top}^{CJ}\,\text{cn bw}}{+}$; $\dfrac{+}{\text{TM3Sb}}$ **X** $\female\,\dfrac{\text{ena}^{210}}{\text{CYO}}$; $\dfrac{\text{fer}^{X8}}{\text{TM6B}}$

Sb $\male$

$\downarrow$

$\dfrac{\text{top}^{CJ}\,\text{cn bw}}{\text{CYO}}$; $\dfrac{\text{ferX8}}{\text{TM3Sb}}$

cn, Sb

B. The crosses and the results

$\dfrac{\text{top}^{CJ}\,\text{cn bw}}{\text{CYO}}$; $\dfrac{+}{+}$ **X** $\dfrac{\text{top}^{CJ}\,\text{cn bw}}{\text{CYO}}$; $\dfrac{\text{ferX8}}{\text{TM3Sb}}$

$\dfrac{\text{top}^{CJ}\,\text{cn bw}}{\text{CYO}}$; $\dfrac{\text{ferX8}}{\text{TM3Sb}}$ **X** $\dfrac{\text{fer}^{X42}}{\text{TM3Sb}}$

	Surviving adults	Eye Phenotype
$\dfrac{\text{top}^{CJ}\,\text{cn bw}}{\text{top}^{CJ}\,\text{cn bw}}$; $\dfrac{\text{ferX8}}{+}$	100%	unaffected
$\dfrac{\text{top}^{CJ}\,\text{cn bw}}{+}$; $\dfrac{\text{ferX8}}{\text{fer}^{X42}}$	7%	unaffected (perhaps slightly suppressed)

Legend figure 3.10:

Construction of the top^{CJ} ; fer^{X8} strain, and the summary of the interactions between *torpedo* mutations and *fer* mutations.

All crosses to determine the effects of top^{CJ} on the fer mutations were done in two ways: Male of strain 1 X Female of strain 2 and Female of strain1 X Male of strain 2.

Figure 3.11

Scanning Electron microscopy of $\frac{top^{CJ}\ cn\ bw}{top^{CJ}\ cn\ bw}\ ;\ \frac{ferX8}{+}$ and $\frac{top^{CJ}\ cn\ bw}{+}\ ;\ \frac{ferX8}{fer_rX42}$ eyes

Legend figure 3.11:

Scanning electron microscopy of mutant eyes.

Magnification is 300X.

A. top^{CJ}/top^{CJ} fly.

B. top^{CJ}/top^{CJ} ; $fer^{X8}/+$ fly.

C. $top^{CJ}/+$; fer^{X8}/fer^{X42} fly.

.

Future directions: other candidates for mutations that may interact with *fer* mutations.

In the previous sections of this chapter , I described the results of experiments where I tested the *fer* mutant alleles for genetic interactions either with mutations in other protein tyrosine kinases or with mutations already known to interact with protein tyrosine kinase mutations. In this section I will discuss several mutations which exhibit phenotypes similar to the *fer* mutant phenotype. I believe that these mutations should also be tested for genetic interactions with the *fer* mutant alleles.

The defect in the development of the macrochaete of the head and thorax in *fer* mutants is very similar to the phenotype of the *Hairless* (*H*) mutation (Bang, Hartenstein et al. 1991; Bang and Posakony 1992). *H* is required at two points during macrochaete development. Early during macrochaete development, *H* is required in the undifferentiated epithelium of the wing disc for the determination of the sensory organ precursor cell, (SOP), which is the cell that will later differentiate into the four cells that make up a macrochaete (Hartenstein and Posakony 1989). Loss of *H* function at this time of macrochaete development results in the failure of the SOP to form, leading to the loss of a macrochaete. Later, *H* is also required for the proper development of the tricogen, the cell which makes the macrochaete bristle, and the tormogen, the cell which makes the socket around the macrochaete bristle. Loss of *H* function during these later stages of macrochaete development causes the tricogen to adopt the tormogen cell fate. This change of cell fate leads to the short bristle and double socket phenotypes observed in weak *H* alleles. Since the *fer* mutations show a similar range of macrochaete

phenotypes, the two genes, H and fer, may function at similar times during macrochaete development and in similar developmental processes.

$Notch$ (N) is a mutation that has been to shown to act at similar times during macrochaete development as H. Experiments using a temperature sensitive N allele (N^{ts1}) have revealed a requirement for N activity during the early stages of macrochaete development, when the SOP is determined, and later during the differentiation of the four cells that make up a macrochaete (Hartenstein and Posakony 1990). Experiments with the N^{ts1} have also revealed a requirement for N function during eye development (Cagan and Ready 1989). The local cell-cell interactions that determine the organization of the cells that make up the compound eye are dependent on N activity. Consequently, the disruption of N function at different times during eye development can lead to an abnormal determination of cell fate which causes defects in different subsets of cells in the developing eye. Loss of N function early in eye development can cause defects in photoreceptor development, while loss of N function later during development can cause defects in bristle development which often lead to a loss of interommatidial bristles. Other defects resulting from a loss of N activity late during eye development include a disorganization of the bristles and defects in differentiation of the secondary and tertiary pigment cells which causes the ommatidia to be abnormally shaped. The fer mutant eyes exhibit a loss and mislocalization of interommatidial bristles and abnormally shaped ommatidia similar to the phenotype observed with the N^{ts1} allele. Genetic experiments have shown that N and H mutations interact genetically, and N mutations interact with Elp alleles of DER (de la Concha, Dietrich et al. 1988; Baker and Rubin 1992). By testing all of these mutations, $N,H,$ and DER for interactions with

fer mutations, we may be able to better understand the role of *fer* in the development of the macrochaete and the compound eye.

There are a large number of mutations known to affect muscle development in *Drosophila* (Deak 1977; Koana and Hotta 1978; Deak, Bellamy et al. 1982; Lindsley and Zimm 1992). Most of these mutations were initially isolated as flightless mutations. The abnormalities in the development of the indirect muscles observed in the *fer* mutants are similar to those observed in other mutants. I believe that there are four mutants which affect muscle development that are particularly good candidates for mutations that might interact with *fer*. These four mutations are *stripe (sr)*, *erect wing (ewg)*, *l (1) myospheroid (l(1)mys*, and *l (1) fibrillardysgenesis (l(1)fdg)*.

sr and *ewg* were originally isolated as flightless mutations. Both of these mutations show a primary defect in the development of the dorsal longitudinal muscles (DLMs), with weaker effects, depending upon the alleles, on the dorsal ventral muscles (DVMs) and the tergal depressor of the throcanter (TDT) (Deak 1977; Koana and Hotta 1978; Deak, Bellamy et al. 1982; Fleming, Zusman et al. 1983; Costello and Wyman 1986; Fleming, DeSimone et al. 1989; Lindsley and Zimm 1992). In addition, lethal alleles of both *sr* and *ewg* exhibit an embryonic CNS phenotype. In *sr* mutant embryos, it appears that fewer than the normal number of neurons differentiate and some neurons have altered projections (De La Pompa, Garcia et al. 1989). *ewg* mutant embryos exhibit numerous interruptions of the longitudinal tracts of the embryonic CNS and many neurons show aberrant projections (De La Pompa, Garcia et al. 1989; Fleming, DeSimone et al. 1989). Certain *ewg* alleles also show defects in retinal development (De La

Pompa, Garcia et al. 1989). Given the similarities in the phenotypes that *fer*, *sr*, and *ewg* mutants exhibit in the indirect flight muscles and the observation that *fer* is expressed in the ventral midline of the CNS late during embryogenesis, the *sr* and *ewg* mutations appear to be a good candidate mutations to test for genetic interactions with *fer*.

lethal (1) myospheroid (*l(1)mys*) is a mutation in the common ß subunit of the *Drosophila* integrins (Newman and Wright 1981; MacKrell, Blumberg et al. 1988; Lindsley and Zimm 1992). The somatic and visceral muscles of *l(1)mys* mutant embryos fail to make their normal attachments with the epidermis. Consequently, the muscles retract from their attachment sites causing the midgut and the nervous system to herniate out of the dorsal suture of the embryo (Newman and Wright 1981; Volk, Fessler et al. 1990). In vertebrates, it is well known that integrin interactions can be regulated by tyrosine phosphorylation of the integrin ß-subunit (Hirst, Horowitz et al. 1986). Like *l(1)mys*, mutations in *fer* also affect muscle development, it would be interesting to test whether *fer* mutations interacted with *l(1)mys* mutations.

The last mutation that I will discuss is *lethal (1) fibrillardysgenesis* (*l(1)fdg*) (Newman and Wright 1983). This mutation causes a disorganization of the myofibril components and abnormal convolutions of the myofibrils. The disruption of myofibril structure observed in *l(1)fdg* mutants is similar to that seen in the *fer* X42/X42 mutant adults (see Figure 2.19). In addition, *l(1)fdg* mutants exhibit defects in the development of the midgut, with mutant embryos failing to make the morphogenetic movements necessary to form the four constrictions normally seen in the midgut. Since *fer* is expressed in the midgut during embryogenesis and *fer* mutant flies exhibit

defects in myofibril structure, *l(1)fdg* appears to be another mutation that should be tested for interactions with *fer* mutations.

Appendix 1

Methods and Materials

Isolation of cDNA clones for the 2.3 kb *dfps-85D* mRNA:

Lambda phage clones were isolated from a *Drosophila melanogaster* adult head cDNA library obtained from Dr. Gerry Rubin at UC-Berkeley. A 1.5 kb fragment (nucleotides +539 - +2029 relative to the AUG start codon in the 3.3 kb mRNA) from the a partial cDNA coding for the 3.3 kb mRNA was used a probe at high stringency. The lambda phage library was plated out at ~20000 plaques per plate and duplicate filters were lifted and processed from each plate according to (Ausubel, Brent et al. 1990). The filters were hybridized at high stringency, 20 mM HEPES (N-2-hydroxyethylpiperazine-N'-2-ethanesulfonic acid) pH 7.0, 2.5X Denhardt's solution (1X Denhardt's is 0.2 mg/ml Ficoll, 0.2 mg/ml Polyvinylpyrrolidone, 0.2 mg/ml Bovine serum albumin), 3X SSC (1X SSC is 0.15 M NaCl, 0.15 M sodium citrate), 0.2 mg/ml salmon sperm DNA, and 50% Formamide (vol/vol) at 42° C. The filters were washed for one hour 1x in 2x SSC, 0.2% sodium dodecyl sulfate (SDS) (wt/vol), 0.1% sodium pyrophosphate (wt/vol) at 42º and 1x in 0.1x SSC, 0.2% SDS, 0.1% sodium pyrophosphate at 42 ºC. The filters were exposed to autoradiograghic film at -70ºC with intensifying screens. Positive plaques were picked using the large end of a pasteur pipet and the phage were resuspended in 1.0 ml of SM buffer (10 mM MgSO4, 10 Mm Tris pH 7.5, 0.1 mg/ml gelatin). Potential positive plaques were replated at lower density and screened again in order to plaque purify the phages. DNA isolated from plaque purified phage clones that hybridized to the probe was subcloned into the EcoR1 site of PUC 19 and restriction mapped. The sequence of one clone, 9C13, was determined by chain termination sequencing according to the

Sequenase Kit protocol. The sequence of both strands of the DNA was analyzed.

Isolation of genomic DNA from the *dfps-85D* locus:

Libraries of *Drosophila* genomic DNA were screened initially using portions of the cDNA as probe and later using the ends of genomic lambda phage clones. The filters were processed as described above. Different lambda phages clones were restriction mapped and the maps of the different clones were compared to determine any overlap between the clones. In addition, Southern blot analysis was done using probes from the ends of the different genomic clones to reveal cross hybridization of different clones. A composite restriction map of the *dfps-85D* locus was generated from the maps of overlapping phage clones. The genomic phage clones were subcloned as EcoR1 restriction fragments into the EcoR1 site of PUC 18 or 19.

Determination of exon-intron boundaries:

Subclones of the genomic lambda clones were sequenced using the double stranded DNA sequencing protocol of the Sequenase™ Kit. The primers used for the sequencing reactions were derived from cDNA sequence. All intron exon boundaries conform to the consensus 5' and 3' splice site sequences as described by Mount (Mount 1982).

The size of the introns was determined in three ways. First some introns were directly sequenced. Second, PCR amplification of the intron by using primers in adjacent exons. PCR reactions were carried out in 10 mM Tris pH 8.0, 50 mM KCl, 2mM $MgCl_2$ and 0.01% gelatin with 0.2mM dNTPs, 12.5 units of Taq polymerase (Perkin Elmer Cetus), 10 pM of each primer, and 50 ng of linearized genomic subclone plasmid DNA. The reactions were run for 45 sec at 94° C, 2 minutes at the melting temperature of the primer

with the lowest melting temperature, and 2 minutes at 72º C for 30 cycles.
The PCR products were sized on a 1.5% Agarose gel. The size of the intron
was then estimated by subtracting the amount of cDNA sequence between
the two primers from the size of the PCR product. The size of the very large
introns was estimated by mapping exons onto the genomic restriction map
and estimating the size of the intron from that map.

**Construction of plasmids used in the S1 nuclease protection analysis
and in situ hybridization to whole mount *Drosophila* embryos:**

The pXbaS1 plasmid was constructed by first PCR amplifying an
801 bp fragment using the genomic subclone plasmid p2.7/6.4 and XbaS1 and
Xbaright primers.

XbaS1: 5' **AGA**CGAGTGTTTCGAGTATCT 3' (-398 - -371 of the 3.3 kb
mRNA)

Xbaright: 5' **AGA**GCTGATGAGAAGCCCAT 3' (+17 - +1 of the 3.3 kb
mRNA)

The amplified fragment was purified from a 1.5% Agarose gel using the Gene
Clean™ protocol. Since the primers contained Xba1 half sites at their 5'
ends, in bold, when the fragment is ligated to itself the Xba1 site is
regenerated. The fragment was ligated to itself according to the standard
DNA ligation reaction of the red book. The ligated fragments were then cut
with Xba1 and cloned into the Xba1 site of PUC 19. Clones with the
appropriate insert were sequenced to determine if the PCR amplifcation had
introduced any mutations, and to determine the orientation of the insert in
the vector.

The p9C13S1 plasmid was derived by digesting the p9C13 cDNA clone
with PvuII and EcoR1. PvuII cuts at a site 166 bp 5' to the AUG start codon

of the 2.3 kb mRNA, and EcoR1 cuts at a site in the polylinker of PUC 19. The 600 bp PvuII-EcoR1 fragment was cloned into the Sma1-EcoR1 sites of PUC 19.

The pEmbprobe was constructed by digesting the 3.3 kb mRNA cDNA clone called pDfps with Pst1. Pst1 cuts at two sites in the cDNA, +686 and +1749. The intervening 1063 bp band was cloned into the Pst1 site of PUC 18.

The pKinprobe plasmid was constructed by cutting pDfps cDNA clone with Pst1 and HindIII. The 1225 bp band that spans from the Pst1 site at +1749 to the HindIII site at +2974 was cloned into the Pst1 and HindIII sites of PUC 18.

Isolation of RNA from different stages of *Drosophila* development:

Adult flies or *Drosophila* at different stages of development were mixed with 2 volumes of 10mM Tris pH7.5, 1mM EDTA, 0.2 M NaCl, and 1.0 % SDS and 1 volume of Phenol. This mixture was homogenized in the polytron tissue mixer for two 30 second bursts. One volume of chloroform was added and the tubes were vortexed for one minute. The samples were spun for 15 minutes at 3500 rpm in the J6M cetrifuge. The aqueous phase and the interphase layer were removed and mixed with 2 volumes of chloroform in Oak Ridge Tubes and vortexed for 2 minutes. The tubes were centrifuged at 18 Krpm for 20 minutes in a J2-22M cetrifuge to compact the interphase layer. The aqueous phase was removed and extracted 3-5 times with phenol/chloroform (1:1). The aqueous was removed and extracted once with chloroform. The RNA was precipitated overnight at -20° C by adding NaCl to a final concetration of 0.2 M and two volumes of ethanol.

Poly A+ RNA was selected on an oligo dT cellulose column according to the protocol in (Ausubel, Brent et al. 1990).

S1 nuclease protection analysis:

Single stranded DNA S1 probes were produced by single primer PCR using either a ^{32}P end labeled primer to produce an end labeled probe or the PCR reaction was done in the presence of ^{32}P dCTP to produce a uniform labeled probe. The following primers were used to make single stranded DNA S1 probes:

5' #1 5' AGCTCAGCGCCGAGTATCTCG 3' (-213 - -234 relative to the AUG start codon of the 3.3 kb mRNA)

fps S1 5' GTTTCGCGGACCAGGAAGTC 3' (+1628 - +1608 relative to the AUG start codon of the 3.3 kb mRNA)

The S1 probe used to map the start site of transcription of the 3.3 kb mRNA was made in a PCR reaction utilizing pXbaS1 plasmid linearized at the Hind III site in the polylinker and the PCR conditions described above with the exception that the cold dCTP was replaced with 50 μCi of 3000mCi/ mM ^{32}P-dCTP. The end labeled probe used to determine the timing of the expression of the two mRNAs during *Drosophila* development was produced in a single primer PCR eaction using a ^{32}P end labeled primer. The fps S1 primer was end labeled with ^{32}P by a standard kinase reaction (Ausubel, Brent et al. 1990). 100 ng of end labeled primer was used in the single primer PCR reaction as described above utilizing the p9C13 S1 plasmid linearized at the BamH1 site of the polylinker as the template.

2.5 volumes of gel loading buffer (90% Foramide, 1X TBE , 0.01% Bromo-phenyl-blue, 0.01% Xylene cyanol) were added to the PCR reactions and the samples were boiled for 5 minutes. The denatured samples were run

on a 6% acrylamide, 7M urea gel. The gel was exposed to autoradiographic film, wet for 10 minutes at room temperature and the labeled band was cut out of the gel. The probe was eluted from the gel for 2hours at 42°C in elution buffer (0.5 M sodium acetate, 0.5 % SDS, and 1mM EDTA pH 8.0). The probe was phenol/ chloroform/ iso-amyl alcohol (25:24:1) extracted and precipitated in 2 volumes of ethanol at -70°C.

500000 counts per minute of probe was mixed with 10 μg of poly A$^+$ selected RNA and allowed to hybridize overnight at 30∞C in hybridization buffer (80% Formamide, 400mM NaCl, 40mM MOPS pH 6.7, 1mM EDTA) in a total volume of 15μl. 240μl of ice cold S1 digestion mix (250mM NaCl, 0.03 M sodium acetate pH 4.6, 1mM ZnSO$_4$, 13μg/ml salmon sperm carrier DNA, 350 units/ml S1 nuclease (Sigma)) were added and the samples were digested for 2 hours at room temperature. The whole digestion reaction was then transfered to a new tube and 10 μg of yeast tRNA carrier was added to each reaction. The reaction was extracted 1X with phenol/chloroform/iso-amyl alcohol (25:24:1) and the protected fragments precipitated in 2 volumes of ethanol at -70°C. The precipitated DNA was resuspended in 10 μl of gel loading buffer and boiled for 5 minutes. The denatured samples were run on a 6% acrylamide, 7 M urea gel. The gel was dried and exposed at room temperature or at -70 °C with an intensifying screen to autoradiographic film.

Primer extension analysis:

The primer extension analysis was done as described in the red book with the exception that Moloney Murine Leukemia Virus RNAse H$^-$ reverse transcriptase (Superscript™ BRL) and the supplied buffer were used in place of AMV reverse transcriptase and its buffer. The primers used in the primer extension reactions were 5' #1 as described above and Race 1.

Race 1: 5' GCTTGGAGCCGCTTCAACTGG 3'

(-293 - -313 relative to the AUG codon of the 2.3 kb mRNA)

Direct RNA Sequencing:

The direct RNA sequencing of the 5' end of the 3.3 kb mRNA was done as described in Geliebter BRL Focus **9:1** pp.5-8 with the following changes. 34 ng of ^{32}P end labeled 5' #1 primer were hybridized to 50µg of poly A$^+$ RNA isolated from 2-24 hour after oviposition embryos in a total volume of 12 µl. The primer was allowed to anneal for 6 hours at 66° C.

RACE cloning of 5' ends of the 3.3 kb and the 2.3 kb mRNAs:

The RACE protocol was modified in the following way (Frohman, Dush et al. 1988). First strand cDNA was synthesized from poly A$^+$ selected RNA from 2-24 hour after oviposition embryos. 10 µg of RNA was mixed with 400 ng of random hexamer oligonucleotide primers in a total volume of 24 µl. The sample was heated for 10 minutes at 70°C and then quick chilled on ice. 8µl of 5X Reaction Buffer (BRL Superscript™), 4µl of 0.1M Dithiothreitol, and 2µl of 10 mM dNTPs were added. This mixture was heated at 37° C for 2 minutes then 5µl (1000 units) of Superscript ™ M-MLV RNAse H⁻ reverse transcriptase were added and the reaction was incubated at 37° C for 1 hour. The cDNA was purified with a Gene Clean ™ Kit according to the kit's protocol. Next the cDNA was tailed with dG residues. 5µl of cDNA representing ~25% of the cDNA were incubated with 2µl of 50mM dGTP (final concentration 0.5µM), 40µl of 5X buffer (supplied with the terminal deoxynucleotide transferase BRL), and 2µl of terminal deoxynucleotide transferase BRL in a total reaction volume of 200 µl. The reaction was incubated for 30 minutes at 37° C. The tailing reaction was

phenol/chloroform/iso-amyl alcohol (25:24:1) extracted and the tailed cDNA was purified by the Gene Clean™ protocol.

PCR reactions using the tailed cDNA were done as described above. The primers used in the PCR reactions were:

For the 3.3 kb mRNA: 5' #1 described above.

For the 2.3 kb mRNA:

1º PCR reaction: Head Race 5' CGCCAGGCTGGGCACGCAATA 3'

(+27 - +6 relative to the AUG start codon of the 2.3 kb mRNA)

2º PCR reaction: Head Race B 5' TCTCGTCCAGCTCTCCAGAAC 3'

(-76 - -97 relative to the AUG start codon of the 2.3 kb mRNA)

Common Primer: Race 2

5' GGATCCGAATTCCCCCCCCCCCCCCCCCC 3'

For the 3.3 kb message a single round of PCR was done with the 5' #1 primer and the Race 2 primer. The PCR reaction was run on a 1.5% gel and the 147 bp band was cut out and purified by the Gene Clean protocol. The ends of the fragment were blunted T4 DNA polymerase and the ends kinased with cold ATP according to (Ausubel, Brent et al. 1990). The fragments were then cut with EcoR1 and purified on an agarose gel. The cut fragments were cloned into the EcoR1-Sma 1 sites of PUC-18. All clones that had inserts were sequenced as described above.

The RACE cloning of the 5' end of the 2.3 kb mRNA required two sets of PCR reactions. The primary PCR reaction for the 2.3 kb message utilized the Head race and Race 2 primers. DNA produced in this reaction was a smear on the gel so DNA from the expected size range ~400-800 bp was cut out and purified by the Gene Clean protocol. This DNA was used in a secondary PCR reaction which utilized the Head Race B and the Race 2

primers. This reaction also produced a smear of DNA from ~300-600 bp which was cut out and purified. The fragments were processed for cloning as described above. All transformed colonies were screened by colony hybridization with a ^{32}P end labeled internal oligo:

Exon A : 5' GTTCCACCTCGAACTCTTTGG 3'.

(-201 - -222 relative to the AUG start codon of the 2.3 kb

mRNA.)

DNA from all positive colonies was sequenced as described above.

In situ hybridization to whole mount *Drosophila* embryos:

Embryos were collected from population cages and their age was measured as hours after oviposition. The embryos were processed and the hybridization conditions are as described in Tautz and Pfeifle (Tautz and Pfeifle 1989).

The single stranded sense and antisense DNA probes specific for the 3.3 kb or the 2.3 kb mRNA were synthesized by single primer PCR as described above with the exception that the final concentration of dNTPs is 200 nM dATP, 200 nM dCTP, 200 nM dGTP, 130nM dTTP, 70nM Digoxigenin-11-dUTP. The primers used in these reactions are as follows:

Seq 7: 5' TGAATAACGATGGTGACT 3' (+1351 - +1369 relative to the

AUG start codon of the 3.3 kb mRNA)

Seq 5: 5' CTGCTTCTCCTGGCAGCG 3' (+1136 - +1118 relative to the

AUG start codon of the 3.3 kb mRNA)

Seq 14: 5' CTCAAGAGCAGGTCGAGA 3' (-72 - -54 in the 2.3 kb

mRNA)

Head race: see above

Seq 8: 5' GCGAGGAAGAGGAATATA 3' (+2053 - +2071 relative to the AUG start codon of the 3.3 kb mRNA)

fpskin: 5' AATTCAAGGCCTCGGGAGCTG 3' (+2131 - +2110 relative to the AUG start codon of the 3.3 kb mRNA)

For the 3.3 kb mRNA specific probes: The sense probe of 398 nucleotides was synthesized using the pEmbprobe plasmid cut at the EcoR1 site of the polylinker as template and the Seq 7 oligo as primer. The antisense probe of 450 nucleotides utilized the pEmbprobe plasmid linearized at the HindIII site of the polylinker an the Seq 5 oligo as primer.

For the 2.3 kb mRNA specific probes: The sense probe of 164 nucleotides was synthesized from the p9C13S1 plasmid linearized at the Nco1 site (at +74 relative to the AUG start codon of the 2.3 kb mRNA) using the Seq 14 oligo as primer. The antisense probe of 186 nucleotides was synthesized from the p9C13S1 plasmid linearized at the BamH1 site in the polylinker using the Head race oligo as primer.

The kinase domain sense probe of 921 nucleotides was synthesized from the pKinprobe plasmid linearized at the HindIII site of the polylinker using the Seq 8 oligo as primer. The kinase domain antisense probe of 382 nucleotides was synthesized from the pKinprobe plasmid linearized at the Pst1 site of the polylinker using the fpskin oligo as primer.

The PCR products were purified by 2X precipitation in 400mM LiCl with two volumes of ethanol. After the immunohistochemistry reaction was completed, the embryos were dehydrated through a 30%, 70%, 2X 100% ethanol series and then cleared in 100% xylenes. The cleared embryos were mounted in Permount. Photographs were taken on a Zeiss Axiophot microscope using Kodal Ektar 100 film.

Fly stocks.

Flies were raised according to the procedures of (Roberts 1986).

The E134 enhancer trap line which contains a P element insertion into the *dfer* locus was kindly provided by Dr. Gerald Rubin at UC-Berkeley. All other fly stocks were obtained from Dr. Tom Kornberg, Dr. Y.N. Jan, or the Bishop laboratory. All markers are described in (Lindsley and Zimm 1992).

Preparation and analysis of *Drosophila* genomic DNA.

DNA was isolated from adult flies as described in (Katzen, Monterras et al. 1991). Southern blot techniques, generation of radioactive probes by random priming, and autoradiography of the blots was done as described in (Ausubel, Brent et al. 1990). Some blots were probed with non-radioactive Genius probes. These probes were synthesized according the Genius Kit manual, and all hybridizations, and development of the signal on these blots were done according to the Genius kit manual.

Preparation and analysis of *Drosophila* RNA.

Total RNA was isolated from adult flies as described above. Northern blot anaysis was done as described in the red book. For the RNA PCR experiments to determine whether the transformed fly lines expressed the rescue P element, the first strand cDNA was synthesized as described for the RACE cloning experiments in chapter 1. The oligos used in the PCR reactions were:

Exon 1 5'CCAGCCTTGTTCAATTATGTT3' (-123 to -102 relative to the AUG codon of the 3.3 kb *dfer* mRNA)

Seq 3 5'ATTCAGGCGTGCTGCGAT3' (+621 to +603 relative to the AUG codon of the 3.3 kb *dfer* mRNA).

Instead of cloning the PCR products, as was done in the RACE protocol, the PCR reactions were run on a gel, and the 500 bp band was cut out and purified by the Gene Clean method. The 500 bp fragment was divided in two tubes. The DNA in one of the tubes was cut with Xba 1and the cut DNA was run side by side with the uncut DNA on a 1.5 % Agarose gel in TBE buffer. The gels were Southern blotted and probed according to the Genius Kit manual.

Construction of the *dfer* mini gene recue P element.

The construction of the P[2345fer] minigene rescue P element is described in Figure A 1. The PCR 1 fragment was generated by PCR using the plasmid p2.7/6.4 as template and the following oligos:

M13 Reverse sequencing primer

Xba Pel 3 5'AGATCTTATTTGGGTCGCGGCTCT3' (-18 to-36

relative to the ATG start codon of the 3.3 kb mRNA.

The PCR 2 fragment was generated using the plasmid pdfps (the insert of this plasmid is the 3.3 kb cDNA clone) and the following primers:

Xba Pel 5 5'AGATCTATAGGGAGTAACGAGAGC 3' (-21- to-3

relative to the ATG start site of the 3.3 kb mRNA.)

Seq 5   5' CTGCTTCTCCTGGCAGCG 3' (+1136 to +1118
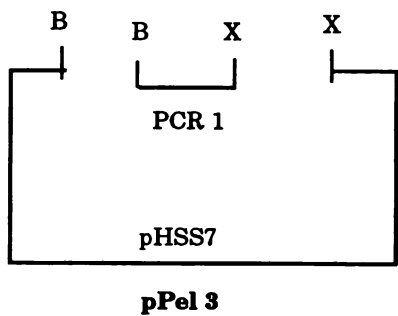
relative to the ATG start site of the 3.3 kb mRNA)

The plasmid pHSS7 and the CasPer Pelement vector are described in Simon, Bowtell et al. 1991.

The P[2345fer] P element construct was purified 2X on CsCl gradients and the plasmid was injected according to the protocol in (Roberts 1986).
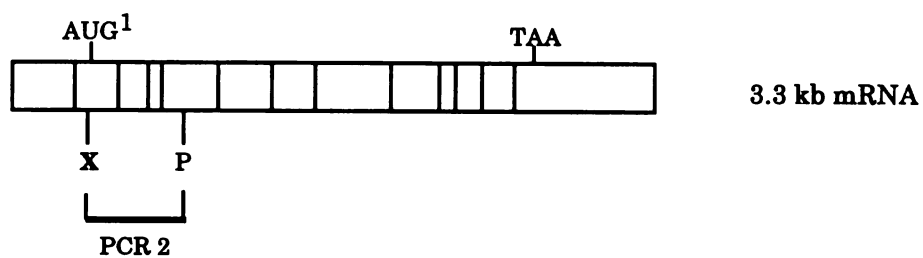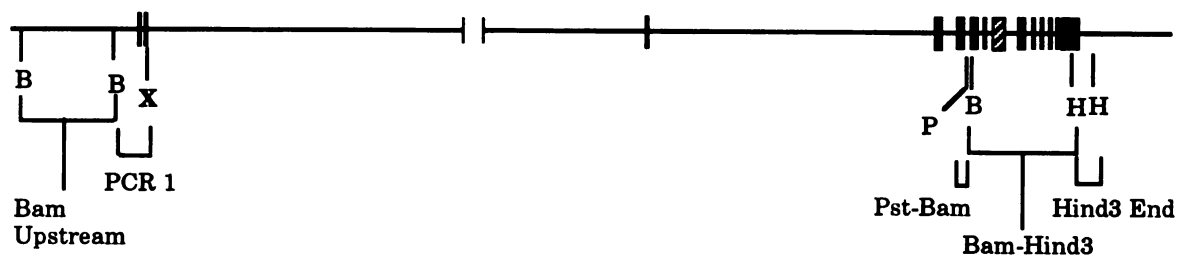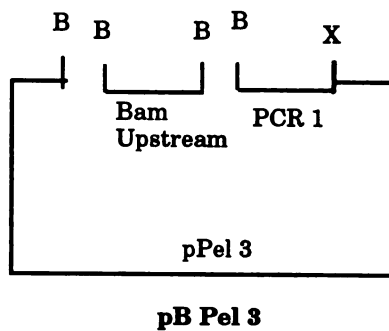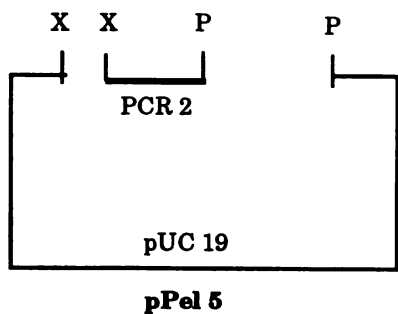
Figure A1 Continued

5.

6.

7.

8.
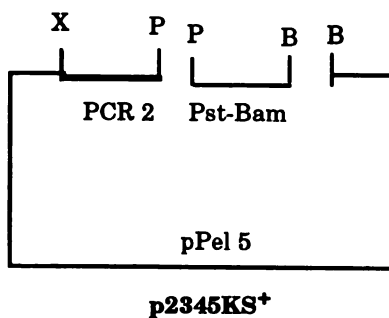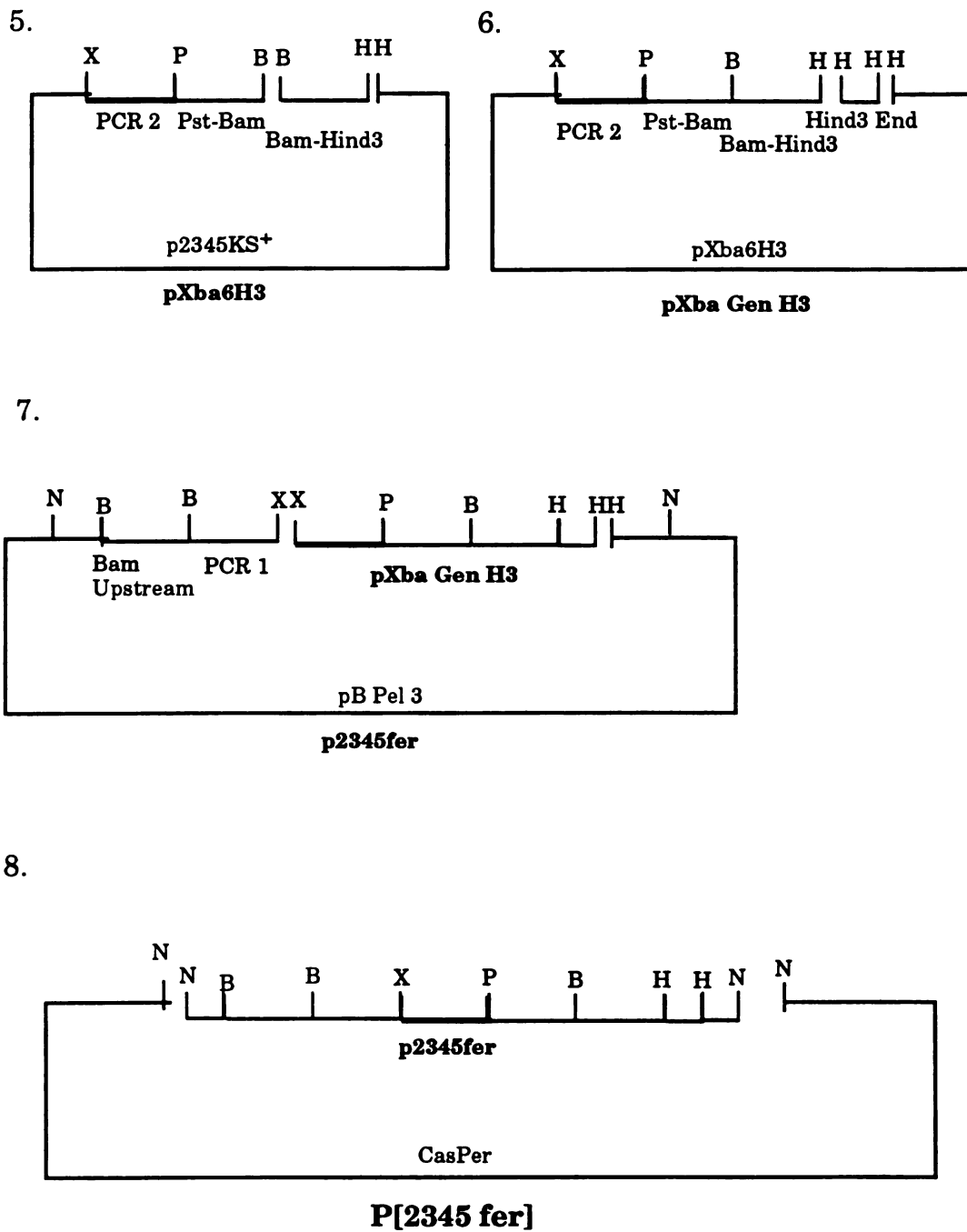
RNA PCR to determine the expression of the P[2345fer] transgene in the transformed lines.

Total RNA was isolated from adult flies and first strand cDNA was synthesized as described above. PCR reactions were carried out on the cDNA as described above using the following oligos:

Exon 1 5' CCAGCCTTGTTCAATTATGTT 3' (-123 to -102 relative to the ATG start site of the 3.3 kb mRNA)

Seq 3 5' ATTCAGGCGTGCTGCGAT 3' (+377 to +356 relative to the ATG start codon of the 3.3 kb mRNA.)

The PCR reaction was gene cleaned, and then the products were divided into two tubes. One tube was cut with Xba 1 and the other tube was incubated with digestion buffer with out Xba 1. The cut and uncut PCR products were run on a 1.5% Agarose gel. The gel was Southern blotted and Probed with a probe made to the 3.3 kb mRNA.

Scanning Electron microscopy of adult flies.

The adult flies were dehydrated in an ethanol series, 25%,50%,75%, and 2X 100% Ethanol for 24 hours at each stage. The specimens were then dried at the critical point using a Autosamdri 814 Critical point Drying Apparatus. The dried specimens were then mounted on to SEM specimen stubs and sputter coated with Gold-palladium. The specimens were examined in a JEOL JSM 840A Scanning Electron Micrscope.

Sections of Drosophila eyes.

The eye sections were done as described in (Kimmel, Heberlein et al. 1990).

Flight tests of control and mutant adult flies.

The flight tests were done as described in (Koana and Hotta 1978) .

Silver staining of thoracic muscle sections.

The adult flies were processed and sectioned as described in (Deak 1977). Pharate adults, both control and fer^{X42}/fer^{X8} mutants, were collected during late pupal stage when the wings and eyes were visible through the pupal case. These specimens were also processed and sectioned as described in (Deak 1977).

Appendix 2

Bibliography

Abraham, N., M. Miceli, et al. (1991). "Enhancement of T-cell responsiveness by the lymphocyte-specific tyrosine protein kinase p56^{lck}." Nature **350**: 62-66.

Ambrosio, L., A. Mahowald, et al. (1989). "Requirement of the *Drosophila raf* homolog for *torso* function." Nature **342**: 288-290.

Appleby, M., J. Gross, et al. (1992). "Defective T cell receptor signaling in mice lacking the thymic isoform of p59^{fyn}." Cell **70**: 751-763.

Atkinson, M. and J. Sheridan (1985). Reduced junctional permeability in cells transformed by different viral oncogenes. Gap Junctions. Cold Spring Harbor NY, Cold Spring Harbor Laboratory. 205-213.

Ausubel, F., R. Brent, et al., Ed. (1990). Current Protocols in Molecular Biology. New York, NY, Wiley Interscience.

Baeuerle, P. and D. Baltimore (1988). "IkB: a specific inhibitor of the NF-kB transcription factor>." Science **242**: 540-546.

Baker, N. and G. Rubin (1992). "*Ellipse* mutations in the *Drosophila* homolog of the EGF receptor affect pattern formation, cell division, and cell death in eye imaginal discs." Developmental Biology **150**: 381-396.

Baker, N. E. and G. M. Rubin (1989). "Effect on eye development of dominant mutations in the Drosophila homolog of the EGF receptor." Nature **340**: 150-153.

Banerjee, U., P. Renfranz, et al. (1987). "Molecular characterization and expression of sevenless, a gene involved in neuronal pattern formation in the Drosophila eye." Cell **49**: 281-291.

Bang, A. and J. Posakony (1992). "The *Drosophila* gene *Hairless* encodes a novel basic protein that controls the alternative cell fates in adult sensory organ development." Genes and Development **6**: 1752-1769.

Bang, A., V. Hartenstein, et al. (1991). "*Hairless* is required for the development of adult sensory organ precursor cells in *Drosophila*." Development **111**: 89-104.

Barbacid, M. (1987). "*Ras* genes." Annual Review of Biochemistry **56**: 779-827.

Bargmann, C., M. Hung, et al. (1986). " Multiple independent activations of the *neu* oncogene by a point mutation in the transmembrane domain of p185." Cell **45**: 649-657.

Biggs, J., E. Hersperger, et al. (1990). "A Drosophila gene that is homologous to a mammalian gene associated with tumor metastasis codes for a nucleoside diphosphate kinase." Cell **63**: 933-940.

Bishop, J. and V. Corces (1988). "Expression of an activated ras gene causes developmental abnormalities in transgenic Drosophila melanogaster." Genes and Development **2**: 567-577.

Bishop, J. M. (1987). "The molecular genetics of Cancer." Science **235**: 305-311.

Bishop, J. M. (1991). "Molecular themes in Oncogenesis." Cell **64**: 235-248.

Bonfini, L. C., C. A. Karlovich, et al. (1992). "The Son of Sevenless gene product: a putative activator of ras." Science **255**: 603-606.

Bryant, P. (1987). Experimental and genetic analysis of growth and cell proliferation in Drosophila imaginal discs. Genetic regulation of Development. New York, Alan R. Liss. 339-372.

Cagan, R. and D. Ready (1989). "*Notch* is required for successive cell decisions in the developing *Drosophila* retina." Genes and Development **3**: 1099-1112.

Cagen, R. and D. Ready (1989). "The emergence of order in the *Drosophila* pupal retina." Developmental Biology **136**: 346-362.

Call, K., T. Glaser, et al. (1990). "Isolation and characterization of a zinc finger polypeptide at the human chromosome 11 Wilms' Tumor locus." Cell **60**: 509-520.

Campos-Ortega, J. and V. Hartenstein (1985). The Embryonic Development of Drosophila melanogaster. Heidelberg, Springer-Verlag.

Campos-Ortega, J. and Y. Jan (1991). "Genetic and molecular bases of neurogenesis in *Drosophila melanogaster*." Annual Review of Neuroscience **in press**:

Cavener, D. (1987). "Comparison of the consensus sequence flanking translational start sites in *Drosophila* and vertebrates." Nucleic Acids Research **15**: 1353-1361.

Clark, S. G., M. J. Stern, et al. (1992). "C. elegans cell-signaling gene Sem-5 encodes a protein with SH2 and SH3 domains." Nature **356**: 340-344.

Clifford, R. and T. Schupach (1989). "Coordinately and differentially mutable activities of *torpedo*, the *Drosophila melanogaster* homolog of the vertebrate EGF receptor gene." Genetics **123**: 771-787.

Cooke, M., K. Abraham, et al. (1991). "Regulation of T cell receptor signaling by a *src* family protein-tyrosine kinase (p59^{fyn})." Cell **65**: 281-291.

Costello, W. and R. Wyman (1986). "Development of an indirect flight muscle in a muscle specific mutant of *Drosophila melanogaster*." Developmental Biology **118**: 247-258.

Crossley, A. . (1978). The morphology and development of the *Drosophila* muscular system. The Genetic and Biology of *Drosophila*. New York, Academic Press. 499-560.

Daniels, S., M. McCarron, et al. (1985). "Dysgenesis induced instability of rosy locus transformation in *Drosophila melanogaster* : analysis of excision events and the selective recovery of control element deletions." Genetics **109**: 95-117.

De La Pompa, J., J. Garcia, et al. (1989). "Genetic analysis of muscle development in *Drosophila melanogaster*." Developmental Biology **131**: 439-454.

de la Concha, A., U. Dietrich, et al. (1988). "Functional interactions of the neurogenic genes of *Drosophila melanogaster*." Genetics **118**: 499-508.

Deak, I. (1977). "Mutations of *Drosophila melanogaster* that affect muscles." Journal Embryology and experimental Morphology **40**: 35-63.

Deak, I., P. Bellamy, et al. (1982). "Mutations affecting the indirect flight muscles of *Drosophila melanogaster*." Journal Embryology and experimental Morphology **69**: 61-81.

Dearolf, C., E. Hersperger, et al. (1988). "Developmental consequences of awd^{b3}, a cell autonomous lethal mutation of *Drosophila* induced by hybrid dysgenesis." Developmental Biology **129**: 159-168.

Doyle, H. and J. M. Bishop (1993). "Torso, a receptor tyrosine kinase required for embryonic pattern formation, shares substrates with the Sevenless and EGF-R pathways in *Drosophila*." Genes and Development **In Press**:

Fearon, E. and B. Vogelstein (1990). "A genetic model for colorectal tumorigenesis." Cell **61**: 759-767.

Fearon, E., K. Cho, et al. (1990). "Identification of a chromosome 18q gene that is altered in colorectal cancers." Science 247: 49-56.

Feldman, R., E. Wang, et al. (1983). "Cytoplasmic localization of the transforming protein of Fujinami Sarcoma Virus: salt sensitive association with subcellular components." Journal of Virology 45: 782-791.

Fernandez, J., M. Bate, et al. (1991). "Development of the indirect flight muscles of Drosophila." Development 113: 67-77.

Fischman, K., J. Edman, et al. (1990). "A murine fer testis-specific transcript (ferT) encodes a truncated Fer protein." Molecular and Cellular Biology 10: 146-153.

Fleming, R., S. DeSimone, et al. (1989). "Molecular isolation and analysis of the erect wing locus in Drosophila melanogaster." Molecular and Cellular Biology 9: 719-725.

Fleming, R., S. Zusman, et al. (1983). "Developmental genetic analysis of lethal alleles at the ewg locus and their effects on muscle development in Drosophila melanogaster." Developmental Genetics : 347-363.

Fortini, M. E., M. A. Simon, et al. (1992). "Signaling by the sevenless protein tyrosine kinase is mimicked by Ras 1 activation." Nature 355: 559-561.

Frohman, M., M. Dush, et al. (1988). "Rapid amplification of full length cDNAs from rare transcripts: Amplification using a single gene-specific oligonucleotide primer." PNAS USA 85: 8998-9002.

Fu, X. (1992). "A transcription factor with SH2 and SH3 domains is directly activated by an interferon alpha-induced cytoplasmic protein tyrosine kinase(s)." Cell 70: 323-335.

Gassmann, M., M. Guttinger, et al. (1992). "Protein tyrosine kinase p59^{fyn} is associated with the T cell receptor-CD3 complex in functional human lymphocytes." European Journal of Immunology 22: 283-286.

Gateff, E. (1982). "Cancer, Genes, and Development: The Drosophila case." Advances in Cancer Research 37: 33-74.

Gateff, E. and B. Mechler (1989). "Tumor-suppressor genes of Drosophila melanogaster." CRC Critical Reviews of Oncogenesis 1: 221-245.

Gaul, U., G. Mardon, et al. (1992). "A putative Ras GTPase Activating Protein acts as a Negative regulator of signaling by the sevenless receptor tyrosine kinase." Cell 68: 1007-1019.

Geisler, R., A. Bergmann, et al. (1992). "*cactus* ,a gene involved in dorsoventral pattern formation of *Drosophila*, is related to the IkB gene family of vertebrates." Cell **71**: 613-621.

Gertler, F., J. Doctor, et al. (1990). "Genetic suppression of mutations in the *Drosophila abl* proto-oncogene homolog." Science **248**: 857-860.

Gertler, F., K. Hill, et al. (1993). "Dosage-sensitive modifiers of Drosophila abl tyrosine kinase function: prospero, a regulator of axonal outgrowth, and disabled, a novel tyrosine kinase substrate." In press :

Gertler, F., R. Bennett, et al. (1989). "Drosophila *abl* Tyrosine Kinase in Embryonic CNS Axons: A Role in Axonogenesis Is Revealed through Dosage-Sensitive Interactions with *disabled.*" Cell **58**: 103-113.

Gilmore, T. (1990). " NF-kB, KBF-1, *dorsal,* and *rel*ated matters." Cell **62**: 841-843.

Govind, S. and R. Steward (1991). "Dorsoventral pattern formation in *Drosophila.*" Trends in Genetics **7**: 119-125.

Gregory, R., K. Kammermeyer, et al. (1987). "Primary sequence and developmental expression of a novel Drosophila melanogaster src gene." Molecular and Cellular Biology **7**: 2119-2127.

Gutmann, E. (1976). "Neurotrophic relations." Annual Review of Physiology **38**: 177-216.

Hafen, E., K. Basler, et al. (1987). "Sevenless, a cell-specific homeotic gene of Drosophila, encodes a putative transmembrane receptor with a tyrosine kinase domain." Science **236**: 55-63.

Hanks, S., A. Quinn, et al. (1988). "The Protein Kinase Family: Conserved Features and Deduced Phylogeny of the Catalytic Domains." Science **241**: 42-52.

Hao, Q., N. Heisterkamp, et al. (1989). "Isolation and sequence analysis of a novel human tyrosine kinase gene." Molecular and Cellular Biology **9**: 1587-1593.

Harihan, I. K., R. w. Carthew, et al. (1991). "The Drosophila Roughened mutation: activation of a rap homolog disrupts eye development and interferes with cell determination." Cell **67**: 717-722.

Hartenstein, V. and J. Posakony (1989). "Development of the adult sensilla on the wing and notum of *Drosophila melanogaster.*" Development **107**: 389-405.

Hartenstein, V. and J. Posakony (1990). "A dual function of the *Notch* gene in Drosophila sensillum development." Developmental Biology **142**: 13-30.

Hartwell, L. (1992). "Defects in a Cell cycle checkpoint may be responsible for the genomic instability of cancer cells." Cell **71**: 543-546.

Henkemeyer, M., F. Gerteler, et al. (1987). "The Drosophila Abelson proto-oncogene homolog: Identification of mutant alleles that have pleitropic effects late in development." Cell **51**: 821-828.

Henkemeyer, M., S. West, et al. (1990). "A Novel Tyrosine Kinase-Independent Function of Drosophila *abl* Correlates with Proper Subcellular Localization." Cell **63**: 949-960.

Herskowitz, I. (1987). "Functional inactivation of genes by dominant negative mutations." Nature **329**: 219-222.

Heuvel, M. v. d., R. Nusse, et al. (1989). "Distribution of the *wingless* Gene Product in Drosophila Embryos: A Protein Involved in Cell-Cell Communication." Cell **59**: 739-749.

Hirst, R., A. Horowitz, et al. (1986). "Phosphorylation of the fibronectin receptor complex in cells transformed by oncogenes that encode tyrosine kinases." PNAS USA **83**: 6470-6474.

Hoffman-Falk, H., P. Einat, et al. (1983). "Drosophila melanogaster DNA clones homologous to vertebrate oncogenes: evidence for a common ancestor to the src and abl cellular genes." Cell **32**: 589-598.

Hoffmann, F. M. (1989). "Role of Drosophila Proto-oncogenes and growth factor homologs during development of the fly." Current Topics in Microbiology and Immunology **147**: 1-29.

Hoffmann, F. M. (1991). "Drosophila *abl* and genetic redundancy in signal transduction." Trends in Genetics :

Huang, C., C. Hammond, et al. (1985). "Nucleotide sequence and topography of chicken *c-fps* genesis of a retroviral oncogene encoding a tyrosine specific protein kinase." Journal of Molecular Biology **181**: 175-186.

Ikeda, K., j. Koenig, et al. (1980). "Organization of identified axons innervating the dorsal longitudinal flight muscle of *Drosophila melanogaster*." Journal of Neurocytology **9**: 799-823.

Ingham, P. (1988). "The molecular genetics of embryonic pattern formation in *Drosophila*." Nature **335**: 25-34.

Jursnich, V., S. Fraser, et al. (1990). "Defective gap junctional communication associated with imaginal disc overgrowth and degeneration caused by mutations of the *dco* gene in Drosophila." Developmental Biology 140: 413-429.

Katzen, A., D. Monterras, et al. (1991). "A gene related to the proto-oncogene *fps/fes* is expressed at diverse times during the life cycle of *Drosophila melanogaster*." Molecular and Cellular Biology 11: 226-239.

Katzen, A., T. Kornberg, et al. (1985). "Isolation of the proto-oncogene c-myb from Drosophila melanogaster." Cell 41: 449-456.

Katzen, A., T. Kornberg, et al. (1991). "Expression during *Drosophila* development of DER, A gene related to *erB-1* and *neu*:: correlations with mutant phenotypes." Developmental Biology 145: 287-301.

Katzen, A., T. Kornberg, et al. (1993). "A role for myb in the cell cycle." Manuscript in preparation.

Kemphues, K., E. Raff, et al. (1980). "Mutation in a testes-specific ß-tubulin in Drosophila: analysis of its effects on meiosis and map location of the gene." Cell 21: 445-451.

Kemphues, K., E. Raff, et al. (1983). "Genetic analysis of ß2t, the structural gene for a testes specific ß-tubulin subunit in Drosophila melanogaster." Genetics 105: 345-356.

Kidd, S. (1992). "Characterization of the *cactus* locus and analysis of the interactionsbetween *cactus* and *dorsal*;." Cell 71: 623-635.

Kidd, S., T. Lockett, et al. (1983). "The *Notch* locus of *Drosophila melanogaster*." Cell 34: 421-433.

Kimmel, B., U. Heberlein, et al. (1990). "The homeo domain protein *rough* is expressed in a subset of cells in the developing *Drosophila* eye where it can specify photoreceptor cell subtype." Genes and Development 4: 712-727.

Klambt, C., J. R. Jacobs, et al. (1991). "The midline of the Drosophila central nervous system: a model for genetic analysis of cell fate, cell migration, and growth cone guidance." Cell 64: 801-815.

Klambt, C., L. Glazer, et al. (1992). "*breathless*, a Drosophila FGF receptor homolog, is essential for the migration of tracheal and specific midline glial cells." Genes and Development 6: 1668-1678.

Klambt, C., S. Muller, et al. (1989). "The Drosophila melanogaster l(2)gl gene encodes a protein in the cadherin cell-adhesion molecule family." Developmental Biology 133: 425-436.

Koana, T. and Y. Hotta (1978). "Isolation and characterization of flightless mutants in *Drosophila melanogaster*." Journal embryology and experimental Morphology **45**: 123-143.

Kopczynski, C., A. Alton, et al. (1988). "*Delta*, a Drosophila neurogenic gene, is transcriptionally complex and encodes a protein related to blood coagulation factors and epidermal growth factor of vertebrates." Genes and Development **2**: 1723-1735.

Korsmeyer, S. (1992). "Chromosomal Translocations in Lymphoid Malignancies Reveal Novel Proto-Oncogenes." Annual Review of Immunology **10**: 785-807.

Lawrence, p. and P. Johnston (1986). "The muscle pattern of a segment of *Drosophila* may be determined by neurons and not the contributing myoblasts." Cell **45**: 505.

Lee, E., H. To, et al. (1988). "Inactivation of the retinoblastoma susceptibility gene in human breast cancers." Science **241**: 218-221.

Lenardo, M. and D. Baltimore (1989). "NF-kB: a pleiotropic mediator of inducible and tissue specific gene control." Cell **58**: 227-229.

Lindsley, D. L. and G. G. Zimm (1992). The Genome of Drosophila melanogaster. San Diego, CA, Academic Press Inc.

Livingstone, L., A. White, et al. (1992). "Altered cell cycle arrest and gene amplification potential accompany loss of wild-type p53." Cell **70**: 923-935.

Livneh, E., L. Glazer, et al. (1985). "The Drosophila EGF receptor gene homolog: conservation of both hormone binding and kinase domain." Cell **40**: 599-607.

Lowenstein, E. J., R. Daly, et al. (1992). "The SH2 and SH3 domain-containing protein GRB2 links receptor tyrosine kinases to ras signaling." Cell **70**: 431-442.

MacKrell, A., B. Blumberg, et al. (1988). "The lethal myospheroid gene of Drosophila encodes a membrane protein homologous to vertebrate integrin ß subunits." PNAS USA **85**: 2633-2637.

Mahoney, P., U. Weber, et al. (1991). "The *Fat* tumor suppressor gene in Drosophila encodes a novel member of the Cadherin gene superfamily." Cell **67**: 853-868.

Marshall, C. (1991). "Tumor suppressor genes." Cell **64**: 313-326.

Mechler, B., W. Mcginnis, et al. (1985). "Molecular cloning of lethal(2)giant larvae, a recessive oncogene of Drosophila melanogaster." EMBO Journal 4: 1551-1557.

Molina, T., K. Kishihara, et al. (1992). "Profound block in thymocyte development in mice lacking p56^{lck}." Nature 357: 161-164.

Mount, S. (1982). "A catalogue of splice junction sequences." Nucleic Acids Research 10: 459-472.

Neuman-Silberberg, F., E. Schejter, et al. (1984). "The Drosophila ras oncogenes: structure and nucleotide sequence." Cell 37: 1027-1033.

Newman, S. and T. Wright (1981). "A Histological and Ultrastructural Analysis of Developmental Defects Produced by the Mutation lethal(1)myospheroid, in Drosophila melanogaster." Developmental Biology 86: 393-402.

Newman, S. and T. Wright (1983). "Lethal(1)fibrillardysgenesis (l(1)fdg), A mutation affecting muscle development in the embryo of Drosophila melanogaster." Developmental Genetics : 329-345.

Nishida, Y., M. Hata, et al. (1988). "Proliferation of both somatic and germ cells is affected in the Drosophila mutants of the raf proto-oncogene." EMBO Journal 7: 775-781.

Nusse, R. (1986). "The activation of cellular oncogenes by retroviral insertion." Trends in Genetics 2: 244-247.

Padgett, R., R. S. Johnson, et al. (1987). "A transcript from a Drosophila pattern gene predicts a protein homologous to the transforming growth factor-ß family." Nature 325: 81-84.

Pawson, T. and G. Gish (1992). "SH2 and SH3 Domains: From structure to function." Cell 71: 359-362.

Pawson, T., K. Letwin, et al. (1989). "The FER gene is evolutionarily conserved and encodes a widely expressed member of the FPS/FES protein-tyrosine kinase family." Molecular and Cellular Biology 9: 5722-5725.

Peles, E., S. Bacus, et al. (1992). "Isolation of the Neu/Her-2 stimulatory ligand: a 44kd glycoprotein that induces differentiation of mammary tumor cells." Cell 69: 205-216.

Perkins, K., G. Dailey, et al. (1988). "Novel Jun and Fos related proteins in Drosophila are functionally homologous to enhancer factor AP-1." EMBO Journal 7: 4265-4273.

Perkins, L., I. Larsen, et al. (1992). "corkscrew encodes a putative protein tyrosine phosphatase that functions to transduce the terminal signal from the receptor tyrosine kinase torso." Cell 70: 225-236.

Petruzelli, L., R. Herrera, et al. (1986). "Isolation of a Drosophila genomic sequence homologous to the kinase domain of the human insulin receptor and detection of the phosphorylated Drosophila receptor with an anti-peptide antibody." PNAS USA 83: 4710-4714.

Pribyl, L., D. Watson, et al. (1988). "The Drosophila ets-2 gene: molecular structure, chromosomal localization, and developmental expression." Developmental Biology 127: 45-53.

Rijsewijk, F., M. Schuermann, et al. (1987). "The Drosophila homolog of the mouse mammary oncogene int-1 is identical to the segment polarity gene wingless." Cell 50: 649-657.

Robbins, P., J. Horowitz, et al. (1990). "Negative regulation of human c-fos expression by the retinoblastoma gene product." Nature 346: 668-671.

Roberts, D., Ed. (1986). Drosophila a Practical approach. Washington DC, IRL Press.

Robinson, L., J. Gibbs, et al. (1987). "CDC25: a component of the RAS-adenylate cyclase pathway in Saccharomyces cerevisiae." Science 235: 1218-1221.

Roebroek, A., J. Schalken, et al. (1987). "Structure of feline cfps/fes proto-oncogene: Genesis of a retroviral oncogene." Journal of Virology 61: 20092016.

Rogge, R., C. Karlovich, et al. (1991). "Genetic dissection of a neurodevelopmental pathway: Son of sevenless functions downstream of the sevenless and EGF receptor tyrosine kinases." Cell 64: 39-48.

Rubin, G. (1991). "Signal transduction and the fate of the R7 photoreceptor in Drosophila." Trends in Genetics 7: 372-376.

Rubin, G. and e. al. (1992). Cold Spring Harbor Symposia on Quantitative Biology in press:

Ruggieri, R. and F. McCormick (1991). "Ras and the awd couple." Nature 353: 390-391.

Rutledge, B., K. Zhang, et al. (1992). "The Drosophila spitz gene encodes a putative EGF-like growth factor involved in dorsal-ventral axis formation and neurogenesis." Genes and Development 6: 1503-1517.

Sager, R. (1989). "Tumor suppressor genes: the puzzle and the promise." Science **246**: 1406-1412.

Samarut, J., B. Mathey-Prevot, et al. (1985). "Preferential expression of the c-fps protein in chicken macrophages and granulocytic cells." Molecular and Cellular Biology **5**: 1067-1072.

Schwab, M. and L. Amler (1990). "Amplification of cellular oncogenes: a predictor of clinical outcome in human cancer." Genes, Chromosomes and Cancer **1**: 181-194.

Schwartzberg, P., A. Stall, et al. (1991). "Mice Homozygous for the abl^{m1} Mutation Show Poor Viability and Depletion of Selected B and T Cell Populations." Cell **65**: 1165-1175.

Shaw, A., K. Amrein, et al. (1989). "The lck tyrosine kinase interacts with the cytoplasmic tail of the CD4 glycoprotein through its unique amino-terminal domain." Cell **59**: 627-636.

Shilo, B-Z and R. Weinberg (1981). "DNA sequences homologous to vertebrate oncogenes are conserved in *Drosophila melanogaster*." PNAS USA **78**:6789-6792.

Shilo, B.-Z. and E. Raz (1991). "Developmental control by the *Drosophila* EGF receptor homolog DER." Trends in Genetics **7**: 388-392.

Simon, M., B. Drees, et al. (1985). "The nucleotide sequence and the tissue specific expression of Drosophila c-src." Cell **42**: 831-840.

Simon, M., D. Bowtell, et al. (1991). "Ras 1 and a putative guanine nucleotide exchange factor perform crucial steps in signaling by the sevenless tyrosine kinase." Cell **67**: 701-716.

Smith, M., S. DeGudicibus, et al. (1986). "Requirement for c-ras during viral oncogene transformation." Nature **320**: 540-543.

Soriano, P., C. Montgomery, et al. (1991). "Targeted disruption of the c-src proto-oncogene leads to Osteopetrosis in mice." Cell **64**: 693-702.

Spofford, J. (1976). Position-effect variegation in *Drosophila*. The Genetics and Biology of Drosophila. New York, Academic Press. 955-1018.

Sprenger, F., L. Stevens, et al. (1989). "The Drosophila gene torso encodes a putative receptor tyrosine kinase." Nature **338**: 478-483.

St. Johnson, R. and W. Gelbart (1987). "Decapentaplegic transcripts are localized along the dorsal-ventral axis of the Drosophila embryo." EMBO Journal **6**: 2785-2791.

Stein, P., H. Lee, et al. (1992). "pp59^{fyn} mutant mice display differential signaling in thymocytes and peripheral T cells." Cell 70: 741-750.

Sternberg, P. and H. Horvitz (1991). "Signal transduction during *C. elegans* vulval induction." Trends in Genetics 7: 366-371.

Steward, R. (1987). "*Dorsal*, an embryonic polarity gene in Drosophila, is homologous to the vertebrate proto-oncogene, c-rel." Science 238: 692-694.

Steward, R., S. Zusman, et al. (1988). "The dorsal protein is distributed in a gradient in early embryos." Cell 55: 487-495.

Straus, D. and A. Weiss (1992). "Genetic evidence for the involvement of the lck tyrosine kinase in signal transduction through the T cell antigen receptor." Cell 70: 585-593.

Tautz, D. and C. Pfeifle (1989). "A non-radioactive *in situ* hybridization method for the localization of specific RNAs in *Drosophila* reveals translational control of the segmentation gene *hunchback*." Chromosoma 98: 81-85.

Teng, D., C. Engele, et al. (1991). "A product of the *prune* locus of Drosophila is similar to mammalian GTPase-activating protein." Nature 353: 437-440.

Tower, J., G. Karpen, et al. (1993). "Preferential transposition of *Drosophila* P elements to nearby chromosomal sites." Genetics 133: 347-359.

Tsuda, L., Y. Inoue, et al. (1993). "A protein kinase similar to MAP kinase Activator acts downstream of the raf kinase in *Drosophila*." Cell 72: 407-414.

Tybulewicz, V., C. Crawford, et al. (1991). "Neonatal lethality and lymphopenia in mice with a homozygous disruption of the *c-abl* proto-oncogene." Cell 65: 1164.

Ullrich, A. and J. Schlessinger (1990). "Signal Transduction by Receptors with Tyrosine Kinase Activity." Cell 61: 203-212.

Van Etten, R., P. Jackson, et al. (1989). "The mouse type IV *c-abl* gene product is a nuclear protein, and activation of transforming ability is associated with cytoplasmic localization." Cell 58: 669-678.

Varmus, H. (1989). An historical overview of oncogenes. Oncogenes and the Molecular Origins of Cancer. New York, Cold Spring Harbor Laboratory Press. 3-44.

Velazquez, L., M. Fellous, et al. (1992). "A protein tyrosine kinase in the interferon alpha/beta signaling pathway." Cell 70: 313-322.

Volk, T., L. Fessler, et al. (1990). "A role for integrin in the formation of sarcomeric cytoarchitecture." Cell 63: 525-536.

Woods, D. and P. Bryant (1989). "Molecular cloning of the *Lethal(1)Discs Large-1* Oncogene of Drosophila." Developmental Biology 134: 222-235.

Woods, D. and P. Bryant (1991). "The Discs-large tumor suppressor gene of Drosophila encodes a guanylate kinase homolog localized at septate junctions." Cell 66: 451-464.

Woolford, J. and K. Beemon (1984). "Transforming proteins of Fujinami and PRCII avian Sarcoma viruses have different subcellular localizations." Virology 135: 168-180.

Xu, G., P. O'Connell, et al. (1990). "The neurofibromatosis type 1 gene encodes a protein related to GAP." Cell 62: 599-608.

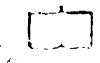Young, J. and G. S. Martin (1984). "Cellular localization of *c-fps* gene product NCP98." Journal of Virology 52: 913-918.